AD_____

Award Number: W81XWH-08-1-0509

TITLE: The Role of BRCA1 Domains and Motifs in Tumor Suppression

PRINCIPAL INVESTIGATOR: Aneliya Velkova

CONTRACTING ORGANIZATION: Moffitt Cancer Center
Tampa, FL 33512

REPORT DATE: August 2011

TYPE OF REPORT: Annual Summary

PREPARED FOR: U.S. Army Medical Research and Materiel Command
Fort Detrick, Maryland 21702-5012

REPORT DOCUMENTATION PAGE

Form Approved
OMB No. 0704-0188

1. REPORT DATE *(DD-MM-YYYY)*	2. REPORT TYPE	3. DATES COVERED *(From - To)*
01-08-2011	Annual Summary	1 AUG 2008 - 31 JUL 2011

4. TITLE AND SUBTITLE

The Role of BRCA1 Domains and Motifs in Tumor Suppression

5a. CONTRACT NUMBER

5b. GRANT NUMBER

W81XWH-08-1-0509

5c. PROGRAM ELEMENT NUMBER

6. AUTHOR(S)

Aneliya Velkova

E-Mail: aneliya.velkova@moffitt.org

5d. PROJECT NUMBER

5e. TASK NUMBER

5f. WORK UNIT NUMBER

7. PERFORMING ORGANIZATION NAME(S) AND ADDRESS(ES)

Moffitt Cancer Center
Tampa, FL 33512

8. PERFORMING ORGANIZATION REPORT NUMBER

9. SPONSORING / MONITORING AGENCY NAME(S) AND ADDRESS(ES)

U.S. Army Medical Research and Materiel Command
Fort Detrick, Maryland 21702-5012

10. SPONSOR/MONITOR'S ACRONYM(S)

11. SPONSOR/MONITOR'S REPORT NUMBER(S)

12. DISTRIBUTION / AVAILABILITY STATEMENT

Approved for Public Release; Distribution Unlimited

13. SUPPLEMENTARY NOTES

14. ABSTRACT

The purpose of this research is to classify BRCA1 variants for which cancer association is not known (called variants of uncertain significance or VUS). To approach this problem we hypothesized that poorly characterized but conserved domains in BRCA1 directly participate in its tumor suppression function. To test this hypothesis we set out to develop: 1. A system of functional assays to test the functions of domains anywhere in coding region of BRCA1. Our results indicate that the intra S phase checkpoint function of BRCA1 can be used for further classification of BRCA1 unclassified variants for their cancer association as well as for analyzing BRCA1 function. 2. We also studied the function of under explored but conserved small motifs in BRCA1. Using as bait in yeast two hybrid screening one of these motifs we identified the cytoskeletal protein Filamin A as a specific BRCA1 binding partner. Their interaction is abrogated by a mutation found in breast cancer families. We systematically evaluated DNA damage signaling after treatment with ionizing radiation in cells that lack Filamin A. We found that these cells have an impaired BRCA1 and Rad51 foci formation and accumulate single stranded DNA. Our data showed that lack of Filamin A leads to an impairment in both HR and NHEJ repair pathways.

15. SUBJECT TERMS

BRCA1, unclassified variants, genetic counseling, Breast cancer treatment

16. SECURITY CLASSIFICATION OF:			17. LIMITATION OF ABSTRACT	18. NUMBER OF PAGES	19a. NAME OF RESPONSIBLE PERSON
a. REPORT	b. ABSTRACT	c. THIS PAGE			USAMRMC
U	U	U	UU	48	19b. TELEPHONE NUMBER *(include area code)*

Table of Contents

Page

Progress report PI Aneliya Velkova BC083181 “The Role of BRCA1 Domains and Motifs in Tumor Suppression “ FINAL REPORT August 2008/August 2011

I. INTRODUCTION: Summary of project objectives and scope of research

Breast cancer is among the most frequent malignancies affecting women. Germline mutations in the breast and ovarian cancer predisposition gene 1 *(BRCA1)* are responsible for the majority of early-onset hereditary breast cancers arising in families with multiple cases [1, 2]. It is estimated that around 10% of all women undergoing testing and about 35-50% of women from minority populations receive non-informative results, due to the finding of a variant for which cancer association is not known. These are called variants of uncertain significance (VUSs). Considering that there are over 1500 alleles of *BRCA1*, one of the most challenging tasks for genetic counseling is to distinguish which are benign and which are cancer predisposing. Previous research has indicated that the likelihood of a variant being deleterious is higher when the variant is located in a structurally and functionally defined protein domain. Thus, the identification of other functional domains is critical to classifying variants. To approach this problem we hypothesized that poorly characterized, conserved domains in the central region of BRCA1 (called motif 6 and coiled-coil domain) directly participate in tumor suppression functions of BRCA1.This proposal aims to test our hypothesis and determine how specific domains and motifs of BRCA1 act to promote tumor suppression. Importantly our research has much broader implications because gene products implicated in breast cancer seem to cluster around DNA damage response pathways [3]. Thus, an understanding of the role of BRCA1 will likely have an impact on other forms of breast cancer not attributable to germline mutations in BRCA1. Both radiation therapy and most of the drugs used for cancer treatment rely on introducing DNA damage in the cells. BRCA1 is a main participant in the cellular response to DNA damage, which makes it a very important factor in modulating the patient’s response to therapy [4].

II. BODY

During the past three years (August 2008/August2011) we achieved the goals described in the two specific aims of this proposal. We choose to test for biological processes in which BRCA1 has been implicated (response to DNA damage and checkpoint control) and that are thought to be the basis for its tumor suppressive action [5-7]. We used BRCA1 full length wild type (WT) and two BRCA1 variants for which cancer association has been determined (by genetic and integrative methods) as deleterious variants: C61G [8], which is located in RING domain and M1775R [9] which is located in the second BRCT domain. We also generated two additional BRCA1 constructs: delta motif 6 (a full length BRCA1 that lacks conserved motif 6), delta coiled-coil domain (a full length BRCA1 that lacks exons 12-13). During this grant period I also collaborated with other lab members in multiple projects (see *Appendix* “Role of BRCA1 in cancer treatment” and “The role of histone H2AX in chromosomal instability”).

Task 1. To determine the functional significance of two poorly characterized domains of BRCA1 (Months 1-24):

a. Generating BRCA1 C61G in pLenti4 BRCA1 full length.
b. Generating BRCA1-null cell lines with reconstituted full-length BRCA1C61G.
c. Verifying the expression levels and subcellular localization of BRCA1 wt and mutants (C61G, M1775R, delta motif 6 and delta exon 12/13) in SUM1315 tet repressor, SUM149 tet repressor and HCC1937 tet repressor cell lines.
d. Colony forming assay with the cell lines stated above after irradiation.
e. Early G2/M checkpoint assay with the cell lines stated above.
f. RDS assay with the cell lines stated above.
g. Assay for intact spindle assembly checkpoint with the cell lines stated above.

Task2. To characterize the interaction between Filamin A and conserved motif 6 (months 18-36).

a. Performing dose response and time coarse analysis in M2, A7, HCT116, HCT116 chk2-/- cell lines.

b. Confirming dose response and time coarse analysis in MCF7 breast cancer cell line.

c. Analysis of early G2/M arrest in MCF7 cells, transfected with small fragment, containing BRCA1-motif 6.

d. Performing G2/M checkpoint recovery assays in M2 cell line transfected with pCMV2 Flag-Filamin A construct and simultaneously with pCMV2 Flag-Filamin A and BRCA1 sh RNA.

III. Key research accomplishments (summary bulleted list can be found at the end of this section)

Task 1. **To determine the functional significance of two poorly characterized domains of BRCA1 (Months 1-24):**

Task 1 (a-g).

Full-length construct of BRCA1 C61G mutant into plenti4 vector was obtained. We expressed full-length BRCA1 and mutants (C61G, M1775R, delta motif 6, delta coiled-coil domain) in HCC1937 cell line. We also tested the expression of the indicated BRCA1 mutants in two additional *BRCA1*-null cell lines SUM1315 and MDA-MB-436.

We initiated our experiments with two available BRCA1 negative cell lines: HCC1937 tet repressor and SUM 1315 tet repressor that were developed in the lab. We infected the cells with lentivirus expressing full length BRCA1 wild type (plentiBRCA1WT). Unfortunately we were not able to achieve the inducible expression of BRCA1 after addition of tetracycline for neither of the cell lines (Fig. 1A). We repeated the infection with the same lentivirus using HCC1937 and SUM 1315 that do not express tet repressor. We needed three consecutive infections for both cell lines to achieve transient expression of BRCA1 (Fig. 2B). The last approach required a high volume of lentivirus that is not practical for routine use. Another problem was that the cells were expressing BRCA1 for very short window of time 24-36 hours. Thus, we could not obtain stable cell lines.

Next, we tested and optimized electroporation of the same BRCA1 constructs using HCC1937 (Fig. 1C) and SUM1315 cell lines. We achieved reproducible levels of expression of BRCA1 2-5 days after electroporation. We concluded that this would be the method of choice to analyze whether different mutants can restore BRCA1 checkpoint function.

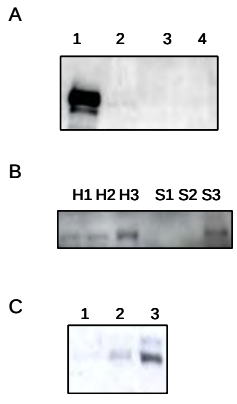

Fig.1 Optimization of BRCA1 expression in different BRCA1-null cell lines. A, B, and C-Western blot analysis of BRCA1 expression is shown. **A)**Testing BRCA1 expression in HCC1937 tet cell line. Lane1-HeLa cell line was used as positive control: lane2-HCC1937 tet parental cell line was used as negative control. Lanes 3 and 4, HCC1937 tet infected with plenti BRCA1 WT plasmid before and after the addition of tetracycline respectively. **B)** Three consecutive infections were necessary with plenti BRAC1 WT lentivirus to detect BRAC1 on western blot. H1, H2, and H3-HCC1937 first, second, and third infection respectively. Similarly, S1, S2, and S3-SUM1315 first, second, and third infection respectively. **C)** Optimization of the electroporation of plenti BRCA1 WT plasmid using HCC1937 cell line. Lane1-HCC1937 electroporated with plenti LacZ plasmid served as a negative control. Lanes 2 and 3-HCC1937 electroporated with plenti BRCA1 WT plasmid, 2 and 5 days after the procedure.

We performed colony forming assays [10] with HCC1937 transfected with pLenti plasmids expressing either BRCA1 wild type or mutant constructs: M1775R, a mutant lacking Motif 6 (delta motif 6), a mutant lacking sequences in exons 12 and 13 that code for the coiled-coil domain (delta 12/13), and BRCA1 C61G mutant. We used HCC1937 cell line transfected with pLenti lacZ plasmid as a negative control. Our experiments indicate that HCC1937 expressing BRCA1 wild type and delta Motif 6, showed better survival after ionizing radiation than HCC1937 expressing lacZ, delta 12/13, C61G or M1775R mutants. This suggests that the RING, coiled-coil and BRCT domains are critical for survival after irradiation.

In order to systematically evaluate the role of different BRCA1 domains in its checkpoint functions we started by analyzing the response of Hela cells (which we used as a positive control) and HCC1937 cells (which does not express functional BRCA1) one hour after ionizing radiation with 6 Gy (early G2/M checkpoint). We stained the cells with phospho Ser-28 -histone H3 (mitotic marker) and analyzed them by flow cytometry [10]. As expected Hela cells presented 80% decrease in the mitotic cell population 1h after irradiation. For HCC1937 cells the decrease in mitotic cells population was 30%, showing that the cell line that do not express BRCA1 (like HCC1937) do not have intact G2/M checkpoint. We continued by testing wt BRCA1 and mutants proposed in this application for early G2/M checkpoint. The results from several independent experiments with multiple samples revealed that this assay does not seem to be sensitive enough in our conditions. This may be due to several reasons:

- Transfection of HCC1937 cells (even with negative control plasmid pLenti lacz) influences the percentage of cells in mitosis.
- The ectopic expression of the BRCA1 mutants is variable. In the G2/M assay we measure the changes in the G2/M phase of the cell cycle, which for HCC1937 cells represent ~2% of the total cell population. Transfection efficiency is well under 100% and this compounds the technical issue.
- SUM1315 and SUM 149 cell lines, which were our other options for BRCA1 negative cell lines [11], behaved as they have intact G2/M checkpoint in our analysis so we conclude that they do not constitute a viable alternative.

Thus, even though we tested all the BRCA1 mutants, proposed in the application we concluded that the early G2/M assay using ectopic transfection is not sensitive enough under these conditions to be used for functional analysis of unclassified variants of BRCA1.

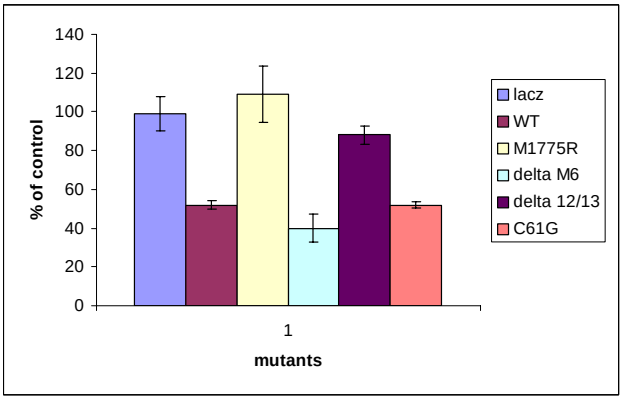

Fig.2 RDS assay. HCC1937 cells were transfected with plenti lacz (used as negative control) or mutants as shown in the diagram. The results are shown as percentage of incorporation of labeled thymidine after irradiation with 20Gy if the incorporation for unirradiated control cells is 100%.

Next, we performed RDS assay [6] using HeLa cells (as positive control) or HCC1937 cell lines. We also tried non-radioactive method to quantify the intra-S-phase checkpoint using BrdU incorporation followed by flow cytometry. We performed RDS assay using HCC1937 cell line, transfected with all the mutants proposed in the application. We used HCC1937 cell line transfected with pLenti lacZ plasmid as a negative control. Our results (Fig. 2) show that Motif 6 (delta M6) and RING domain (C61G mutant) are not required for the intra-S-phase checkpoint function of BRCA1 in HCC1937 cell line. On the other hand the coil-coiled (delta 12/13) and BRCT (M1775R) domains are necessary for the intra-S-phase checkpoint in HCC1937 cell line. We conclude that the RDS assay can be used for testing the function of BRCA1 VUSs and plan to increase the number of variants that we will be testing for the future. We also plan to use this assay routinely in our laboratory to understand the mechanism by which BRCA1 controls the intra-S-phase checkpoint. These results constitute the basis of a planned manuscript submission.

Next, we used HCC1937 cell line transfected with pLenty lac z (as negative control) or with pLenti BRCA1 wild type (as positive control) and analyzed phospho-histone H3 positive cells after nocodazole treatment (spindle assembly checkpoint) [12]. There was no difference between the two samples (positive and negative control) in any of the time points examined *i.e.* the wild type BRCA1 could not reconstitute the spindle assembly checkpoint in HCC1937 cell line. Unfortunately, the function of BRCA1 in spindle assembly checkpoint has been extensively tested in mouse embryonic fibroblasts [12] not in human breast cancer epithelial cell lines. We speculate that the difference may be species specific. Thus, we conclude that the spindle assembly assay cannot discriminate different alleles of BRCA1.

This set of experiments establish an assay system that is able to assess the role of any domain in the full length BRCA1 on biological processes in which BRCA1 has been implicated (long term survival after irradiation and the intra-S-phase checkpoint). This information (in combination with other methods) can be used further for classification of missense variants anywhere in the coding region of BRCA1.

Task2. To characterize the interaction between Filamin A and conserved motif 6 (months 18-36).

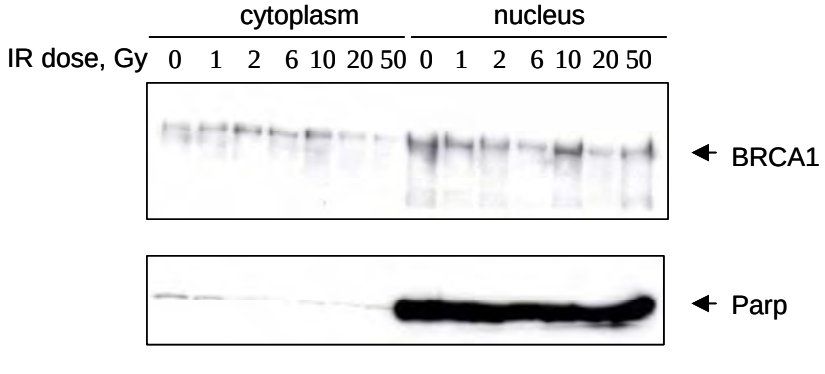

Fig. 3 Analysis of BRCA1 distribution in MCF7 cell line. BRCA1 western blot in nuclear and cytoplasmic fractions are shown after the indicated dose of irradiation.

2a. Performing dose response and time course analysis in M2, A7, HCT116, HCT116 chk2-/- cell lines. We started by analyzing BRCA1 levels in the cytoplasmic fraction of A7 (Filamin A positive) and M2 (Filamin A negative cell line). At all time points tested M2 cell lines showed significantly lower levels of BRCA1 as expected. We choose 10 Gy (maximum levels of BRCA1 in A7 cells) and performed detailed time course analysis (0-24h) of BRCA1 distribution in several cell lines. Next, we analyzed the BRCA1-P-988 antibody. Unfortunately, these experiments revealed several shortcomings of this reagent. First,

this phospho-specific antibody recognizes a band corresponding to BRCA1 in HCT116 *CHK2* $^{-/-}$ cell line. Phosphorylation of Ser-988 in BRCA1 is thought to be mediated by CHK2 [13]. Thus, this cell line should not present with this phospho epitope. Second, we used shRNAs against BRCA1 to make sure that the antibody indeed recognizes the correct (BRCA1) epitope. There was no difference between scrambled shRNA and shRNA for BRCA1 when using phospho-BRCA1-988 for western blot, although the endogenous BRCA1 was effectively silenced. Thus we conclude that this reagent (BRCA1-P-988 antibody) cannot be used with confidence. At this time there is no other alternative vendor or antibody.

2b. Confirming dose response and time course analysis in MCF7 breast cancer cell line.
We started by analyzing BRCA1 levels in the cytoplasmic fraction of MCF7 breast cancer cell line. The distribution of BRCA1 in the nucleus and in the cytoplasm of MCF7 cell line is shown on Fig.3. We choose 10 Gy (maximum levels of BRCA1 in MCF7 cells) and performed detailed time course analysis (0-24h) of BRCA1 distribution (Fig.4).

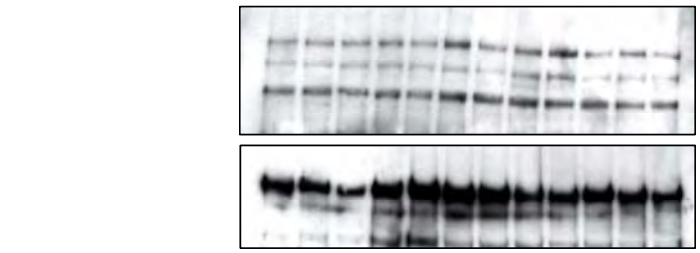

Fig. 4 Time course analysis of BRCA1 distribution in the cytoplasmic (upper panel) and nuclear (lower panel) fractions of MCF7 cell line. Western blots for BRCA1 are shown at the indicated time.

2c. Analysis of early G2/M arrest in MCF7 cells transfected with small fragment, containing BRCA1-motif 6.
We transfected MCF7 breast cancer cell line with either vector expressing GST, or GST-141-240 construct that contains the region of BRCA1 that binds to Filamin A. We performed detailed checkpoint recovery experiments as described in the proposal (Fig.5). The results indicated that there was no difference in the markers tested between the control samples and the samples expressing GST-141-240 BRCA1 fragment. We should point out that the ectopic expression of GST-141-240 construct in MCF7 cell line showed much higher level of degradation that in the other cell lines tested. Also, MCF7 cell line is hemizygous for BRCA1 and thus, it expresses less BRCA1 if compared to cell lines that are homozygous of wild type BRCA1. The levels of BRCA1 might interfere not only with the interaction between the GST-141-240 fragment and Filamin A, but also with the checkpoint recovery process.
After a detailed analysis of the binding regions between BRCA1 and Filamin A we confirmed that motif 6 of BRCA1 contribute to the binding to Filamin A. However, the main region of BRCA1 that is responsible for the binding to Filamin A is another conserved motif within the BRCA1 N-terminus called motif 2. Please, refer to fig.1 and fig.2 of the paper “Identification of Filamin A as a BRCA1-interacting protein required for efficient DNA repair. 2010, Cell Cycle 2010; 9(7): 1-13, which is attached in the appendices of this report. Moreover, introduction of BRCA1 mutation Y179C in motif 2 disrupts the binding between BRCA1 and Filamin A. Y179C mutation of BRCA1 was found in families with breast and ovarian cancer. Thus, these experiments analyzed the role of Motif 6 and Motif 2 in cell cycle regulation (refer to the first page of the appendices of this report where the paper is attached).

2d. Performing G2/M checkpoint recovery assays in M2 cell line transfected with pCMV2 Flag-Filamin A construct and simultaneously with pCMV2 Flag-Filamin A and BRCA1 shRNA.

Next, we analyzed the G2/M checkpoint recovery in M2 cell line transfected with pCMV2 Flag-Filamin A construct or with an empty vector. Please, refer to fig. 5a, b, c, d of the paper “Identification of Filamin A as a BRCA1-interacting protein required for efficient DNA repair. 2010, Cell Cycle 2010; 9(7): 1-13, which is attached in the appendices of this report. We also compared the checkpoint

recovery of M2 cell line transfected simultaneously with pCMV2 Flag-Filamin A and BRCA1 shRNA. Unfortunately, down regulation of BRCA1 have pleiotropic effects on the cell because it affects all the stages of DNA damage response (including DNA repair, signaling, recovery, and the cell cycle checkpoints).

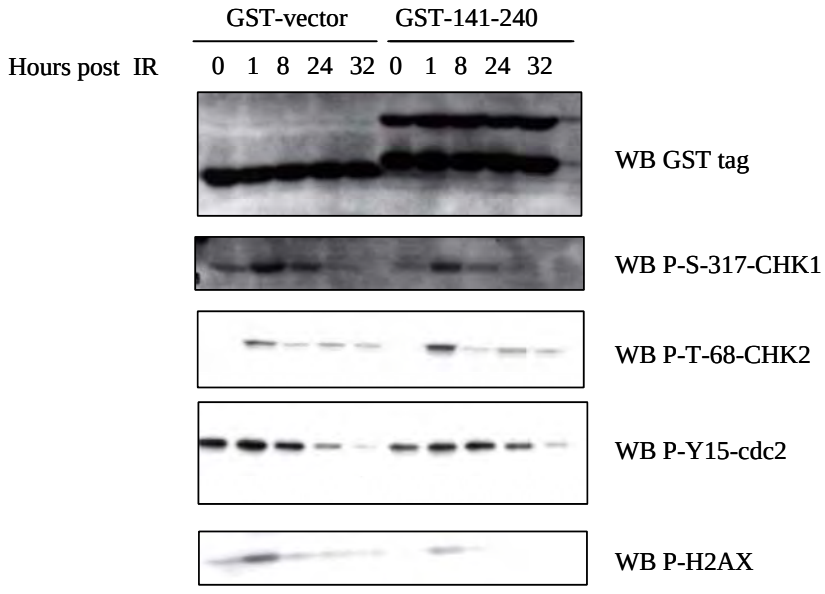

Fig. 5 Analysis of G2/M checkpoint recovery in MCF7 cell line, transfected with GST-vector or GST-141-240 BRCA1 construct. Western blots with the indicated antibodies are shown.

This makes harder exploring the effect of Filamin A combined with BRCA1 deficiency. To overcome this problem we took advantage of two reagents that we generated while investigating the interaction between BRCA1 and Filamin A. We compared the checkpoint recovery of A7 cell line (Filamin A positive) transfected with either GST-141-240 wild type fragment (which binds to Filamin A) or GST-141-240 Y179C mutant (which does not bind to Filamin A). For detailed results, please, refer to fig. 5 d of the paper "Identification of Filamin A as a BRCA1-interacting protein required for efficient DNA repair. 2010, Cell Cycle 2010; 9(7): 1-13, which is attached in the appendices of this report. Based on these results we concluded that:

1. The interaction between BRCA1 and Filamin A is specific because BRCA1 mutation Y179C found in patients with breast and ovarian cancer disrupts the interaction.
2. Filamin A participates in the BRCA1-dependent regulation of the DNA damage response.

IV. Reportable outcomes

1.Publications:

The DOD pre-doctoral fellowship gave me an opportunity to collaborate with other lab members and to participate as a co-author in several papers, which are attached. The DOD pre-doctoral fellowship also gave me an opportunity to publish a first author paper, which is attached. This paper was also featured in the cover of Cell Cycle journal (attached) and in a *News & Views* piece (attached).

1. De Ligio, J. T., **A. Velkova**, et al. (2009). "Can the status of the breast and ovarian cancer susceptibility gene 1 product (BRCA1) predict response to taxane-based cancer therapy?" Anticancer Agents Med Chem 9(5): 543-9.

2. Rios-Doria, J., **A. Velkova**, et al. (2009). "Ectopic expression of histone H2AX mutants reveals a role for its post-translational modifications." Cancer Biol Ther 8(5): 422-34.

3. **Velkova A,** Carvalho MA, Johnson JO, Tavtigian SV, Monteiro AN. Identification of Filamin A as a BRCA1-interacting protein required for efficient DNA repair. 2010, Cell Cycle 2010; 9(7): 1-13

2.Thesis defense:

Defended a doctoral dissertation for Ph.D. degree in Cancer Biology-May 16, 2011 for this and previous work.

3. Collaboration with other lab members

Projects-Role of BRCA1 in cancer treatment and the role of histone H2AX in chromosomal instability.

4. Meetings:

1. As part of my training I participated in Gordon Research Conference "Mammalian DNA repair"-February 8-13 2009 in Ventura, California. This conference had a significant impact on improving my knowledge not only in DNA repair but also in Breast cancer treatment.

2. As part of my training I participated in Gordon Research Conference "Mutagenesis" August 1-6 2010 in Waterville, ME. I presented a poster entitled "Identification of Filamin A as a BRCA1 interacting protein required for efficient DNA repair".

3. As part of my training I participated in the 5th Annual NIH Graduate Students Research Festival October 25-26, 2010, Bethesda, Maryland. I presented a poster entitled "The role of BRCA1 domains and motifs in tumor suppression". The purpose of the festival was to meet graduate students with NIH investigators with whom they will be interest to pursue post-doctoral training. The participation in the festival was competitive and restricted to only 200 graduate students from all over the USA. My DOD pre-doctoral fellowship was acknowledged. The abstract with which I participated in this event is attached in the supplementary section of these report.

4. Poster presentation "The Role of BRCA1 Domains and Motifs in Tumor Suppression" at the Era of Hope 2011 conference August 3-5, 2011, Orlando FL.

V. Bulleted list of key research and training accomplishments (Whole grant period):

- Cloning and expression of full length BRCA1 C61G mutant (tasks 1a and 1b)
- Optimization of BRCA1 full-length expression (WT or mutants) in several cell lines (task1c)
- Verifying the expression level of BRCA1 full-length (WT or mutants) in HCC1937 cell line (task1c)
- Optimization of colony forming assay after irradiation (task1d)
- Performing colony forming assay after irradiation (task1d)
- Performing early G2/M checkpoint assay (task 1e)
- Optimization of early G2/M checkpoint assay (task 1e)
- Optimization of Radio-Resistant DNA synthesis assay (task 1f)
- Performing Radio-Resistant DNA synthesis assay (task 1f)
- Optimization of spindle assembly checkpoint assay (task 1g)
- Performing spindle assembly checkpoint assay (task 1g)

- Performing dose response and time course analysis in M2, A7, HCT116, HCT116 chk2-/- cell lines (task 2a)
- Confirming dose response and time course analysis in MCF7 breast cancer cell line (task2b) Analysis of early G2/M arrest in MCF7 cells transfected with small fragment, containing BRCA1-motif 6.
- Performing G2/M checkpoint recovery assays in M2 cell line transfected with pCMV2 Flag-Filamin A construct and simultaneously with pCMV2 Flag-Filamin A and BRCA1 shRNA.

- **Review article** entitled "Can the status of the breast and ovarian cancer susceptibility gene 1 (BRCA1) predict response to taxane-based cancer therapy", Anticancer Agents Med Chem 9(5): 543-9 by De Ligio, J. T., **A. Velkova**, et al. (2009). " (*Appendix*)

- **Manuscript entitled** "Ectopic expression of histone H2AX mutants reveals a role for its post-translational modifications." Cancer Biol Ther 8(5): 422-34, by Rios-Doria, J., **A. Velkova**, et al. (2009). (*Appendix*)

- **Manuscript entitled** "Identification of Filamin A as a BRCA1-interacting protein required for efficient DNA repair", Cell Cycle 2010; 9(7): 1-13, 2010, by **Velkova A,** et al. This paper was also featured on the cover of Cell Cycle journal (attached) and in a *News & Views* piece (*Appendix*).

- **Abstract and poster presentation**: Gordon Research Conference "Mutagenesis" August 1-6, 2010 in Waterville, ME. I presented a poster entitled "Identification of Filamin A as a BRCA1 interacting protein required for efficient DNA repair".

- **Abstract and poster presentation** in the 5th Annual NIH Graduate Students Research Festival October 25-26, 2010, Bethesda, Maryland. (*Appendix*).

- **Defense of PhD thesis** on May 16th, 2011 for this and previous work.

Conclusion:

The purpose of this research is to classify *BRCA1* variants for which cancer association is not known (variants of uncertain significance, VUS). To approach this problem we hypothesized that poorly characterized but conserved domains in BRCA1 directly participate in its tumor suppression function. To test this hypothesis we choose a global approach analyzing several BRCA1 domains and point mutants in functions that have previously been attributed to BRCA1: long term survival after irradiation, early G2/M checkpoint, intra S phase checkpoint, and spindle assembly checkpoint. We analyzed all the BRCA1 mutants proposed in this application. Our analysis revealed that the coiled-coil domain of BRCA1 is important for the intra-S-phase checkpoint function of BRCA1. We also characterized two conserved motifs of BRCA1: Motif 6 (proposed in this application) and Motif 2 (as a new finding). In addition, we identified Filamin A, as an interacting partner of BRCA1 Motif 2 and Motif 6, which is required for efficient DNA repair. BRCA1 mutation, found in breast and ovarian cancer patients disrupts the binding between Filamin A and BRCA1. Cells, lacking Filmain A display a diminished ionizing radiation induced BRCA1 focus formation and a slow kinetics of Rad51 focus formation. Moreover, BRCA1/Filamin A complex might control end processing and proper checkpoint signaling in mammalian cells. The results obtained in this grant, will have a significant impact not only to understand BRCA1 role as a tumor suppressor in breast cancer but also to help patients that are carriers of BRCA1 mutation to make informed clinical decisions. In addition, our findings have implications for our understanding of the response to irradiation-induced DNA damage, which is a significant part of cancer treatment.

References:

1. Easton, D.F., et al., *Genetic linkage analysis in familial breast and ovarian cancer: results from 214 families. The Breast Cancer Linkage Consortium.* Am J Hum Genet, 1993. **52**(4): p. 678-701.
2. Miki, Y., et al., *A strong candidate for the breast and ovarian cancer susceptibility gene BRCA1.* Science, 1994. **266**(5182): p. 66-71.
3. Dapic, V., M.A. Carvalho, and A.N. Monteiro, *Breast cancer susceptibility and the DNA damage response.* Cancer Control, 2005. **12**(2): p. 127-36.
4. Narod, S.A. and W.D. Foulkes, *BRCA1 and BRCA2: 1994 and beyond.* Nat Rev Cancer, 2004. **4**(9): p. 665-76.
5. Joukov, V., et al., *The BRCA1/BARD1 heterodimer modulates ran-dependent mitotic spindle assembly.* Cell, 2006. **127**(3): p. 539-52.
6. Xu, B., S. Kim, and M.B. Kastan, *Involvement of Brca1 in S-phase and G(2)-phase checkpoints after ionizing irradiation.* Mol Cell Biol, 2001. **21**(10): p. 3445-50.
7. Moynahan, M.E., et al., *Brca1 controls homology-directed DNA repair.* Mol Cell, 1999. **4**(4): p. 511-8.
8. Hashizume, R., et al., *The RING heterodimer BRCA1-BARD1 is a ubiquitin ligase inactivated by a breast cancer-derived mutation.* J Biol Chem, 2001. **276**(18): p. 14537-40.
9. Williams, R.S. and J.N. Glover, *Structural consequences of a cancer-causing BRCA1-BRCT missense mutation.* J Biol Chem, 2003. **278**(4): p. 2630-5.
10. Xu, B., et al., *Two molecularly distinct G(2)/M checkpoints are induced by ionizing irradiation.* Mol Cell Biol, 2002. **22**(4): p. 1049-59.
11. Elstrodt, F., et al., *BRCA1 mutation analysis of 41 human breast cancer cell lines reveals three new deleterious mutants.* Cancer Res, 2006. **66**(1): p. 41-5.
12. Deng, C.X., *BRCA1: cell cycle checkpoint, genetic instability, DNA damage response and cancer evolution.* Nucleic Acids Res, 2006. **34**(5): p. 1416-26.
13. Lee, J.S., et al., *hCds1-mediated phosphorylation of BRCA1 regulates the DNA damage response.* Nature, 2000. **404**(6774): p. 201-4.

Cell Cycle 9:7, 1421-1433; April 1, 2010; © 2010 Landes Bioscience

Identification of filamin A as a BRCA1-interacting protein required for efficient DNA repair

Aneliya Velkova,[1,2] Marcelo A. Carvalho,[1,†] Joseph O. Johnson,[3] Sean V. Tavtigian[4] and Alvaro N.A. Monteiro[1,*]

[1]Risk Assessment, Detection and Intervention Program; and [3]Analytic Microscopy Core; H. Lee Moffitt Cancer Center & Research Institute; Tampa, FL USA; [2]University of South Florida Cancer Biology PhD Program; Tampa, FL USA; [4]Department of Oncological Sciences; Huntsman Cancer Institute; University of Utah, Salt Lake City, UT USA

[†]Current address: Instituto Federal do Rio de Janeiro; Rio de Janeiro, RJ Brazil

Key words: BRCA1, filamin A, DNA-PK, non-homologous end joining, DNA damage, DNA repair

Abbreviations: ATM, ataxia-telangiectasia mutated; ATR, ATM and Rad3-related; ATRIP, ATR-interacting protein; DDR, DNA damage response; DMEM, dulbecco's modified eagle medium; DNA-PKcs, DNA protein kinase catalytic subunit; DSB, double stranded breaks; FLNA, filamin A; γ-H2AX, histone H2AX phosphorylated at serine 139; GFP, green fluorescent protein; GST, glutathione-sulfo-transferase; GT, glutathione; IR, ionizing radiation; MRN, Mre11/Rad50/NBS1 complex; NHEJ, non-homologous end joining; PI3K, phosphoinositide-3-kinase; RPA, replication protein A; ssDNA, single stranded DNA

The product of the breast and ovarian cancer susceptibility gene BRCA1 has been implicated in several aspects of the DNA damage response but its biochemical function in these processes has remained elusive. In order to probe BRCA1 function we conducted a yeast two-hybrid screening to identify interacting partners to a conserved motif (Motif 6) in the central region of BRCA1. Here we report the identification of the actin-binding protein Filamin A (FLNA) as a BRCA1 partner and demonstrate that FLNA is required for efficient regulation of early stages of DNA repair processes. Cells lacking FLNA display a diminished BRCA1 IR-induced focus formation and a delayed kinetics of Rad51 focus formation. In addition, our data also demonstrate that FLNA is required to stabilize the interaction between components of the DNA-PK holoenzyme, DNA-PKcs and Ku86 in a BRCA1-independent fashion. Our data is consistent with a model in which absence of FLNA compromises homologous recombination and non-homologous end joining. Our findings have implications for the response to radiation-induced DNA damage.

Introduction

The presence of DNA damage triggers a series of events collectively known as the DNA Damage Response (DDR) pathway.[1,2] Its biological role is to promote efficient DNA repair and to coordinate this activity with cell cycle progression. Injuries to DNA primarily activate three PI3K related kinases ATM, ATR and DNA-PK which are recruited to DNA breaks by the Mre11/Rad50/NBS1 complex, ATRIP and Ku86, respectively.[3] This process is guided by different DNA structures: ATM and DNA-PK are activated by double stranded breaks (DBS) and ATR is activated by Replication Protein A (RPA) coated single stranded DNA (ssDNA).[1]

Two main mechanisms exist to promote DSB repair. The error-prone non-homologous end joining (NHEJ) is functional in all phases of the cell cycle, while the error-free homologous recombination (HR) only functions in S and G_2 phases.[1,2] HR is initiated by ssDNA resulting from resection of DNA ends at the DSB.[1] RPA then binds ssDNA with very high affinity and is visualized as nuclear foci detected by immunofluorescence.[4] The RPA-coated ssDNA is the substrate for RAD51 recombinase, which is loaded by BRCA2 and mediates the DNA pairing during HR.[1,5] RAD51 co-localizes with the tumor suppressors BRCA1 and BRCA2 in radiation-induced nuclear foci.[6,7] BRCA1 and BRCA2 are part of a complex that controls RAD51 function and the efficiency of HR.[5,8]

Germline mutations in *BRCA1* lead to increased predisposition to breast and ovarian cancer.[9,10] Cloning of *BRCA1* in 1994 made possible the genetic testing of individuals with strong family history of breast cancer and set the stage for an intensive effort to understand its biological functions and the nature of its tumor suppressive activities.[11,12] However, 15 years later it is still not clear which of its many activities can be related directly to its role as tumor suppressor.

BRCA1 has been implicated in several aspects of the DNA damage response (DDR). Its role in the DDR seems to span a wide range of activities from damage signaling to participation in repair and the coordination of cell cycle checkpoints.[1,13-15] In particular, BRCA1 has been implicated in HR,[16] microhomology-mediated[17] and NHEJ DNA repair.[18,19]

*Correspondence to: Alvaro N.A. Monteiro; Email: alvaro.monteiro@moffitt.org
Submitted: 12/10/09; Revised: 01/08/10; Accepted: 01/19/10
Previously published online: www.landesbioscience.com/journals/cc/article/11256

Our laboratory has focused on a systematic analysis of domains and motifs in BRCA1 as a means to understand its biochemical functions.[20] Here we analyzed a conserved region, called Motif 6, spanning amino acids 845–869 coded by BRCA1's large exon 11.[21,22] Using a yeast two hybrid screen we identified the actin-binding protein Filamin A (FLNA) as an interacting partner of BRCA1. Interestingly, FLNA has been shown to interact with BRCA2 and to participate in the DDR.[23-25] Cells lacking FLNA exhibit prolonged checkpoint activation leading to accumulation of cells in G_2/M after ionizing radiation.[23]

We show that BRCA1 and FLNA interact in mammalian cells and this interaction is mediated by Motif 6 and by another uncharacterized region in BRCA1 N-terminus called Motif 2.[21] Binding to BRCA1 is mediated by the C-terminus of FLNA, a region that includes its dimerization domain. Introduction of a BRCA1 missense variant found in individuals with family history of breast cancer abrogates the interaction. Lack of FLNA leads to a broad defect in DNA repair with accumulation of ssDNA combined with the hyperactivation of ATM and ATR-mediated signaling. We show that this phenotype is due to a combined failure of Ku86 and DNA-PKcs to form stable complexes, and to defects in BRCA1 and Rad51 focus formation implicating FLNA in the control of DNA repair.

Results

BRCA1 motif 6 interacts with filamin A. In order to identify interactors to the conserved Motif 6 of BRCA1 spanning amino acid residues 845–869 (**Suppl. Fig. 1A**) we performed a yeast two-hybrid screening against a human mammary gland cDNA library. Two overlapping clones coding for human Filamin A (FLNA; OMIM # 300017), spanning amino acid residues 2443–2647 and 2477–2647 (**Suppl. Fig. 1B**), were identified. This region includes repeat 23, the hinge region, and repeat 24 in the C-terminus FLNA (**Suppl. Fig. 1B**).[26] We mapped the minimal region of FLNA that interacts with BRCA1 Motif 6 by testing binding of a series of FLNA deletion mutants (**Suppl. Fig. 1B**). Only the fragment aa 2477–2647 was able to bind BRCA1 Motif 6 (**Suppl. Fig. 1B**).

Next, we tested whether endogenous FLNA interacted with endogenous BRCA1 in mammalian cells. Immunoprecipitation using a specific monoclonal antibody against BRCA1 pulled down FLNA in HeLa and HCT116 cells (**Fig. 1A**). In addition, immunoprecipitation using an antibody against FLNA was able to pull down BRCA1 (**Fig. 1A**). Thus, BRCA1 and FLNA interact in vivo and the interaction is mediated by the C-terminus of FLNA.

Because FLNA and BRCA1 have been demonstrated to be primarily cytoplasmic and nuclear, respectively, we biochemically fractionated HCT116 cells to determine in which subcellular compartment the interaction occurs (**Suppl. Fig. 1C**). We found that FLNA is expressed in the nucleus and cytoplasm and BRCA1 can be co-immunoprecipitated by FLNA in the nuclear fraction (**Suppl. Fig. 1C**). We also determined that the interaction is direct as bacterially expressed GST-tagged BRCA1 (aa 141–302) can pull down bacterially expressed His-tagged FLNA C-terminus (**Suppl. Fig. 1D**).

BRCA1 binding to FLNA is mediated primarily by BRCA1 motif 2. In the course of our yeast experiments we noted that the interaction between Motif 6 and FLNA was relatively weak (data not shown). Thus, we hypothesized that other regions in BRCA1 might contribute to binding. We co-expressed in-frame fusions of GST to deletion fragments of BRCA1 and a FLAG-tagged FLNA fragment (aa 2477–2647) in 293FT cells (**Fig. 1B**) to assess each region's contribution to binding.

We immunoprecipitated FLAG-FLNA using α-FLAG agarose beads and the eluate with FLAG-peptide was separated by SDS-PAGE. Western blot against FLNA and BRCA1 confirmed that FLAG-FLNA was properly folded and interacted with endogenous BRCA1, respectively (**Fig. 1C**, left). Western blot against GST revealed interaction of FLNA with different fragments of BRCA1 under low stringency (**Fig. 1C**, left). Interaction with fragments 1 (aa 1–324), 3 (aa 502–802) and 4 (aa 758–1064) was detected even under high stringency conditions (**Fig. 1C**, right). Reverse pull-downs of endogenous FLNA using GT-beads confirmed that the interaction is mediated by BRCA1 fragments 1, 3 and 4 (**Fig. 1D**). In both experiments, BRCA1 fragment 1 showed the strongest interaction (**Fig. 1C and D**).

Fragment 1 (aa 1–324) includes the RING finger (aa 1–101)[11] and nuclear export signals (aa 22–30 and aa 81–99).[27,28] To determine whether the interaction was mediated by these motifs we used deletion mutants of BRCA1 fragment 1 (**Fig. 2A**). Initially, we identified BRCA1 residues 141–240 as the interacting region to FLNA (aa 2477–2647) (**Fig. 2A**). Further mapping identified residues 160–190 as the minimal region required for binding (**Fig. 2B**). This region, called Motif 2, had been previously identified as conserved motif in *BRCA1* orthologs.[21,22]

To assess whether BRCA1 and FLNA interaction might contribute to breast cancer we searched the Breast Cancer Information Core database (research.nhgri.nih.gov/bic/) for variants in this region. Variant Y179C is a frequent missense change recorded in the database (BIC Database). Introduction of BRCA1 Y179C mutant significantly reduced BRCA1 interaction to FLAG-FLNA aa 2477–2647 and to endogenous FLNA (**Fig. 2C**) further demonstrating the specificity of the interaction. Because other regions in BRCA1 besides Motif 2 also contributed to the binding we investigated whether the Y179C mutation would disrupt binding to FLNA in the context of full length BRCA1. Introduction of the Y179C mutation significantly reduced the interaction in the full length context as compared to wild type BRCA1 (**Fig. 2C**, right). In summary, these experiments demonstrate that Motif 2 primarily mediates the interaction to FLNA. Taken together these data raised the possibility that lack of FLNA might impair BRCA1 foci formation after DNA damage. Thus, the following experiments were directed at assessing the role of the interaction in the DNA damage response.

FLNA-null cells are deficient in DSB repair. To further characterize the functional significance of FLNA/BRCA1 interaction we obtained the M2 melanoma cell line which lacks FLNA and its counterpart A7 which was obtained by reconstituting M2 cells with full length FLNA cDNA.[29] First, we assessed the kinetics of double strand break (DSB) repair after ionizing radiation (IR). We irradiated or mock treated the $FLNA^-$ and $FLNA^+$ cell lines and

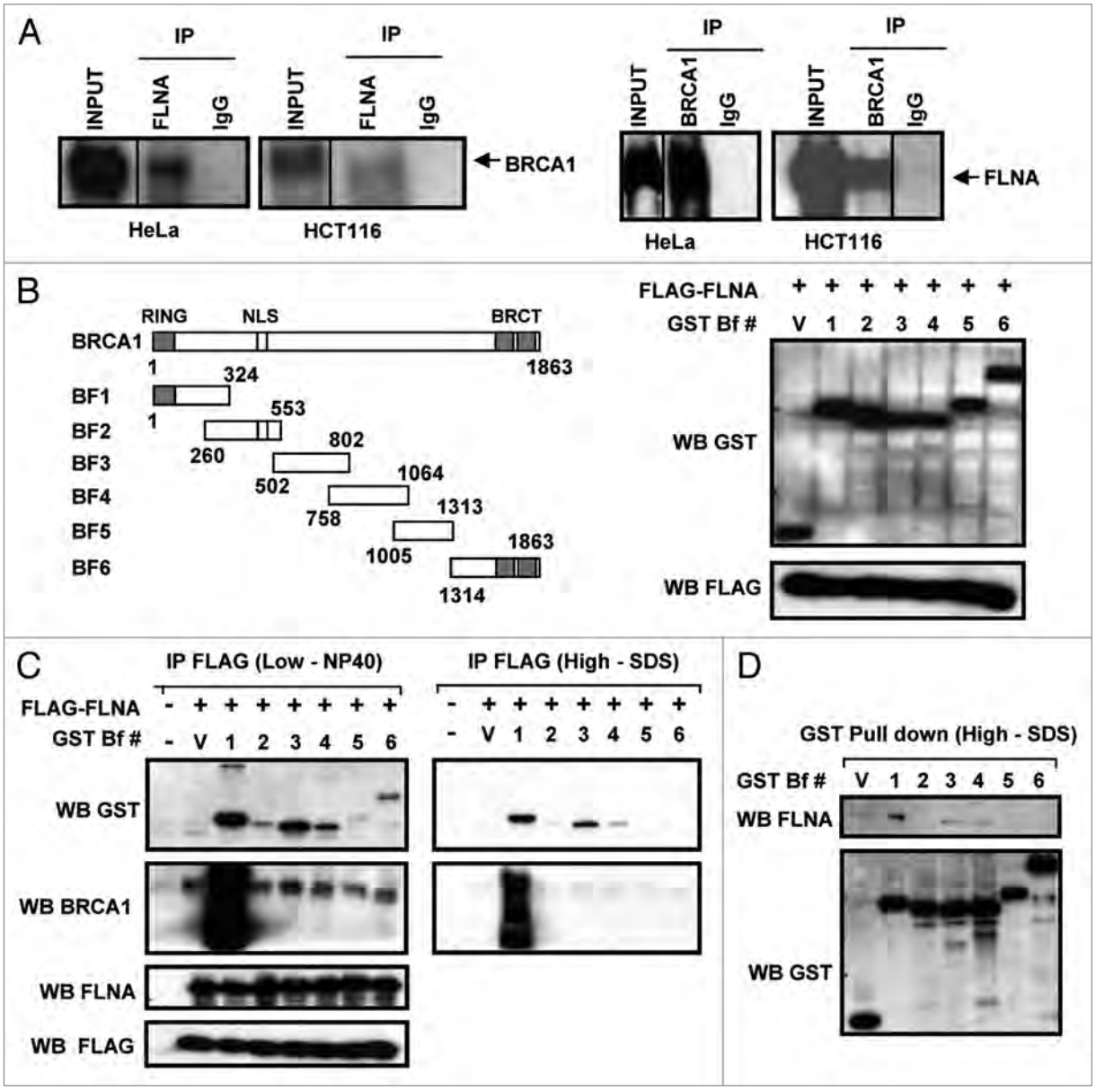

Figure 1. Interaction of Filamin A and BRCA1 in mammalian cells. (A) Left, co-immunoprecipitation of endogenous BRCA1 with FLNA in HeLa and HCT116 cells showing interaction of endogenous BRCA1 and FLNA. Right, reverse reaction showing co-immunoprecipitation of endogenous FLNA with BRCA1. Vertical lines indicate where lanes were digitally removed. Figures are not a composite of lanes from two different blots but from the same blot. (B) Left, diagram of deletion constructs used to map the BRCA1 interaction site to FLNA. RING, RING finger domain; NLS, nuclear localization signals; BRCT, BRCA1 C-terminal domains. Right, co-expression of GST-fragments of BRCA1 and FLAG-FLNA (aa 2477–2647) in 293FT cells. Lower molecular weight band obtained in the empty vector (V) transfection corresponds to GST. (C) Co-immunoprecipitation of BRCA1 fragments (WB GST), endogenous BRCA1 (WB BRCA1) with FLAG-FLNA (aa 2477–2647) under low (left panel) and high (right panel) stringency conditions. Note that endogenous FLNA is also immunoprecipitated by FLAG-FLNA (aa 2477–2647) confirming it is in the native conformation (WB FLNA). Strong reactivity shown for GST BF1 is due to recognition of the GST-BRCA1 fragment that contains the epitope for the antibody. (D) GST-pull down experiments show that GST-BRCA1 fragments 1, 3 and 4 can precipitate endogenous FLNA (WB FLNA).

collected cells at several time points after IR. We monitored the presence of DSB with an antibody against histone H2AX phosphorylated at Serine 139 (called γ-H2AX), a marker for DSBs.[30] Whereas the FLNA$^+$ cell line efficiently repaired DSBs and by 8 h after IR there was no detectable γ-H2AX (**Fig. 3A**), FLNA$^-$ cells had a sustained high level of γ-H2AX for up to 32 h after IR. We confirmed this observation using Comet assays (**Fig. 3B**).

FLNA deficiency does not cause a defect in sensing DNA damage. Next, we assessed whether cells lacking FLNA had a compromised DNA damage signaling. Thus, we tested whether ATM and ATR were properly activated upon DNA damage. Phosphorylation of ATM S1981 was not compromised in FLNA$^-$ cells (**Fig. 3C**, Top). Likewise, phosphorylation of CHK2 T68 and CHK1 S317, markers of ATM and ATR activation, respectively,

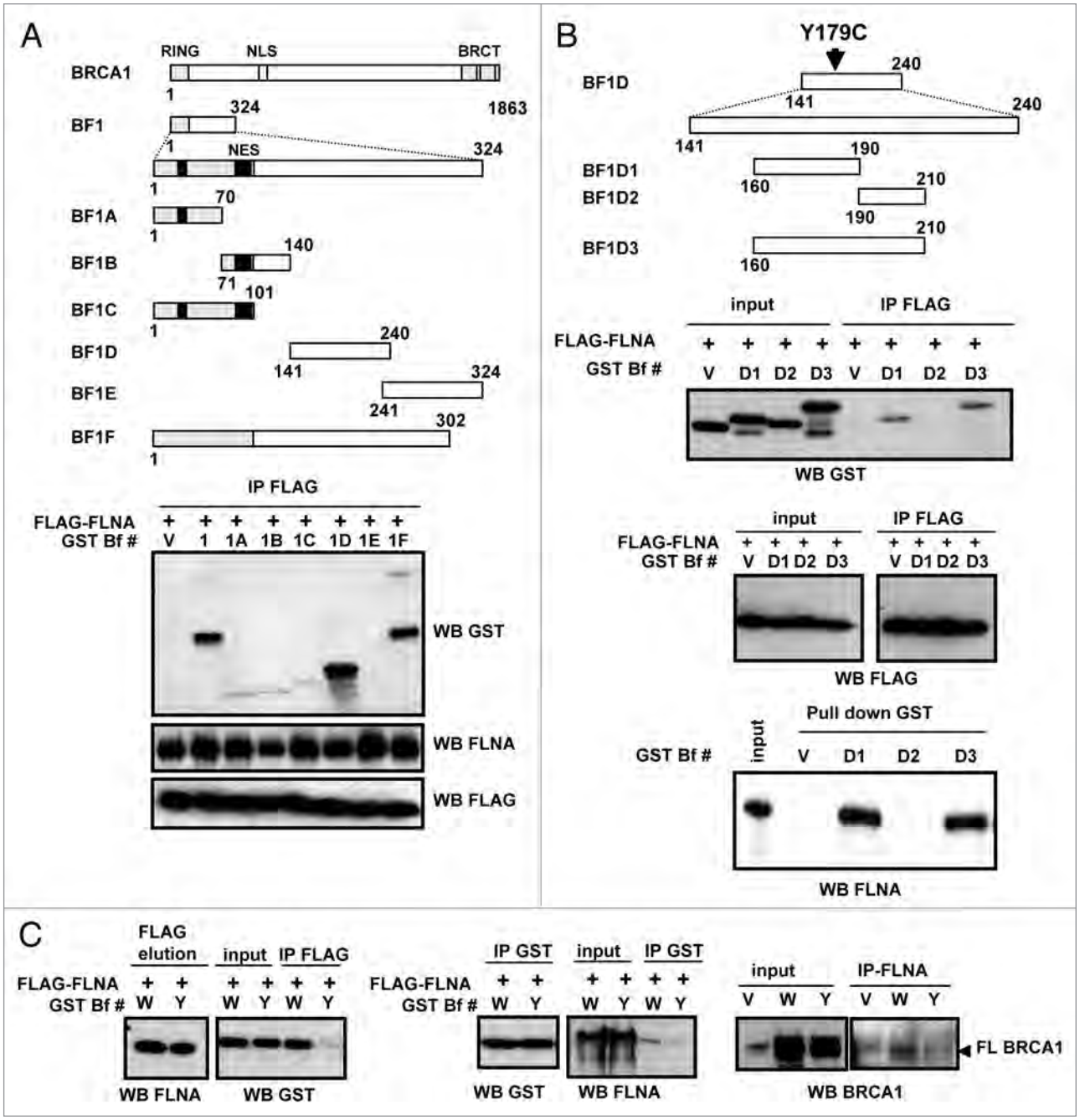

Figure 2. Fine mapping of the interaction regions in BRCA1. (A) Upper, diagram of deletion constructs used to map the interaction site to FLNA. NES, nuclear export sequence (black boxes). Lower, FLAG-FLNA (aa 2477–2647) interacts strongly with GST-BRCA1 fragments BF1 (aa 1–324), BF1D (aa 141–240) and BF1F (aa 1–302). (B) First, diagram of deletion constructs of fragment aa 141–240 used to map the interaction site to FLNA. The location of the missense variant Y179C is indicated. Second, FLAG-FLNA (aa 2477–2647) co-immunoprecipitates with GST-BRCA1 fragments BF1D1 (aa 160–190) and BF1D3 (aa 160–210). V, GST; D1, GST-BRCA1 fragment BF1D1 (aa 160–190); D2, GST-BRCA1 fragment BF1D2 (aa 190–210); D3, GST-BRCA1 fragments BF1D3 (aa 160–210). Third, control for expression levels. Fourth, GST-BRCA1 fragments BF1D1 (aa 160–190) and BF1D3 (aa 160–210) can pull down endogenous FLNA. (C) Introduction of BRCA1 Y179C mutation significantly reduces BRCA1 interaction to FLAG-FLNA aa 2477–2647 (Left) and to endogenous FLNA (Middle). W, wild type GST-BRCA1 fragment BF1D (aa 141–240); Y, GST-BRCA1 fragment BF1D with Y179C mutation. Right, Introduction of BRCA1 Y179C mutation into a full length BRCA1 context significantly reduces interaction to endogenous FLNA. W, wild type full length BRCA1; Y, full length BRCA1 carrying a Y179C mutation.

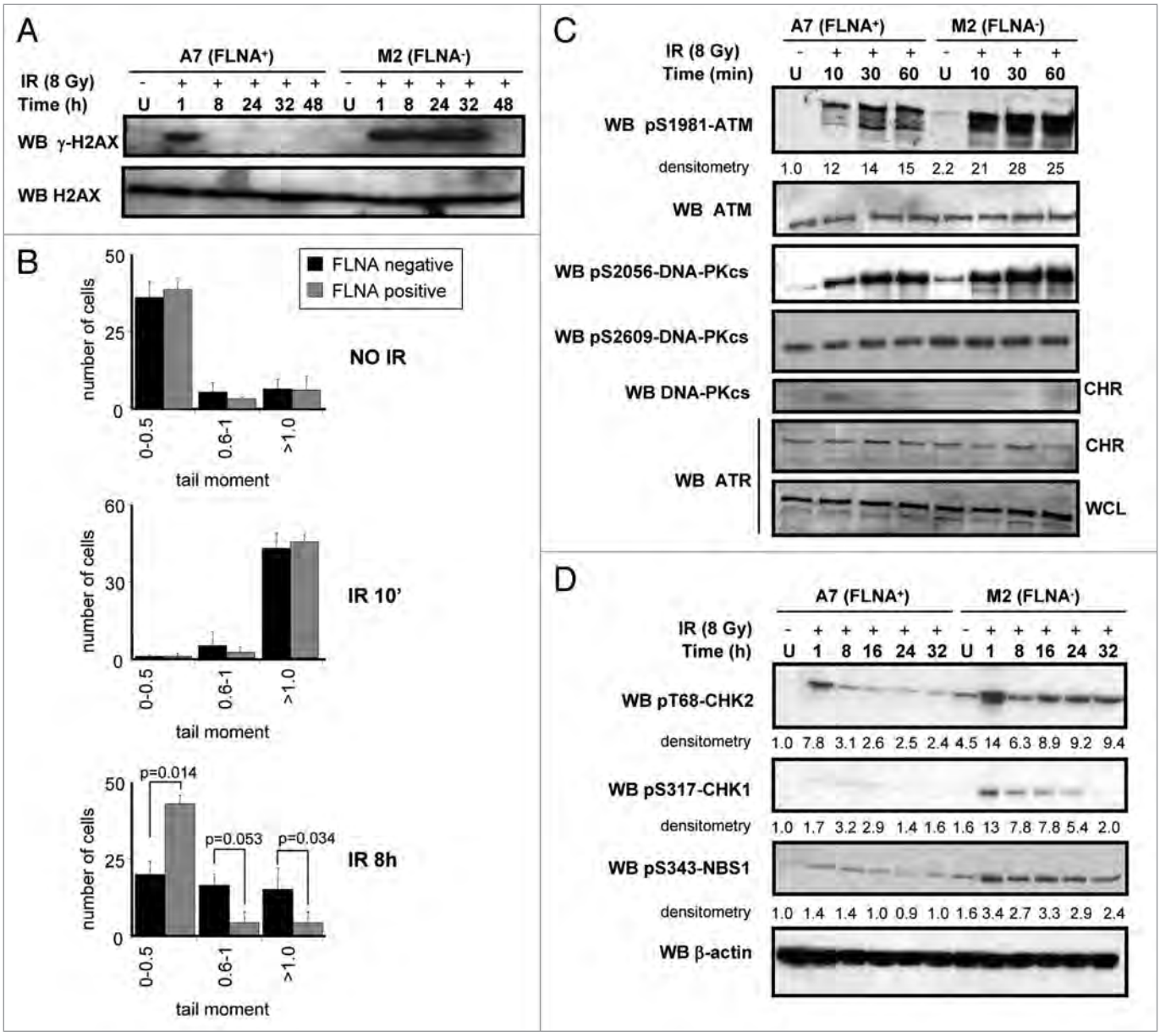

Figure 3. FLNA-null cells are deficient in repair but show no impairment in activating the DNA damage response. (A) FLNA$^+$ (A7) and FLNA$^-$ (M2) cells were irradiated with 8 Gy or mock-treated (U) and harvested at the indicated time points. While FLNA$^+$ cells repair most of the DSBs (as measured by γ-H2AX) by 8 h, FLNA$^-$ cells show significant unrepaired DSBs even after 32 h post-IR (Top). Bottom, shows total levels of H2AX as a loading control. (B) FLNA$^+$ (A7) and FLNA$^-$ (M2) cells were irradiated with 8 Gy or mock-treated (NO IR) and harvested at the indicated time points and comet assays were performed under neutral conditions. A two-tailed Student's t test was performed and p values are shown for statistically significant differences. (C) Top two, ATM activation as measured by phosphorylation of S1981 is not compromised in FLNA$^-$ cells. Blot for total ATM is used as a loading control. Note significantly higher levels of pS1981-ATM in FLNA$^-$ cells. Middle three, no significant difference was observed in levels of DNA-PKcs S2056 or S2609 phosphorylation but recruitment of DNA-PKcs to chromatin is defective in FLNA$^-$ cells. Bottom two, ATR presence in chromatin (CHR) is shown. Blot for ATR levels in whole cell lysates is used a loading control. (D) CHK2, CHK1 and NBS1 activation as measured by pT68-CHK2, pS317-CHK1 and pS343-NBS1, respectively is not compromised in FLNA$^-$ cells. Note consistently higher levels of pT68-CHK2, pS317-CHK1 and pS343-NBS1 in FLNA$^-$ cells. β-actin is used a loading control.

did not show a defect (**Fig. 3D**). Intriguingly, we consistently observed higher levels of phosphorylation of ATM, CHK2 and CHK1 in cells lacking FLNA (**Fig. 3C and D**) indicating an upregulation of ATM and ATR signaling. These results confirmed previous data by Meng et al.[23] showing a sustained activation of CHK2 and CHK1 in FLNA-deficient cells following damage.

FLNA deficiency impairs BRCA1 and Rad51 foci formation. To determine whether the deficiency in repair was due to defective recruitment of factors required for the DDR we performed immunofluorescence analysis in non-irradiated or irradiated cells at 1 and 24 h after IR. Accumulation of γ-H2AX and pS343-NBS1, early markers of DNA damage, was comparable

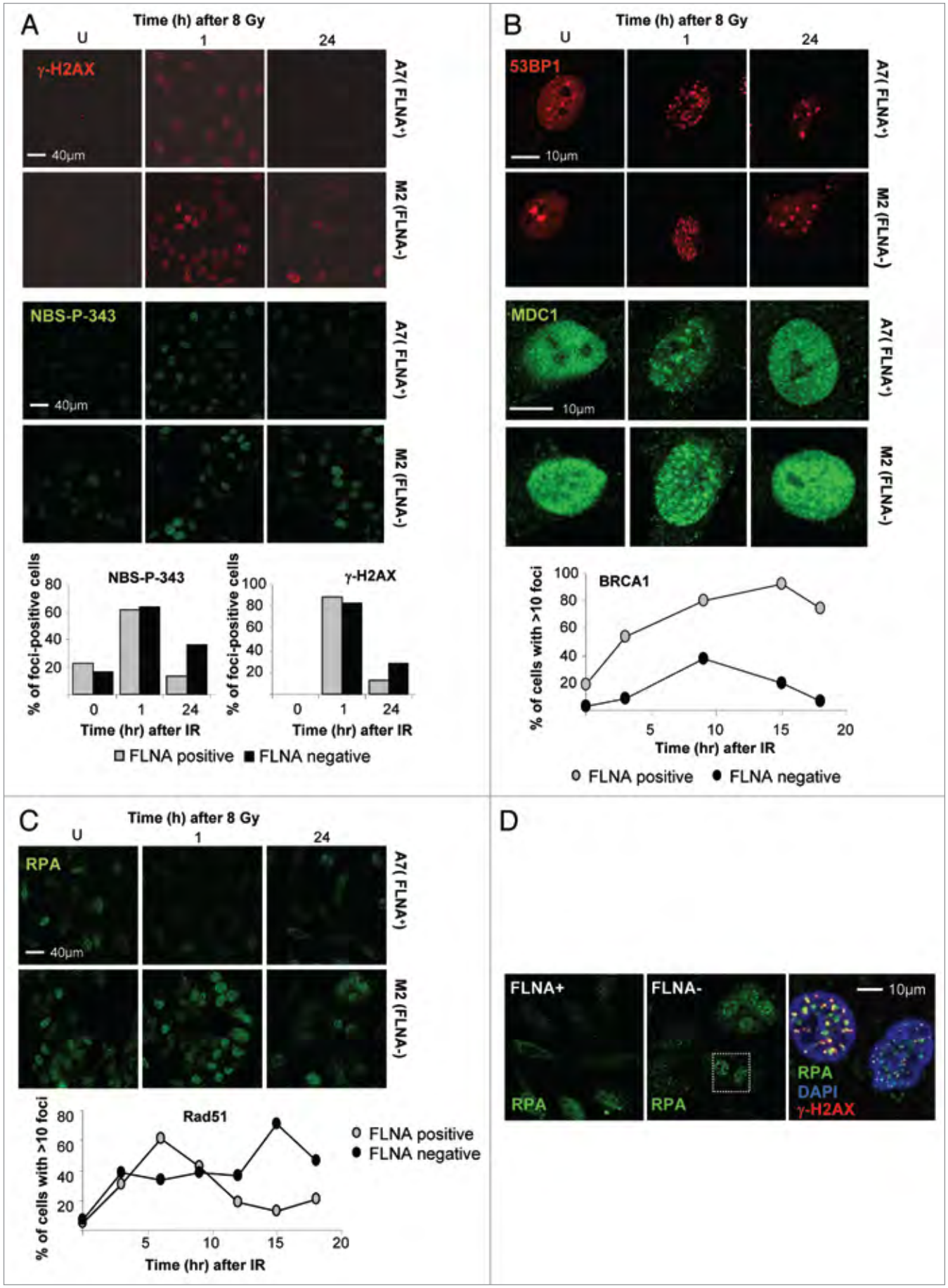
A
Time (h) after 8 Gy
U
1
24
γ-H2AX
40μm
A7(FLNA+)
M2 (FLNA-)
NBS-P-343
40μm
A7(FLNA+)
M2 (FLNA-)
NBS-P-343
% of foci-positive cells
80
60
40
20
0
1
24
Time (hr) after IR
γ-H2AX
% of foci-positive cells
100
80
60
40
20
0
1
24
Time (hr) after IR
FLNA positive
FLNA negative
B
Time (h) after 8 Gy
U
1
24
53BP1
10μm
A7(FLNA+)
M2 (FLNA-)
MDC1
10μm
A7(FLNA+)
M2 (FLNA-)
BRCA1
% of cells with >10 foci
100
80
60
40
20
5
10
15
20
Time (hr) after IR
FLNA positive
FLNA negative
C
Time (h) after 8 Gy
U
1
24
RPA
40μm
A7(FLNA+)
M2 (FLNA-)
Rad51
% of cells with >10 foci
80
60
40
20
5
10
15
20
Time (hr) after IR
FLNA positive
FLNA negative
D
FLNA+
RPA
FLNA-
RPA
10μm
RPA
DAPI
γ-H2AX

Figure 4 (See opposite page). Recruitment of DNA damage response factors to IR-induced foci. (A) Early markers of DNA damage γ-H2AX (red) and phosphoserine 343 NBS1 (green) form foci irrespective of FLNA status. Note maintenance of foci after 24 h only in FLNA$^-$ cells. Lower, show quantification of foci-positive cells (≥20 foci). (B) Recruitment of DNA damage response mediator proteins 53BP1 (red, top) and MDC1 (green, middle) was also comparable at early time points. BRCA1 foci formation was compromised in FLNA-deficient cells (lower). (C) Recruitment of repair factor p34 RPA (green, top) did not show any difference between the cell lines at the early time points. FLNA-deficient cells displayed a delayed kinetics of Rad51 foci formation (bottom). In (A–C) representative results from two independent experiments are shown. In each experiment one slide was scored per time point with at least 50 (A) or 100 (B and C) cells scored per slide. Mock-treated cells are indicated by (U). (D) FLNA-deficient cells present with large chromatin-bound RPA foci at 24 h after IR. Higher magnification of FLNA$^+$ and FLNA$^-$ cells after 24 h post-IR. Left, shows FLNA$^+$ cells stained for RPA (green). Middle, shows FLNA$^-$ cells stained for RPA (green). Note that nuclear foci are significantly larger than in FLNA$^+$ cells. Right, shows a blow up of the inset (white square in middle) with staining for DAPI (blue), RPA (green) and γ-H2AX (red).

in both cell lines at 1 h (**Fig. 4A**). In order to determine if there were small differences we quantified foci-positive cells (**Fig. 4A**, lower). Results were comparable in both cell lines at 0 and 1 hr after IR, but FLNA-negative cells showed increased number of foci-positive cells after 24 hr. Likewise, recruitment of mediator proteins MDC1, 53BP1, was also comparable at 1 h (**Fig. 4B**). Finally, repair factor RPA did not show any difference between the cell lines at 1 h (**Fig. 4C**). Consistent with our western blot results (**Fig. 3**) where we detected abnormally high levels of γ-H2AX, pT68-CHK2 and pS317-CHK1 at 24 h, we detected persistent foci of γ-H2AX, pS343-NBS1 and RPA at 24 h after irradiation only in FLNA-deficient cells (**Fig. 4A–C**). Thus, the repair defect in FLNA-deficient cells was not due to a failure to initiate the DNA damage response.

Next, we investigated the ability of BRCA1 and Rad51 to form IR-induced foci. A detailed analysis showed that FLNA-deficient cells are unable to efficiently form BRCA1 IR-induced foci as compared to FLNA-proficient cells (**Fig. 4B** and bottom). Although Rad51 displayed a comparable initial response at 3 h after IR, it failed to mount a response comparable to FLNA-proficient cells at 6 h after IR. Rad51 presented a delayed kinetics of foci formation with a peak at 15 h in FLNA-deficient cells (**Fig. 4C** and bottom). Taken together these data suggest that the compromised repair capacity in FLNA-deficient cells may be, at least partially, mechanistically tied to inefficient HR.

Lack of FLNA leads to accumulation of ssDNA after DNA damage. During our analysis we noted that RPA foci in FLNA-deficient cells were not only persistent 24 h after damage but were also significantly larger (**Fig. 4D**). To determine whether those foci were associated with chromatin we pre-extracted cells with Triton X100 before fixation. This method has been successfully used to detect only the fraction of RPA tightly bound to chromatin.[31] Interestingly, FLNA-deficient cells accumulate large chromatin-bound RPA foci whereas FLNA$^+$ cells present fewer and smaller chromatin-bound RPA foci at 24 h after IR (**Fig. 4D**). Whereas most FLNA$^+$ cells have recovered from G_2/M arrest and represent an asynchronous population at 24 h, most FLNA$^-$ cells remain arrested in G_2/M at 24 h after IR.[23] Thus, these large tracts of ssDNA found in FLNA$^-$ cells are unlikely to be due to replication foci.

Expression of BRCA1-interacting fragment of FLNA or FLNA-interaction fragment of BRCA1 phenocopies loss of FLNA. To gain more insight of the mechanism by which FLNA participates in DNA repair we transfected FLNA$^+$ and FLNA$^-$ cell lines with flag-tagged Filamin A aa 2477–2647 construct (BRCA1-interacting fragment). For the sake of simplicity we will refer to this FLNA BRCA1-interacting fragment as FLNA-Bf. At 24 h post transfection we irradiated cells with 8 Gy IR and collected samples at different time points. Transfection of FLNA-Bf did not lead to checkpoint recovery in FLNA$^-$ cells as measured by phosphorylation of CDC2 Y15 (**Fig. 5A**). Interestingly, transfection of the same fragment in FLNA$^+$ cells led to a similar phenotype as that found for FLNA$^-$ cells as shown by phosphorylation of CDC2 Y15 and H2AX S139 (**Fig. 5B**). We also confirmed that expression of FLNA-Bf acts in a dominant negative fashion in a stable transfection context (**Fig. 5C**). We generated HCT116 cells stably expressing GFP-FLNA-Bf or GFP alone that were mock-treated and irradiated. Cells expressing GFP-FLNA-Bf retained high levels of phosphorylated H2AX up to 32 h after damage while cells expressing GFP alone showed levels returning to unirradiated levels at 8 h after damage (**Fig. 5C**).

Next we asked whether expression of a GST-tagged BRCA1 FLNA-interacting fragment (BRCA1-Ff) could also lead to a dominant negative phenotype (**Fig. 5D**). In order to verify the specificity of the interaction we transfected a mutated BRCA1-Ff carrying the Y179C mutation and determined whether it lead to a dominant negative phenotype. Introduction of the Y179C mutation (**Fig. 2C**) significantly reduced the BRCA1-FLNA interaction. The wild type BRCA1-FLNA-Ff led to increased and sustained phosphorylation of CDC2 Y15 and H2AX (**Fig. 5D**) while the BRCA1-Ff Y179C (**Fig. 5D**) displayed a dominant negative effect that is intermediate between vector control (**Fig. 5B**) and the wild type construct (BRCA1-Ff; **Fig. 5D**). This intermediate effect could be due to the residual binding of BRCA1-Y179C mutant to FLNA. Alternatively, this could also be due to the inability of the mutant to disrupt the binding of FLNA to other regions of endogenous BRCA1 that participate in the interaction (**Fig. 1C and D**).

FLNA is required for efficient interactions between DNA-PKcs and Ku86. Our previous experiments demonstrated that FLNA$^-$ cells displayed defective DNA repair, showed signs of compromised HR, and accumulated large tracts of ssDNA. Because mammalian cells also repair DSBs using non homologous end joining (NHEJ) we hypothesized that lack of FLNA also had an impact on the NHEJ pathway.

First, we tested whether FLAG-FLNA aa 2477–2647 interacted with NHEJ factors. FLAG-FLNA aa 2477–2647 immunoprecipitated DNA-PKcs in 293FT cells independent of DNA damage (**Fig. 6A**). To determine whether FLNA was required for the stability of the Ku86/DNA-PKcs complex we performed immunoprecipitation experiments in FLNA$^+$ and FLNA$^-$ cell lines in the presence or absence of irradiation (**Fig. 6B**). Interestingly,

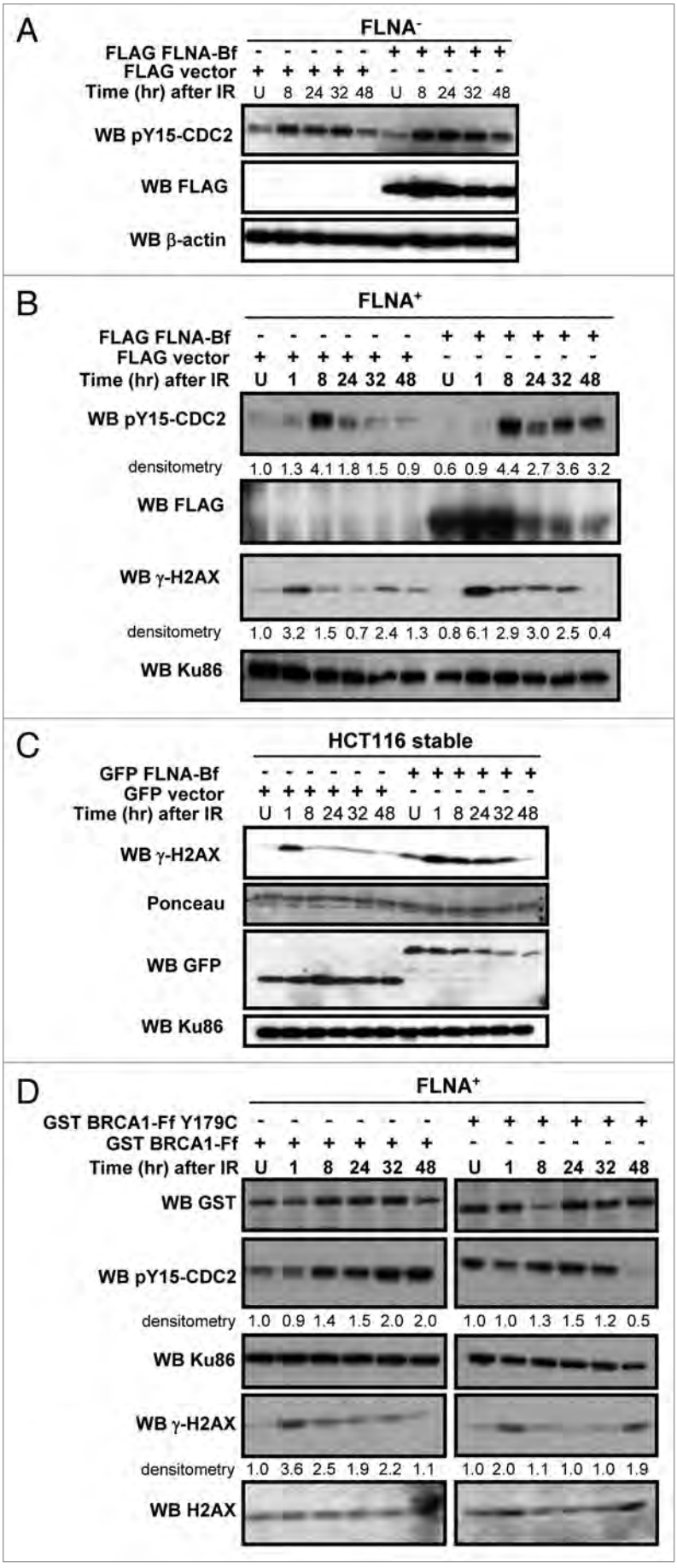

Figure 5. Expression of BRCA1-interacting fragment of FLNA or FLNA-interaction fragment of BRCA1 phenocopies loss of FLNA. (A) FLNA$^-$ cells were transfected with an empty FLAG vector or a FLAG FLNA-Bf constructs. Cells were mock-treated (U) or treated with 8 Gy IR and cells were collected at different time points. Expression of FLAG FLNA-Bf was unable to reverse the recovery defect. (B) FLNA$^+$ cells were transfected with empty FLAG vector or a FLAG FLNA-Bf constructs. Cells were mock-treated (U) or treated with 8 Gy IR and cells were collected at different time points. Cells expressing of FLAG FLNA-Bf displayed a phenotype similar to FLNA$^-$ cells. (C) HCT166 cells stably expressing FLAG FLNA-Bf displayed a phenotype similar to FLNA$^-$ cells. (D) FLNA$^+$ cells were transfected with a GST BRCA1-Ff or a GST BRCA1-Ff Y179C. Cells were mock-treated (U) or treated with 8 Gy IR and cells were collected at different time points. Only cells expressing of GST BRCA1-Ff but not GST BRCA1-Ff Y179C displayed a phenotype similar to FLNA$^-$ cells, confirming that the effect is specific.

in FLNA$^-$ cells Ku86 and DNA-PKcs complex formation was compromised in IR-treated and untreated cells (**Fig. 6B**).

Next we tested whether FLNA was required for Ku86 loading onto chromatin after DNA damage. Ku86 was efficiently recruited to chromatin upon DNA damage in the presence and absence of FLNA (**Fig. 6C**) while we detected DNA-PKcs in chromatin only in the presence of FLNA (**Fig. 3B**). Interestingly, loading of Ku86 onto chromatin persisted longer and with consistently higher levels in FLNA$^-$ than in FLNA$^+$ cells (**Fig. 6C**).

Finally, we tested whether BRCA1 was required to stabilize the interaction between DNA-PKcs and Ku86. We examined *BRCA1*-deficient HCC1937 cell line[32] and a HCC1937 derivative reconstituted with full length BRCA1 (gift from Junjie Chen). Complex formation between Ku86 and DNA-PKcs was not dependent on BRCA1 under IR-treated or untreated conditions (**Suppl. Fig. 2B**).

In summary, our results indicate that cells lacking FLNA have a defect in the two principal mechanisms for double strand break repair. Mechanistically, FLNA impacts on HR by contributing to efficient recruitment of BRCA1 and Rad51 to IR-induced foci, and on NHEJ by promoting the stability of the DNA-PKcs and Ku86 complex.

Discussion

In this paper we shed light on the mechanism by which Filamin A (FLNA) is required for efficient DNA repair. Our data indicates that lack of FLNA impacts on HR and NHEJ. FLNA is an actin-binding protein and its inactivation leads to an array of disorders such as otopalatodigital spectrum disorder, Melnick-Needles syndrome and periventricular heterotopia.[26] Although of unclear significance, at least two families carrying germline mutations in *BRCA1*

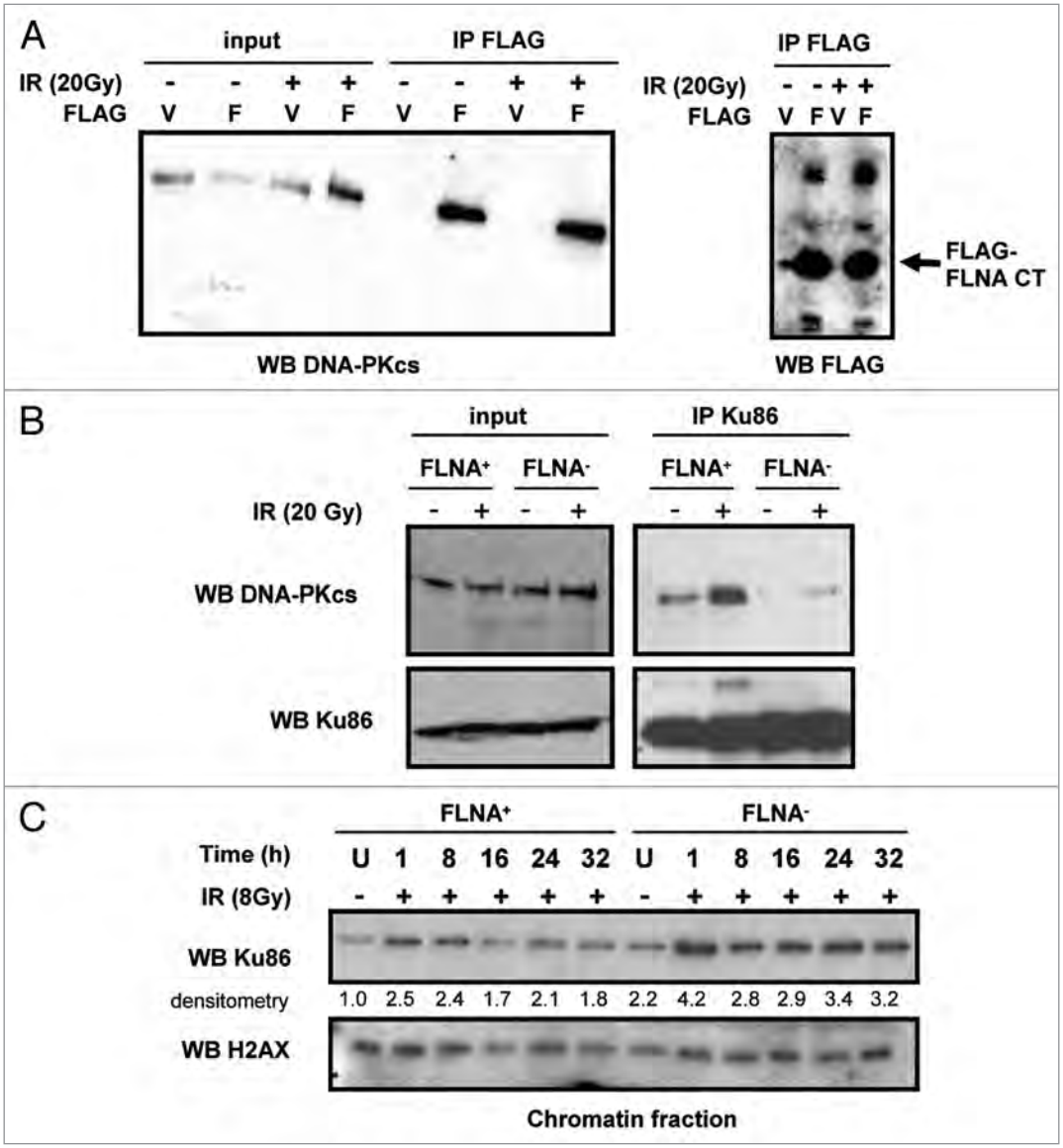

Figure 6. FLNA interacts in vivo with DNA-PKcs and mediates its interaction to Ku86. (A) Left, 293FT cells were transfected with FLAG-FLNA aa 2477–2647 (F) or empty FLAG vector (V) and mock-treated or irradiated with 20 Gy. Cells were collected after 1 h and immunoprecipitated using α-FLAG antibody. FLAG-FLNA aa 2477–2647 co-immunoprecipitates DNA-PKcs in the presence and absence of IR. Right, control for expression and the efficiency of the immunoprecipitation. (B) The interaction between DNA-PKcs and Ku86 is compromised in cells lacking FLNA. Left, shows that levels of DNA-PKcs and Ku86 are similar in both cell lines and in the presence and absence of irradiation. Right, shows that Ku86 and DNA-PKcs interact in FLNA$^+$ cells in the absence of damage and complex formation is significantly increased in the presence of irradiation. Complex formation in the presence and absence of IR is severely compromised in FLNA$^-$ cells. (C) Loading of Ku86 onto chromatin after DNA damage is increased in FLNA$^-$ cells. Histone H2AX levels are used as a loading control.

have been shown to manifest ventricular heterotopia.[33,34] FLNA interacts with a variety of proteins, including BRCA2,[25] and deficiency in FLNA leads to sensitivity to DNA damage and a defect in the recovery from G_2 arrest.[23] Thus, we investigated further its role in the DNA damage response.

FLNA binds BRCA1 using its extreme C-terminus which contains its dimerization domain. BRCA1 interaction with FLNA is mediated by a 30 amino acid region in the N-terminus of BRCA1 which contains a conserved domain called Motif 2.[21] Introduction of the Y179C mutation in Motif 2 significantly decreases the interaction. Analyses by the Align GV-GD method or by a yeast-based recombination assay suggest that Y179C may act as a deleterious mutation.[35,36] On the other hand, this variant has been found co-occurring in trans with a known deleterious mutation, which indicates that it is unlikely to have severe effects.[37] Thus, the Y179C may constitute a hypomorphic mutation with moderate effects on breast cancer predisposition. Of note, Motif 2 is close to the region that has been implicated in binding of BRCA1 to Ku86.[38]

In order to dissect the molecular role of FLNA in the DDR we took advantage of a well-characterized genetically-defined system. A melanoma cell line lacking FLNA was isolated and subsequently

reconstituted with FLNA yielding a pair of cell lines in which the only difference is the presence or absence of FLNA.[29] When we irradiated FLNA$^-$ and FLNA$^+$ cells, we noticed that FLNA$^-$ took much longer to resolve DSBs (**Fig. 3A and B**). To elucidate the mechanism underlying the repair defect we systematically investigated the proficiency of damage signaling in FLNA$^-$ cells.

Initially we investigated the recruitment and activation kinetics of the upstream kinases, as well as their downstream substrates after DNA damage. We found that FLNA deficiency led to the hyperactivation of ATM as judged by phosphorylation of ATM S1981 and CHK2 T68, surrogate markers of ATM activation.[39-41] Similarly, lack of FLNA also led to a hyperactivation of ATR, as measured by CHK1 S317 phosphorylation, a marker for ATR activation.[42] Moreover, we also found sustained levels of phosphorylation of NBS1 S343 to be higher in FLNA$^-$ cells. Although the role of NBS1 phosphorylation in the DNA damage signaling is poorly understood, it is generally thought to reflect ATM and ATR activation.[43,44] We also determined that major mediator proteins BRCA1, MDC1 and 53BP1 formed IR-induced foci irrespective of FLNA status. However, BRCA1 foci formation was significantly impaired in FLNA-deficient cells. In addition, Rad51 foci formation displayed a delayed kinetics in cells lacking FLNA. These data indicate that FLNA-deficient cells have impaired homologous recombination. Indeed, during the preparation of this manuscript Yue et al. showed that FLNA-deficient cells have a reduced ability to repair I-SceI-induced DSBs.[45]

During the course of our experiments we noticed a consistent increase in the number of FLNA$^-$ cells displaying IR-induced RPA foci. These foci progressively increased in size at later time points after IR. RPA is a ssDNA binding protein and participates in DNA metabolism processes where there is generation of ssDNA such as replication, repair and recombination.[46,47] Phosphorylation leads to inability of RPA to associate with the replication centers and leads to the association with DNA damage-induced foci instead.[48] Interestingly, lack of NHEJ proteins DNA-PKcs and Ku86, which together with Ku70 form the active DNA-PK complex, leads to accumulation of ssDNA in S phase.[49] Thus, we further investigated how the lack of FLNA impacted on DNA-PK complex formation.

Remarkably, Ku86 failed to interact with DNA-PKcs in the absence of FLNA. The reduced stability of the interaction is not due to Ku86 failure to load onto chromatin, as FLNA$^-$ cells displayed sustained higher levels of chromatin-bound Ku86 than FLNA$^+$ cells after damage. Ku86 is one of the first molecules to bind DNA ends after DSBs[50] and recruits DNA-PKcs via its C-terminus.[3] Taken together these results establish that lack of FLNA results in an unstable association of Ku86 and DNA-PKcs impairing the function of the complex. This impaired DNA-PK activity leads to a continuous build up of ssDNA and Ku86 on chromatin.

Over 16 phosphorylation sites have been identified in DNA-PKcs although their role is still poorly understood. Nevertheless, DNA-PKcs phosphorylation status is thought to influence its activity.[51] DNA-PKcs interacts with Ku86 and free ends of DNA in an unphosphorylated form,[52] and autophosphorylation is required for NHEJ progression.[53] Thus, we investigated the status of the two major phosphorylation clusters in DNA-PKcs, namely the 2056 and 2609 clusters. Clusters 2056 and 2609 were consistently phosphorylated upon treatment with IR irrespective of FLNA status. The fact that DNA-PKcs is phosphorylated upon damage in the absence of FLNA suggests that DNA-PKcs is interacting with the Ku86/DNA complex albeit transiently. Alternatively, it is possible that phosphorylation of DNA-PKcs is not mediated by autophosphorylation at the synaptic complex but rather via hyperactive ATM and ATR in FLNA-deficient cells.

We showed that FLNA and BRCA1 interact and that FLNA deficiency leads to a marked decrease in BRCA1 foci formation after damage. To investigate further the role of BRCA1 we tested whether expression of the BRCA1 FLNA-interacting fragment in FLNA-proficient cells could also act in a dominant negative fashion leading to a phenotype similar to FLNA-deficient cells. Strikingly, expression of the BRCA1-Ff lead to a defect in DNA repair as judged by CDC2 pY15 and γ-H2AX markers. This effect is specific because expression of BRCA1-Ff containing a mutation that disrupts FLNA/BRCA1 interaction does not lead to the same phenotype. Taken together, these data establish that BRCA1 participates in the FLNA-dependent regulation of the DNA damage response.

Our data shows that absence of FLNA leads to defective DSB repair. The defect is a combined result of compromised HR and NHEJ processes. At this stage we cannot distinguish whether FLNA-deficiency leads to a defective step that is common to both pathways or, alternatively, it impacts different steps in these pathways. In fact, the interplay between these two arms of the DNA repair process is not fully understood,[54] in particular after IR, which generates an array of different DNA modifications. The observed phenotype is consistent with a model in which Ku86 recognizes and binds free ends of DNA, but in the absence of FLNA, fails to make a stable complex with DNA-PKcs. We propose that unstable Ku86/DNA-PKcs interaction results in impaired end processing, accumulation of ssDNA, and hyperactivation of DNA damage signaling.

In addition, in FLNA-deficient cells BRCA1 displays impaired foci formation suggesting that FLNA also plays a role in stabilizing BRCA1 at the DSBs. BRCA1 colocalizes with Rad50/Mre11/NBS1 complex at IR-induced foci[55,56] and inhibits Mre11 exonuclease activity.[57] Thus, the diminished amounts of BRCA1 at IR-foci may lead to an unregulated Mre11 exonuclease activity with formation of the observed extended tracts of RPA-coated ssDNA in FLNA-deficient cells (**Fig. 4C and D**). BRCA1 has also been implicated in the regulation of Rad51,[7,58] although the mechanism by which it happens is obscure.[59] The kinetics of Rad51 foci formation in FLNA-deficient cells suggests that there is no problem in the initial recruitment to foci (see **Fig. 4C**, bottom, 3 h time point). The extended plateau observed in Rad51 foci (from 3 to 12 h after IR) may indicate an accumulation of DSBs that do not fulfill the end processing requirements for efficient Rad51 loading. Although further research will be needed to test this proposed model, it provides a tractable system to dissect the interplay between different processes involved in DNA repair.

It is possible that FLNA provides a framework for the assembly of factors in the synaptic complex. While unrepaired DNA in

yeast (which lacks recognizable DNA-PKcs and FLNA orthologs) migrates to so-called DNA repair centers,[60] the picture is different in mammalian cells where broken chromosome ends are essentially immobile.[61,62] It will be interesting to determine whether lack of FLNA affects the mobility of broken ends.

Materials and Methods

Constructs. GST-fusion fragments of BRCA1 in the mammalian expression vector pEBG BF 1-6 were a gift from Toru Ouchi. BRCA1 fragments BF1A (aa 1–70), BF1B (aa 71–140), BF1C (aa 1–101), BF1D (aa 141–240), BF1D1 (aa 160–190), BF1D2 (aa 190–210), BF1D3 (aa 160–210), BF1E (aa 241–324) and BF1F (aa 1–302) were obtained by PCR using pEBG BF1 as template (primer sequences are available upon request). The PCR products were digested and cloned into pEBG vector[63] and sequenced. Construct BF1D Y179C was obtained by site directed mutagenesis using BF1D as template for the PCR reaction. FLAG FLNA-Bf was obtained by cloning a PCR fragment of FLNA (aa 2477–2647) in frame to FLAG in pCMV2-FLAG vector.

Cell lines and transfections. The FLNA-deficient M2 melanoma cell line and its isogenic cell line, A7, reconstituted with full length FLNA cDNA[29] (gift from Thomas Stossel) was grown in MEM (Sigma) with 8% newborn calf serum (Sigma) and 2% fetal bovine serum (FBS; SAFC Biosciences, Lenexa, KS). A7 cells were grown in the presence of 0.2 mg/ml G418 (Fisher). HeLa (ATCC, Manassas, VA) was grown in DMEM with 5% FBS (Sigma). HCT116 (ATCC) was grown in McCoy's with 10% FBS. 293FT (InVitrogen) cells were grown in DMEM media (Sigma) with 10% FBS. Tissue culture media was supplemented with penicillin and streptomycin. Transfections were performed using Fugene 6 (Roche) according to the manufacturer's instructions.

Antibodies. The following antibodies, peptides and beads were used: α-BRCA1 mouse monoclonal antibody MS110 (Ab-1; Calbiochem; San Diego, CA) and SG11 (gift from Livingston D); α-Filamin A mouse monoclonal antibody PM6/317 (Chemicon International); α-FLAG M2 mouse monoclonal antibody (Sigma); 3xFLAG-peptide (Sigma); α-GST goat polyclonal antibody (Pharmacia Biotech); GT-sepharose 4B beads (GE Healthcare); α-Ku86 monoclonal antibody B-1 and α-Rad51 rabbit polyclonal antibody H-92 (Santa Cruz Biotechnology, Inc., Santa Cruz, CA); α-TP53BP1 mouse monoclonal antibody and α-phosphoserine 343-NBS1 mouse monoclonal antibody (Upstate Biotechnology); α-p34 RPA mouse monoclonal antibody Ab-1 and α-DNA-PKcs mouse monoclonal antibodies Ab-2 (Neomarkers, Freemont, CA); α-phosphoserine 2056 DNA-PKcs rabbit polyclonal antibody (Abcam, Cambridge, MA); α-phosphoserine 2609 DNA-PKcs rabbit polyclonal antibody (Novus Biologicals); α-MDC1 (SIGMA); γ-H2AX rabbit polyclonal;α-H2AX; α-phosphoserine 1981 ATM; α-ATM; α-ATR; α-phosphothreonine 68 CHK2; α-phosphoserine 317 CHK1 (Cell Signaling); α-β actin (Sigma). Conjugates for immunofluorescence were Alexa fluor 488 or 555 Molecular Probes.

Immunoprecipitation, pull-downs, western blot analysis and densitometry. Whole cell extracts were prepared by lyzing cells in a mild RIPA buffer (120 mM NaCl, 50 mM Tris pH 7.4, 1% NP40, 1 mM EDTA, protease inhibitors, 4 mM PMSF) lacking harsher SDS, sodium deoxycholate, and Triton X-100 detergents. The same buffer was used for immunoprecipitation. For high stringency immunoprecipitations the RIPA buffer was supplemented with 0.5% SDS. Antibodies (1 μg) were pre-incubated with protein A/G agarose beads (Santa Cruz Biotechnology, Inc.,), washed twice in RIPA buffer and incubated with the cell extracts overnight at 4°C. After incubation, the slurry were pelleted by centrifugation (2,000 rpm) and washed twice by removing the supernatant. Sample buffer was added to the beads and boiled for 10 min. For GST-pull downs, cell extracts were incubated with GT-beads, washed in RIPA buffer, and boiled.

Samples for western blot analysis were separated by SDS-PAGE and gels were electroblotted on a wet apparatus to a PVDF membrane. The PVDF membrane was blocked with 5% milk in TBS buffer containing 0.1% Tween (TBS-Tween) for 1 h. The membrane was washed three times in TBS-Tween and the antibody was added in 0.5% milk in TBS-Tween. The membrane was washed three times in TBS-Tween and incubated with the appropriate conjugate. After final washes Blots were incubated with ECL (Millipore, Billerica, MA).

Chromatin fractions were obtained by lyzing the cells with mild RIPA buffer and centrifuging at 14,000 rpm for 5 min. The pellet was then washed twice in mild RIPA and extracted with acid extraction buffer (0.5 M HCl, 10% Glycerol, 100 mM BME) and subsequently neutralized using 40 mM Tris pH 7.4 with protease inhibitors and NaOH.

Western blot data was quantified by densitometry using AlphaEaseFC v 3.1.2. Each lane was normalized using the corresponding loading controls and then expressed as a fold change relative to the untreated $FLNA^+$ cells in each blot.

Immunofluorescence. For BRCA1 analysis cells were fixed with 4% formaldehyde for 5 min followed by 5 min incubation with 100% ethanol. Cells were permeabilized with 0.25% Triton X-100 in PBS for 10 min, washed with PBS, and then blocked for 30 min with 5% BSA in PBS at room temperature (RT). After blocking, BRCA1 monoclonal antibody (SG11; kind gift from David Livingston) was added to 1% BSA in PBS for 1 h RT. Cells were washed and goat α-mouse Alexa Fluor 488 (Molecular Probes) was added for an additional 1 h RT.

For all other antibodies, cells were plated onto chamber slides and after 24 h they were washed with cytoskeleton buffer (10 mM HEPES/KOH pH 7.4, 300 mM sucrose, 100 mM NaCl, 3 mM $MgCl_2$) and fixed with 4% formaldehyde for 30 min RT. For analysis of chromatin bound RPA cells were pre-extracted for 2 min on ice with cytoskeleton buffersupplemented with 0.5% Triton X-100 before fixation.[64] After fixation cells were permeabilized with 0.25% Triton X-100 in PBS for 5 min RT and then washed and blocked with 5% BSA in PBS for 30 min RT. Primary and secondary antibodies in 1% BSA in PBS were added for 1 h each.

Cells were washed and mounted with Prolong Gold medium (Molecular Probes). Images were taken on a Leica Confocal Microscope. For quantification of BRCA1 and Rad51 immunofluorescence foci approximately 100 cells were scored per each

time point. Cells were scored as foci-positive if they presented with more than 10 foci per cell (an example can be found in **Supp. Fig. 2A**). For γ-H2AX and NBS-P-343 at least 50 cells per time point were counted for each condition. Cells were scored as foci-positive if they presented with more than 20 foci per cell. A threshold of 20 foci was chosen based on the number of foci found in unirradiated samples using the described antibodies. Determination of foci number per cell was done using Definiens Developer XD 1.1 (Definiens AD, Germany). A rule set was developed to segment nuclei based on the DAPI stain and then segment foci within the nucleus based on an intensity threshold. Representative results from at least two independent experiments are shown instead of statistical data on a small number of measurements with variability as recently recommended.[65]

Comet assay. Comet assays were performed in neutral conditions using a comet assay kit (Trevigen, Gaithersburg, MD) according to manufacturer's instructions. Briefly, cells were collected at the indicated time points, combined in low melting agarose (Trevigen, Gaithersburg, MD), spread over the comet slide area and allowed to set. Then, slides were immersed in lysis buffer for 30 min at 4°C. Electrophoresis was run in TBE buffer for 20 min at 1 V/cm voltage. Image analysis was done with Comet Analysis System 2.3.3 software (Loats Associates Inc., Westminster, MD).

Acknowledgements

The authors are indebted to members of the Monteiro Lab for helpful discussions and to Marcus Smolka and Ed Seto for a critical reading of the manuscript, to David Livingston and Arcangela De Nicolo for a generous gift of SG-11 antibody; Thomas Stossel for the M2 and A7 cell lines; Junjie Chen for the HCC1937-BRCA1wt cells; and Toru Ouchi for GST-BRCA1 constructs. This paper is dedicated to the memory of Hidesaburo Hanafusa, Professor Emeritus of the Rockefeller University, who passed away on March 15, 2009.

Financial disclosure

This work was supported by a predoctoral fellowship [BC083181] to A.V. from the US Department of Defense Breast Cancer Research Program; a National Institutes of Health grant [CA116167]; a grant from the Florida Breast Cancer Coalition Foundation to A.M.; and supported in part by the Analytic Microscopy and the Molecular Biology cores at the H.L. Moffitt Cancer Center & Research Institute.

Note

Supplementary materials can be found at:
www.landesbioscience.com/supplement/VelkovaCC9-7-Sup.pdf

References

1. Jackson SP, Bartek J. The DNA-damage response in human biology and disease. Nature 2009; 461:1071-8.
2. Harper JW, Elledge SJ. The DNA damage response: ten years after. Mol Cell 2007; 28:739-45.
3. Falck J, Coates J, Jackson SP. Conserved modes of recruitment of ATM, ATR and DNA-PKcs to sites of DNA damage. Nature 2005; 434:605-11.
4. Raderschall E, Golub EI, Haaf T. Nuclear foci of mammalian recombination proteins are located at single-stranded DNA regions formed after DNA damage. Proc Natl Acad Sci USA 1999; 96:1921-6.
5. San Filippo J, Sung P, Klein H. Mechanism of eukaryotic homologous recombination. Annu Rev Biochem 2008; 77:229-57.
6. Scully R, Chen J, Plug A, Xiao Y, Weaver D, Feunteun J, et al. Association of BRCA1 with Rad51 in mitotic and meiotic cells. Cell 1997; 88:265-75.
7. Chen J, Silver DP, Walpita D, Cantor SB, Gazdar AF, Tomlinson G, et al. Stable interaction between the products of the BRCA1 and BRCA2 tumor suppressor genes in mitotic and meiotic cells. Mol Cell 1998; 2:317-28.
8. Greenberg RA, Sobhian B, Pathania S, Cantor SB, Nakatani Y, Livingston DM. Multifactorial contributions to an acute DNA damage response by BRCA1/BARD1-containing complexes. Genes Dev 2006; 20:34-46.
9. Ford D, Easton DF, Bishop DT, Narod SA, Goldgar DE. Risks of cancer in BRCA1-mutation carriers. Breast Cancer Linkage Consortium. Lancet 1994; 343:692-5.
10. Easton DF, Bishop DT, Ford D, Crockford GP. Genetic linkage analysis in familial breast and ovarian cancer: results from 214 families. The Breast Cancer Linkage Consortium. Am J Hum Genet 1993; 52:678-701.
11. Miki Y, Swensen J, Shattuck-Eidens D, Futreal PA, Harshman K, Tavtigian S, et al. A strong candidate for the breast and ovarian cancer susceptibility gene BRCA1. Science 1994; 266:66-71.
12. Friedman LS, Ostermeyer EA, Szabo CI, Dowd P, Lynch ED, Rowell SE, et al. Confirmation of BRCA1 by analysis of germline mutations linked to breast and ovarian cancer in ten families. Nat Genet 1994; 8:399-404.
13. Narod SA, Foulkes WD. BRCA1 and BRCA2: 1994 and beyond. Nat Rev Cancer 2004; 4:665-76.
14. Scully R, Livingston D. In search of the tumour-suppressor functions of BRCA1 and BRCA2. Nature 2000; 408:429-32.
15. Venkitaraman AR. Cancer Susceptibility and the Functions of BRCA1 and BRCA2. Cell 2002; 108:171-82.
16. Moynahan ME, Chiu JW, Koller BH, Jasin M. Brca1 controls homology-directed DNA repair. Mol Cell 1999; 4:511-8.
17. Zhong Q, Chen CF, Chen PL, Lee WH. BRCA1 facilitates microhomology-mediated end joining of DNA double strand breaks. J Biol Chem 2002; 277:28641-7.
18. Zhuang J, Zhang J, Willers H, Wang H, Chung JH, van Gent DC, et al. Checkpoint kinase 2-mediated phosphorylation of BRCA1 regulates the fidelity of nonhomologous end-joining. Cancer Res 2006; 66:1401-8.
19. Wang HC, Chou WC, Shieh SY, Shen CY. Ataxia telangiectasia mutated and checkpoint kinase 2 regulate BRCA1 to promote the fidelity of DNA end-joining. Cancer Res 2006; 66:1391-400.
20. Carvalho MA, Marsillac SM, Karchin R, Manoukian S, Grist S, Swaby RF, et al. Determination of Cancer Risk Associated with Germ Line BRCA1 Missense Variants by Functional Analysis. Cancer Res 2007; 67:1494-501.
21. Orelli BJ, Logsdon JM Jr, Bishop DK. Nine novel conserved motifs in BRCA1 identified by the chicken orthologue. Oncogene 2001; 20:4433-8.
22. Abkevich V, Zharkikh A, Deffenbaugh AM, Frank D, Chen Y, Shattuck D, et al. Analysis of missense variation in human BRCA1 in the context of interspecific sequence variation. J Med Genet 2004; 41:492-507.
23. Meng X, Yuan Y, Maestas A, Shen Z. Recovery from DNA damage-induced G_2 arrest requires actin-binding protein filamin-A/actin-binding protein 280. J Biol Chem 2004; 279:6098-105.
24. Yue J, Wang Q, Lu H, Brenneman M, Fan F, Shen Z. The cytoskeleton protein filamin-A is required for an efficient recombinational DNA double strand break repair. Cancer Res 2009; 69:7978-85.
25. Yuan Y, Shen Z. Interaction with BRCA2 suggests a role for filamin-1 (hsFLNa) in DNA damage response. J Biol Chem 2001; 276:48318-24.
26. Feng Y, Walsh CA. The many faces of filamin: a versatile molecular scaffold for cell motility and signalling. Nat Cell Biol 2004; 6:1034-8.
27. Rodriguez JA, Henderson BR. Identification of a functional nuclear export sequence in BRCA1. J Biol Chem 2000; 275:38589-96.
28. Thompson ME, Robinson-Benion CL, Holt JT. An amino-terminal motif functions as a second nuclear export sequence in BRCA1. J Biol Chem 2005; 280:21854-7.
29. Cunningham CC, Gorlin JB, Kwiatkowski DJ, Hartwig JH, Janmey PA, Byers HR, et al. Actin-binding protein requirement for cortical stability and efficient locomotion. Science 1992; 255:325-7.
30. Rogakou EP, Boon C, Redon C, Bonner WM. Megabase chromatin domains involved in DNA double-strand breaks in vivo. J Cell Biol 1999; 146:905-16.
31. Dimitrova DS, Gilbert DM. Stability and nuclear distribution of mammalian replication protein A heterotrimeric complex. Exp Cell Res 2000; 254:321-7.
32. Tomlinson GE, Chen TT, Stastny VA, Virmani AK, Spillman MA, Tonk V, et al. Characterization of a breast cancer cell line derived from a germ-line BRCA1 mutation carrier. Cancer Res 1998; 58:3237-42.
33. Eccles DM, Barker S, Pilz DT, Kennedy C. Neuronal migration defect in a BRCA1 gene carrier: possible focal nullisomy? J Med Genet 2003; 40:24.
34. Eccles D, Bunyan D, Barker S, Castle B. BRCA1 mutation and neuronal migration defect: implications for chemoprevention. J Med Genet 2005; 42:42.
35. Tavtigian SV, Deffenbaugh AM, Yin L, Judkins T, Scholl T, Samollow PB, et al. Comprehensive statistical study of 452 BRCA1 missense substitutions with classification of eight recurrent substitutions as neutral. J Med Genet 2006; 43:295-305.
36. Caligo MA, Bonatti F, Guidugli L, Aretini P, Galli A. A yeast recombination assay to characterize human BRCA1 missense variants of unknown pathological significance. Hum Mutat 2009; 30:123-33.

37. Judkins T, Hendrickson BC, Deffenbaugh AM, Eliason K, Leclair B, Norton MJ, et al. Application of embryonic lethal or other obvious phenotypes to characterize the clinical significance of genetic variants found in trans with known deleterious mutations. Cancer Res 2005; 65:10096-103.
38. Wei L, Lan L, Hong Z, Yasui A, Ishioka C, Chiba N. Rapid recruitment of BRCA1 to DNA double-strand breaks is dependent on its association with Ku80. Mol Cell Biol 2008; 28:7380-93.
39. Bakkenist CJ, Kastan MB. DNA damage activates ATM through intermolecular autophosphorylation and dimer dissociation. Nature 2003; 421:499-506.
40. Matsuoka S, Rotman G, Ogawa A, Shiloh Y, Tamai K, Elledge SJ. Ataxia telangiectasia-mutated phosphorylates Chk2 in vivo and in vitro. Proc Natl Acad Sci USA 2000; 97:10389-94.
41. Melchionna R, Chen XB, Blasina A, McGowan CH. Threonine 68 is required for radiation-induced phosphorylation and activation of Cds1. Nat Cell Biol 2000; 2:762-5.
42. Cimprich KA, Cortez D. ATR: an essential regulator of genome integrity. Nat Rev Mol Cell Biol 2008; 9:616-27.
43. Gatei M, Young D, Cerosaletti KM, Desai-Mehta A, Spring K, Kozlov S, et al. ATM-dependent phosphorylation of nibrin in response to radiation exposure. Nat Genet 2000; 25:115-9.
44. D'Amours D, Jackson SP. The Mre11 complex: at the crossroads of dna repair and checkpoint signalling. Nat Rev Mol Cell Biol 2002; 3:317-27.
45. Yue J, Wang Q, Lu H, Brenneman M, Fan F, Shen Z. The cytoskeleton protein filamin-A is required for an efficient recombinational DNA double strand break repair. Cancer Res 2009; 69:7978-85.
46. Iftode C, Daniely Y, Borowiec JA. Replication protein A (RPA): the eukaryotic SSB. Crit Rev Biochem Mol Biol 1999; 34:141-80.
47. Golub EI, Gupta RC, Haaf T, Wold MS, Radding CM. Interaction of human rad51 recombination protein with single-stranded DNA binding protein, RPA. Nucleic Acids Res 1998; 26:5388-93.
48. Vassin VM, Wold MS, Borowiec JA. Replication protein A (RPA) phosphorylation prevents RPA association with replication centers. Mol Cell Biol 2004; 24:1930-43.
49. Karlsson KH, Stenerlow B. Extensive ssDNA end formation at DNA double-strand breaks in non-homologous end-joining deficient cells during the S phase. BMC Mol Biol 2007; 8:97.
50. Mahaney BL, Meek K, Lees-Miller SP. Repair of ionizing radiation-induced DNA double-strand breaks by non-homologous end-joining. Biochem J 2009; 417:639-50.
51. Weterings E, Chen DJ. DNA-dependent protein kinase in nonhomologous end joining: a lock with multiple keys? J Cell Biol 2007; 179:183-6.
52. Calsou P, Frit P, Humbert O, Muller C, Chen DJ, Salles B. The DNA-dependent protein kinase catalytic activity regulates DNA end processing by means of Ku entry into DNA. J Biol Chem 1999; 274:7848-56.
53. Reddy YV, Ding Q, Lees-Miller SP, Meek K, Ramsden DA. Non-homologous end joining requires that the DNA-PK complex undergo an autophosphorylation-dependent rearrangement at DNA ends. J Biol Chem 2004; 279:39408-13.
54. Yun MH, Hiom K. CtIP-BRCA1 modulates the choice of DNA double-strand-break repair pathway throughout the cell cycle. Nature 2009; 459:460-3.
55. Wu X, Petrini JH, Heine WF, Weaver DT, Livingston DM, Chen J. Independence of R/M/N focus formation and the presence of intact BRCA1. Science 2000; 289:11.
56. Zhong Q, Chen CF, Li S, Chen Y, Wang CC, Xiao J, et al. Association of BRCA1 with the hRad50-hMre11-p95 complex and the DNA damage response. Science 1999; 285:747-50.
57. Paull TT, Cortez D, Bowers B, Elledge SJ, Gellert M. Direct DNA binding by Brca1. Proc Natl Acad Sci USA 2001; 98:6086-91.
58. Chen JJ, Silver D, Cantor S, Livingston DM, Scully R. BRCA1, BRCA2 and Rad51 operate in a common DNA damage response pathway. Cancer Res 1999; 59:1752-6.
59. Cousineau I, Abaji C, Belmaaza A. BRCA1 regulates RAD51 function in response to DNA damage and suppresses spontaneous sister chromatid replication slippage: implications for sister chromatid cohesion, genome stability and carcinogenesis. Cancer Res 2005; 65:11384-91.
60. Lisby M, Mortensen UH, Rothstein R. Colocalization of multiple DNA double-strand breaks at a single Rad52 repair centre. Nat Cell Biol 2003; 5:572-7.
61. Misteli T, Soutoglou E. The emerging role of nuclear architecture in DNA repair and genome maintenance. Nat Rev Mol Cell Biol 2009; 10:243-54.
62. Soutoglou E, Dorn JF, Sengupta K, Jasin M, Nussenzweig A, Ried T, et al. Positional stability of single double-strand breaks in mammalian cells. Nat Cell Biol 2007; 9:675-82.
63. Tanaka M, Gupta R, Mayer BJ. Differential inhibition of signaling pathways by dominant-negative SH2/SH3 adapter proteins. Mol Cell Biol 1995; 15:6829-37.
64. Dimitrova DS, Todorov IT, Melendy T, Gilbert DM. Mcm2, but not RPA, is a component of the mammalian early G_1-phase prereplication complex. J Cell Biol 1999; 146:709-22.
65. Editorial. How robust is your data? Nat Cell Biol 2009; 11:667-70.

CellCycle

Volume 9 • Issue 7 • April 1, 2010

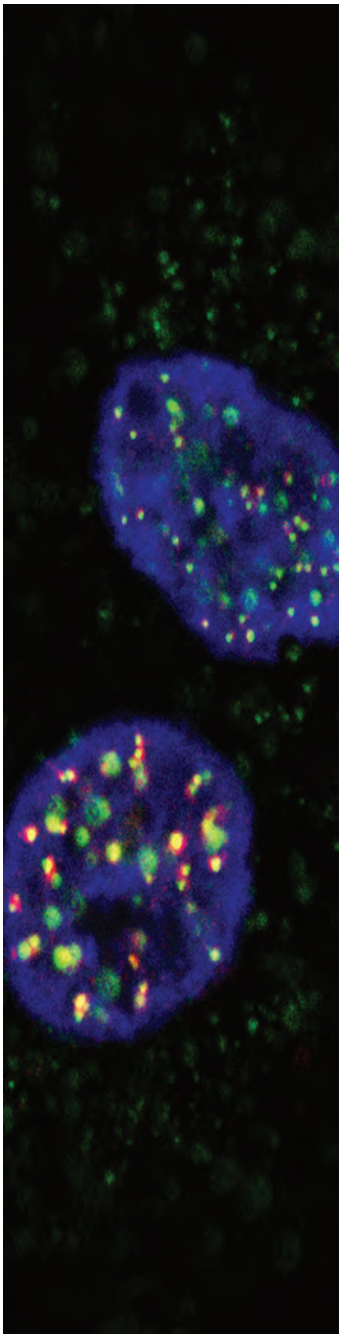

docks to the centromere is still unknown.[10] The data presented here suggest that the tertiary DNA structure is important for CPC docking to the centromere and it would be interesting to appreciate if DNA structure contributes directly to recruitment of the CPC to the inner centromere or if CPC docking is mediated through other chromatin binding proteins.

In summary, this work provides strong indications that the CPC can directly regulate the mitotic checkpoint and can prevent anaphase onset independently of its microtubule destabilizing activity. However, the mechanism by which the CPC is involved in signaling to the mitotic checkpoint remains unclear and future work that addresses these issues will be required.

Acknowledgements

We thank Dr. Gerben Vader for useful comments and The Netherlands Organization for Scientific Research (Vidi 917.66.332) for support.

References

1. Musacchio A, et al. Nat Rev Mol Cell Biol 2007; 8:379-93.
2. Ruchaud S, et al. Nat Rev Mol Cell Biol 2007; 8:798-812.
3. Pinsky BA, et al. Nat Cell Biol 2006; 8:78-83.
4. Kallio MJ, et al. FASEB J 2001; 15:2721-3.
5. Hauf S, et al. J Cell Biol 2003; 161:281-94.
6. Vader G, et al. Mol Biol Cell 2007; 18:4553-64.
7. Ditchfield C, et al. J Cell Biol 2003; 161:267-80.
8. Liu D, et al. Science 2009; 323:1350-3.
9. Emanuele MJ, et al. J Cell Biol 2008; 181:241-54.
10. Vader G, et al. J Cell Biol 2006; 173:833-7.

Filamins and the potential of complexity

Comment on: Velkova A, et al. Cell Cycle 2010; 9:1421–33.

Thomas P. Stossel; Harvard Medical School; Boston, MA USA; Email: Tstossel@partners.org

"Filamin," the name given by Wang and Singer to a high molecular-weight protein they identified in chicken gizzard smooth muscle, has become generic for a family of proteins, the first example of which was purified from rabbit lung macrophages. Humans express three filamin genes, filamin A, the first identified and most abundant filamin of nonmuscle tissues, filamin B, also widely expressed in nonmuscle cells and now known to be the variant named by Wang and Singer, and filamin C, mainly found in muscle cells.[1]

Initial research on filamins focused on their actin filament crosslinking properties and established that they very efficiently create elastic actin gels by promoting orthogonal branching of cross-linked actin filaments.[2] Structural analysis of filamin molecules has revealed how as extended dimers with multiple actin-binding domains they accomplish such branching.[3] Increasingly sophisticated studies on the elasticity of filamin-actin networks have implicated filamins, particularly filamin A, as mediators of the mechanical resistance of many living cells.[4]

In recent years identification of an astonishingly large number of filamin A, binding partners, including diverse membrane proteins, signaling intermediates and transcription factors has dominated filamin research (Figure 1).[5] Since homozygous filamin A deficiency is embryonic lethal,[6] a growing list of degenerative diseases associated with filamin mutations probably reflects functional disruption of filamin-partner interactions.[7-9] The paper by Velkova et al. in the previous issue of *Cell Cycle* describing a role for filamin A in DNA repair function of BRCA-1 adds cancer to the disease list. Since the filamin-partner binding must in many cases be cell-specific and temporally limited, for example, during embryonic development, targeting the binding interfaces might provide relatively specific and minimally toxic therapies for diseases. If posterity can rise to this challenge, it would exemplify how complexity, while daunting, can be useful.

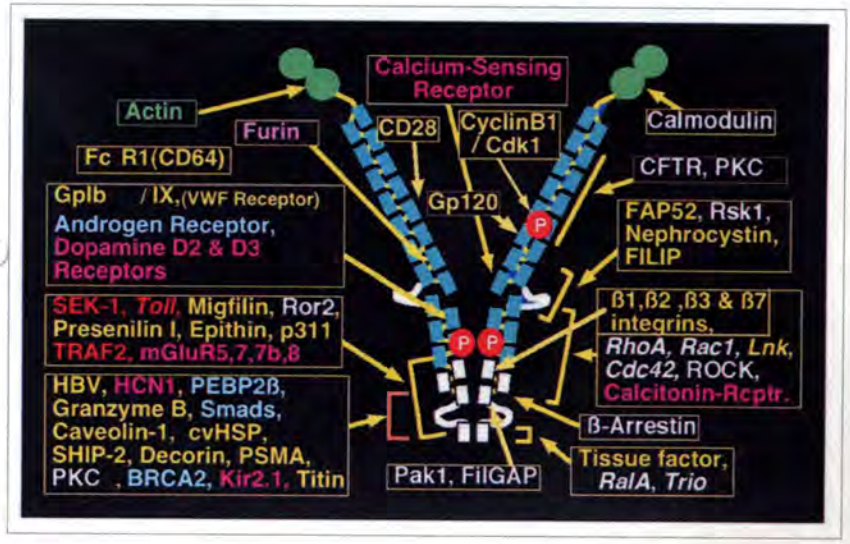

Figure 1. Filamin A binding partners and their location on its subunits.

References.

1. Stossel T, et al. Nat Rev Cell Mol Biol 2001; 2:138-45.
2. Hartwig JH, et al. J Mol Biol 1981; 145:563-81.
3. Nakamura F, et al. J Cell Biol 2007; 179:1011-25.
4. Koenderink G, et al. Proc Natl Acad Sci USA 2009; 106:15192-7.
5. Zhou A-X, et al. Trends Cell Biol 2010; 20:113-22.
6. Feng Y, et al. Proc Natl Acad Sci USA 2006; 103:19836-41.
7. Robertson S, et al. Am J Med Genet A 2006; 140A:1726-36.
8. Kyndt F, et al. Circulation 2007; 115:40-9.
9. Schröder R, et al. Brain Pathol 2009; 19:483-92.

Can the Status of the Breast and Ovarian Cancer Susceptibility Gene 1 Product (BRCA1) Predict Response to Taxane-Based Cancer Therapy?

J. Thomas DeLigio[1,#], Aneliya Velkova[2,3], Diego A.R. Zorio[1,#] and Alvaro N.A. Monteiro[2,*]

[1]*Taxolog, Inc., Tallahassee, FL 32303, USA;* [2]*Risk Assessment, Detection, and Intervention Program, H. Lee Moffitt Cancer Center & Research Institute, Tampa, FL 33612, USA;* [3]*University of South Florida Cancer Biology PhD Program, Tampa, FL 33612, USA and* [#]*Present Address: Florida State University, Dept. Chemistry, 740 DLC, Tallahassee, FL 32306, USA*

Abstract: Taxanes (paclitaxel and docetaxel) are currently used to treat ovarian, breast, lung, and head and neck cancers. Despite its clinical success taxane-based treatment could be significantly improved by identifying those patients whose tumors are more likely to present a clinical response. In this mini-review we discuss the accumulating evidence indicating that the breast and ovarian cancer susceptibility gene product BRCA1 mediates cellular response to taxanes. We review data from *in vitro*, animal, and clinical studies, and discuss them in context of response to therapy. We argue that levels of BRCA1 in tumors may provide a predictive marker for the response to treatment with taxanes. In addition, the study of the role of BRCA1 in the mechanism of action of taxanes might reveal alternative approaches to avoid resistance.

Key Words: Taxol, taxane, BRCA1, cancer, biomarker, microtubule, tubulin, chemotherapy.

ISOLATION AND CHARACTERIZATION OF TAXOL

Isolation of Taxol from the bark of the pacific yew tree, *Taxus brevifolia,* permanently changed the map of cancer treatment and research. Enthusiasm surrounding this finding ran high in both chemical and biological circles as the taxane ring proved to be a novel structure with anti-cancer properties (Fig. (**1**)) [1]. Because of Taxol's wide spectrum of anti-tumor activity, the need to understand how this compound worked became a priority. It was not until the early 1970's when Susan Horwitz and colleagues reported that Taxol inhibited cell division of exponentially growing HeLa cells at low concentrations with no secondary effects in nucleic acid metabolism or protein synthesis [2]. Using *in vitro* microtubule assembly assays, they showed that, contrary to previous plant-derived compounds, such as colchicines which inhibit microtubule assembly, Taxol promoted and stabilized microtubule assembly (rendering cells into late G2/M blockage) [2]. Taxol was also shown to be effective in blocking cell replication in mouse fibroblasts and inhibiting 3T3 fibroblasts migration, indicating that the Taxol-microtubule interaction could have an impact in several morphological and physiological processes critical for cell survival, migration, and replication [3].

Microtubules, considered to be the main component of the cellular skeleton, are composed of heterodimers of α and β-tubulin which are ~40% homologous. An abundance of isotype forms for both α and β co-exist in the cell, which undergo several post-translational modifications [4]. Each subunit has a guanine triphosphate (GTP) nucleotide binding site and hydrolysis only occurs on GTP bound to the β-subunit during microtubule assembly [4]. The precise mechanism by which Taxol interacts with microtubules was characterized in detail using photoaffinity Taxol analogues. This approach mapped the region to the β-tubulin subunit in which Taxol binding occurs [5-7]. The predicted region was later demonstrated to be in agreement with the crystal structure of the α,β-tubulin dimer at 3.7 Å resolution [8]. This was further corroborated by functional studies that demonstrated Taxol-resistant human ovarian cancer cells and Chinese hamster ovarian cells had β-tubulin mutations effectively compromising Taxol driven polymerization [9,10].

*Address correspondence to this author at the H. Lee Moffitt Cancer Center, 12902 Magnolia Drive, Tampa, FL 33612, USA; Tel: 813-7456321; Fax: 813-7451720; E-mail: alvaro.monteiro@moffitt.org

CLINICAL SUCCESS OF TAXANES

Taxanes have been well incorporated in adjuvant and neoadjuvant chemotherapeutic drug regimens given to patients with operable or metastatic breast cancer [11]. Several phase III trials have addressed the effects of using either paclitaxel or docetaxel (Fig. (**1**)) in combination with typical first line treatment protocols such as 5-fluorouracil (5-FU), doxorubicin, and cyclophosphamide. In cases of paclitaxel treatment used in adjuvant therapy, significant increases in disease-free survival (DFS) were recorded for up to six years post treatment [12-14]. Docetaxel given in combination with doxorubicin and cyclophosphamide as adjuvant therapy showed marked decreases in DFS as compared to 5-FU/doxorubicin/cyclophosphamide in the Breast Cancer International Research Group phase III study [15]. However, using docetaxel as a neoadjuvant to surgery following treatment with doxorubicin/cyclophosphamide showed improved clinical and pathological complete response rates, as well as increased overall clinical response rates [16]. A similar result was also observed in a University of Aberdeen phase II trial that looked at neoadjuvant treatment of locally advanced breast cancer with anthracycline therapy in combination with docetaxel; significant results were accomplished establishing a basis for using docetaxel as standard neoadjuvant therapy [17].

Retrospective evaluation of HER2 status in patients was undertaken by The Cancer and Leukemia Group B (CALGB) trial, and their findings indicated increased benefits from treatment when patients were found to have HER2-positive tumor cells versus HER2-negative patients [18]. Further, specific molecular subtyping of HER2 has proven beneficial to predicting efficacy of treatment as shown in CALGB 9344 and CALGB 9741 trials [18]. Inasmuch as molecular subtyping of breast cancer cells by their HER2 or Estrogen Receptor (ER) status may provide useful diagnostic data to the clinician, the challenge to identify additional predictors of treatment response presents the next phase in realizing the goal of personalized medicine.

The use of taxanes in several additional types of cancers has also been studied, namely non-small cell lung cancer (NSCLC), ovarian cancer, and head and neck squamous cell carcinoma (HNSCC). Phase II studies have examined the use of docetaxel in combination with gemcitabine as a second line treatment in NSCLC with promising results [19]. In a randomized, open-label, phase III trial comparing treatment with the standard first line platinum containing regimen (paclitaxel plus carboplatin) versus a platinum-free

1871-5206/09 $55.00+.00

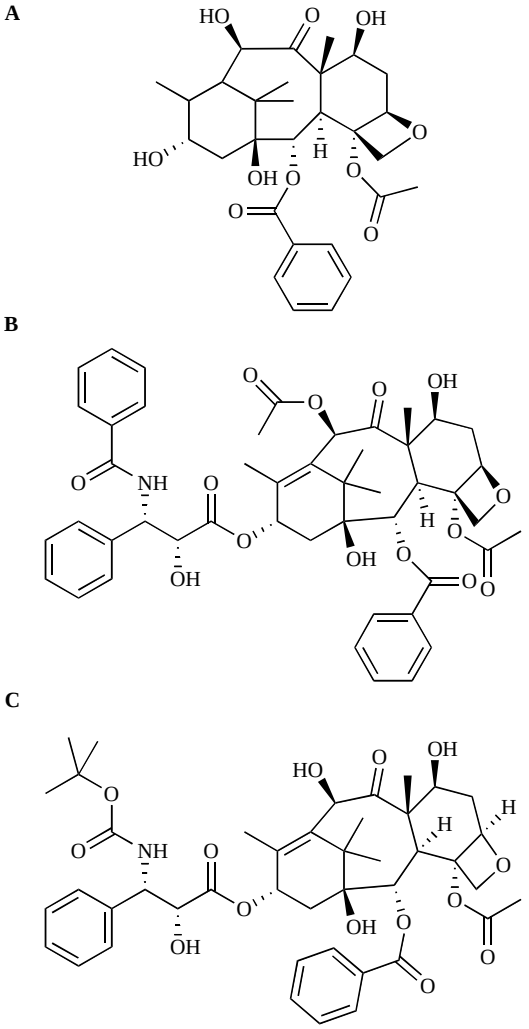

Fig. (1). Structural formulas for **A** (*2aR,4S,4aS,6R,9S,11S,12S,12aR,12bS*)-12b-(Acetyloxy)-12-(benzoyloxy)-1,2a,3,4,4a,6,9,10,11,12,12a,12b-dodecahydro-4,6,9,11-tetrahydroxy-4a,8,13,13-tetramethyl-7,11-methano-5*H*-cyclodeca(3,4)benz(1,2-b) oxet-5-one, 10-deacetylbaccatin (10-DAB), **B** (2α,4α,5β,7β,10β,13α)-4,10-bis(acetyloxy)-13-{[(2*R*,3*S*)-3-(benzoylamino)-2-hydroxy-3-phenylpropanoyl]oxy}-1,7-dihydroxy-9-oxo-5,20-epoxytax-11-en-2-yl benzoate, Taxol (paclitaxel) and **C** (2*R*,3*S*)-*N*-carboxy-3-phenylisoserine, *N*-tert-butyl ester, 13-ester with 5,20-epoxy-1,2,4,7,10,13-hexahydroxytax-11-en-9-one 4-acetate 2-benzoate, trihydrate, Taxotere (docetaxel).

experimental regimen (triplet of vinorelbine, gemcitabine, and docetaxel), researchers found treatment efficacy to be equivalent with unique toxicity profiles [20]. No superiority over either treatment was recorded in this study thus allowing for greater options to patients [20,21]. Taxane-based chemotherapy has also become the first line treatment in ovarian cancer [22]. Studies have shown a marked improvement in progression-free survival rates of patients treated with a combination of taxane (paclitaxel or docetaxel) and cisplatin over cisplatin/cyclophosphamide [23,24]. These types of combination therapy approaches have become the cornerstone of treating cisplatin-resistant ovarian cancer [25].

The treatment of HNSCC with docetaxel as induction chemotherapy has also been established in clinical trials. Combinations of docetaxel and cisplatin have been shown to exhibit upwards of fifty-three percent overall response rates in these patients [26]. More recently a randomized phase III trial compared docetaxel, cisplatin, and 5-fluorouracil (5-FU) versus cisplatin and 5-FU alone (both groups receiving follow-up chemoradiotherapy). The results showed significantly higher overall response rates in the taxane comprising treatment group versus cisplatin and 5-FU alone (72% versus 64%, respectively) [27]. Taken together, these data serve to illustrate the establishment of taxanes in treatment of many types of cancers as a standard chemotherapeutic option.

Although we continue to learn a great deal about taxane response in past and present clinical trials, continuous improvement in determining drug efficacy either as a single agent or as an adjuvant therapy exists. Chemoresistance determinants [11], new drug formulations and the search of derivatives with better therapeutic index [28] are good examples of areas in which improvements could be achieved. In addition, identifying markers in tumors prior to treatment could help researchers and clinicians in designing future clinical trials with higher predicted response rates. For example, it has been demonstrated that inhibition of Aurora Kinase A in conjunction with paclitaxel treatment synergistically enhanced apoptosis induction in HNSCC cells and xenografts [29]. Based on the current literature, we propose that the breast and ovarian cancer susceptibility gene 1 (BRCA1) protein could be a potential predictive marker for taxane treatment. Furthermore, understanding the role of BRCA1 in taxane response could aid in streamlining the clinical approach to improved chemotherapeutic therapy.

BRCA1

BRCA1 [OMIM #113705] was mapped to chromosome 17q21 and isolated by positional cloning in 1994 as a breast and ovarian cancer susceptibility gene [30-33]. *BRCA1* germline mutations have been attributed to a considerable increase in the risk of developing breast (56-80% versus 11% in the general population) and ovarian cancer (15-60% versus 1.4-2.5%) with early onset of the disease [33]. *BRCA1* is rarely mutated in sporadic breast cancers but epigenetic inactivation of *BRCA1* has been documented in high grade sporadic tumors suggesting that it also plays a role in non-familial cases [34,35]. The gene encodes a nuclear phosphoprotein that plays a role in a number of different biological processes such as DNA damage response, cell cycle control, and regulation of transcription, but it is not yet clear which molecular function(s) are major contributors to the gene's tumor suppressive activity (reviewed in refs. [36-40]).

BRCA1 AND RESISTANCE TO MICROTUBULE-DISRUPTING DRUGS

Cells lacking BRCA1 are prone to apoptosis and are more sensitive to DNA damaging agents [41,42]. Conversely, a series of experiments have suggested that low levels of BRCA1 in cell lines correlate with resistance to taxanes and vinca alkaloids (Table **1**) [42-47]. While this proved true for breast cancer cell lines, it was not observed in one ovarian cancer cell line [48] and no clear sensitivity differences were found in lymphocytes from BRCA1 mutation carriers [49]. Thus, cell culture experiments suggest that BRCA1 is required for sensitivity to microtubule poisons but this may vary with gene dosage as well as with cell type.

The evidence highlighting the role of BRCA1 in taxane sensitivity is not limited to studies with cell lines. In a *K14cre; Brca1*$^{F/F}$*; p53*$^{F/F}$ mouse (targeted deletion of *Brca1* and *p53* in the mammary gland) spontaneous tumors became invariably resistant to docetaxel but not to cisplatin [50]. Acquired resistance in this case might be due to increased drug elimination *via* upregulated transport proteins. But even if this is the case, one can imagine that by targeting tumors that are more sensitive (high BRCA1 levels) will preclude the accumulation of genetic or epigenetic changes needed to develop resistance. A different mouse model in which ovarian explants from *K5-TVA; Brca1*$^{lox/lox}$*; p53*$^{lox/lox}$ (targeted deletion of *Brca1* and *p53* combined with the expression of the avian receptor TVA) [51] are cotransduced *ex vivo* with *Cre* and *Myc*, and injected subcutaneously in nude mice illustrate once again potential cell type differences. When treated *in vitro* with paclitaxel, *Brca1*$^{-/-}$ or *Brca1*$^{+/+}$ cell lines showed comparable sensitivity [52].

Table 1. Sensitivity to Microtubule-Interfering Drugs in Cell Lines

Cells	BRCA1 Status	IC_{50}	Drug [Exposure Time] & Assay Used
Comparison across breast cancer cell lines			
HCC1937	ER^{neg}, one deleted allele and one C-terminally truncated allele.	>2μM	Paclitaxel [48h] & MTT (Tassone *et al*. 2003; ref. [45])
MCF-7	ER^{pos}, hemizygous for wild type BRCA1	0.1-0.2 μM	
MDA-MB231	Homozygous for wt BRCA1	10-20 nM	
Comparison across isogenic breast cancer cell lines			
HCCBR116	HCC1937 transfected with wt BRCA1	7.73 nM	Paclitaxel [72h] & MTT (Gilmore *et al*. 2004; ref. [43]).
HCCEV1	HCC1937 transfected with empty vector	6.21 μM	
MBR62-bcl2	MCF-7 derivative stably transfected with tet-inducible wt BRCA1 (induced)	7.7 nM	Paclitaxel [72h] & cell counting (Quinn *et al*. 2003; ref. [42]).
MBR62-bcl2	MCF-7 derivative stably transfected with tet-inducible wt BRCA1 (non-induced)	96.4 pM	
T47D	T47D ($BRCA1^{+/+}$ and ER^{pos}) transfected with a control siRNA	2.2 μM	Paclitaxel [72h] & cell counting (Quinn *et al*. 2003; ref. [42]).
T47D	T47D transfected with a BRCA1 siRNA	>0.1 mM	
HCCBR116	HCC1937 transfected with wt BRCA1	7.7 nM	Paclitaxel [72h] & cell counting (Quinn *et al*. 2003; ref. [42]).
HCCEV1	HCC1937 transfected with empty vector	6.2 μM	
HCCBR116		1.9 nM	Vinorelbine [72h] & cell counting (Quinn *et al*. 2003; ref. [42]).
HCCEV1		17 μM	
HCCBR18	HCC1937 transfected with wt BRCA1	0.3 nM	Paclitaxel [72h] & cell counting (Quinn *et al*. 2003; ref. [42]).
HCCEV2	HCC1937 transfected with empty vector	1.6 μM	
HCCBR mix	HCC1937 transfected with wt BRCA1	1.5 nM	Paclitaxel [72h] & cell counting (Quinn *et al*. 2003; ref. [42]).
HCCEV3	HCC1937 transfected with empty vector	10.7 μM	
MCF-7	MCF-7 transfected with a control siRNA	36 nM*	Paclitaxel [72h] & WST-1 cleavage (Chabalier *et al*. 2006; ref. [46]). *IC_{25} shown.
MCF-7	MCF-7 transfected with a BRCA1 siRNA	4.1 nM*	

THE MECHANISM OF BRCA1 RESPONSE

Although the mechanism by which cells require BRCA1 to respond to taxanes is largely unknown, three modes of action have been proposed and none of them are mutually exclusive. The first mechanism is a differential apoptotic response; the second confers a requirement in spindle-assembly checkpoint; and the third provides a role in centrosome-mediated microtubule stability.

It has been proposed that resistance of BRCA1-deficient cells to taxanes is correlated to a defective apoptotic response but it has not yet been formally demonstrated [42]. The induction of ectopic BRCA1 expression led to an increased sensitivity to paclitaxel in a derivative of the human mammary carcinoma cell line MDA435 when compared to a non-induced control. Treatment triggered cell cycle arrest in G2/M phase and a dramatic increase in apoptosis, with concomitant induction at the transcriptional level of GADD45 by BRCA1 [44]. Interestingly, treatment of A375 and DLD1 cells (melanoma and colon cancer, respectively) with paclitaxel and/ or docetaxel also causes transcriptional induction of GADD45 (DeLigio and Zorio, unpublished data).

A rybozyme-based strategy to inhibit expression of BRCA1 in breast epithelial HBL100 cells caused decreased sensitivity to mitotic-spindle poisons Taxol and vincristine [47]. Upon treatment with Taxol there was a strong increase in JNK phosphorylation and subsequent apoptosis in BRCA1-expressing versus non-expressing cells. This observation was consistent with previous data showing that BRCA1 can enhance apoptosis through a pathway involving H-Ras, MEKK4, JNK, and activation of caspases 8 and 9 [53].

By stabilizing microtubules, paclitaxel disrupts mitotic spindle assembly and triggers the spindle checkpoint [54]. BRCA1 participation in spindle assembly checkpoint signaling is confirmed by the experiments that show targeted knockdown of BRCA1 in MCF7 cells increases resistance to paclitaxel. MCF7 cells exhibited premature sister chromatid separation after treatment with the drug suggesting that the role of BRCA1 in the response to paclitaxel may need spindle assembly checkpoint signaling [46]. This hypothesis is supported by the fact that BRCA1 is important for transcriptional regulation of spindle assembly checkpoint proteins BUBR1 [46] and MAD2 [55]. These proteins (BUBR1, MAD2, and BRCA1) have a critical role in mitotic microtubule organization and spindle pole assembly in *Xenopus* egg extracts and cultured mammalian HeLa cells. The BRCA1/BARD1 heterodimer controls efficient transport to the spindle poles of microtubule associated protein TPX2 [56]. This function was partially dependent upon BRCA1/ BARD1 ubiquitin ligase activity. Among the phenotypes observed in BRCA1-depleted cells were compromised mitotic exit, chromosome segregation defects, and micronucleus formation [56]. Defects in the spindle checkpoint have been associated with resistance to taxanes [57,58]. Thus, it is conceivable that BRCA1 also modulates taxane sensitivity through its effects on the spindle checkpoint. A completely inactive checkpoint seems to be lethal, while a weakened (signal produced but not sustained) checkpoint leads to chromosome instability [59]. Absent or low levels of BRCA1 may act as a hypomorphic mutation and allow for a defective or attenuated spindle assembly checkpoint.

In addition to its role in the spindle-assembly checkpoint, BRCA1 is also involved in the regulation of centrosome function [60]. The hypophosphorylated form of BRCA1 has been found associated with centrosomes during mitosis [61]. BRCA1 (amino acids 504-803) interacts with γ-tubulin, and over expression of this fragment causes accumulation of mitotic cells with multiple centrosomes and abnormal spindles; which in turn interferes with cell growth and induces apoptosis in COS7 cells [62].

Transient inhibition of BRCA1 in cells derived from mammary tissues also leads to amplification and fragmentation of centrosomes [63]. Important activity relationships have been divulged *in vitro* regarding ubiquitination of centrosomal proteins by BRCA1/

BARD1. Specifically, this protein complex monoubiquitinates γ-tubulin at lysine residues 48 and 344. Individually mutating γ-tubulin to abolish BRCA1 ubiquitination at these residues has shown BRCA1 controls both centrosome duplication and its microtubule nucleation properties in different stages of the cell cycle [64].

BRCA1 AS A MARKER FOR CLINICAL OUTCOME

Despite the evidence from *in vitro* studies showing a trend towards cells that have no BRCA1 (or express lower BRCA1 levels) being more resistant to taxanes, a positive correlation in clinical studies would prove noteworthy. In the few studies published so far focusing on breast, ovarian, and most recently, lung cancer, a case for this relationship is starting to emerge.

Absence of BRCA1 expression in primary tumors of metastatic breast cancer patients who were treated with taxanes was identified as an independent predictor of shorter time to progression, although there was no clear correlation with clinical tumor response [65]. On the other hand, a study in primary breast cancers failed to see a correlation between BRCA1 levels (grouped as either high or low expressers) and resistance to docetaxel [66]. However, in a study comparing *BRCA1* germ-line mutation carriers and non-carriers, response rates to neoadjuvant docetaxel treatment in the carrier group was limited while non-carriers showed a high number of complete or partial responses [67].

Patients with familial ovarian cancers (which included carriers and non-carriers of the 5382insC founder truncating mutation in BRCA1) responded less favorably to treatment with paclitaxel and cisplatin or carboplatin than patients with sporadic tumors [68]. In addition, a recent study in sporadic ovarian cancer patients provided evidence that *BRCA1* mRNA expression levels can be used as a predictive marker of survival. The overall median survival for high *BRCA1* expressing patients was increased after taxane-containing chemotherapy [69].

A detailed review of the clinical studies described in the previous paragraphs reveal important limitations in design and methodology. They all have small sample sizes which may lack sufficient power to detect effects. Many do not provide patient genotyping information and in many cases treatment combined several other classes of chemotherapy drugs with taxanes. More importantly, they vary widely in how BRCA1 status was determined (e.g. quantitative RT-PCR or immunohistochemistry) and how differences in levels were considered for (e.g. continuous or discrete). Nevertheless, those limitations are more likely to underestimate differences. Thus, the correlative clinical results, combined with the *in vitro* data, provide a solid starting point for the hypothesis that BRCA1 can be used as a marker of clinical outcome after treatment with taxanes.

Low BRCA1 protein expression, due to promoter methylation, was shown to be a common feature in NSCLC samples [70]. Researchers found that patients subjected to neoadjuvant therapy with gemcitabine/cisplatin whose tumors expressed low levels of *BRCA1* mRNA had a better outcome than those expressing high levels [71]. In conflict to these results, one study of NSCLC patients treated with gemcitabine/cisplatin or epirubicin/gemcitabine did not show any predictive value using comparisons of BRCA1 levels in the tumors as measured by immunohistochemistry [72]. However, analysis of mRNA expression levels in metastatic malignant effusions from NSCLC patients revealed *BRCA1* expression level as positively correlated to docetaxel sensitivity [73]. Finally, overexpression of *BRCA1* mRNA was strongly associated with poor survival (Hazard Ratio: 1.98; 95% confidence interval 1.11-6) in chemonaive NSCLC patients [74]. Thus, although these studies also suffer from limitations (e.g. using mRNA measurements without also analyzing protein levels), they provide preliminary evidence supporting the role of BRCA1 status as a marker for outcome in lung cancer. In light of this evidence, the Spanish Lung Cancer Group has initiated a BRCA1 Expression Customization (BREC) study to test the usefulness of BRCA1 in current and future customized therapy of NSCLC [75]. This exploratory evaluation attempts to expose BRCA1 as a potential genetic marker given the hypothesis that low BRCA1 levels correlate with increased sensitivity to DNA damaging agents such as cisplatin. The results of the BREC study regarding time to progression of disease and BRCA1 levels will be highly anticipated in that its implications reach toward a targeted and efficient approach to chemotherapy with taxanes and/or DNA damaging agents in NSCLC.

CONCLUSION

BRCA1 plays an important role in the cell's response to chemotherapy. In the past few years several lines of evidence have indicated that the status of BRCA1 protein influences the ability of cells to respond to agents that cause DNA damage. Recently, data has emerged suggesting that the status of BRCA1 may also influence response to agents that do not cause direct DNA damage, such as microtubule inhibitors. If this role of BRCA1 is confirmed, BRCA1 may represent an ideal biomarker with the ability to predict response to a wide array of agents currently used in cancer therapy.

ACKNOWLEDGEMENTS

Work in the Monteiro Lab is supported by a DoD predoctoral fellowship BC083181 (A.V.), NIH award CA92309, a grant from the Florida Breast Cancer Coalition Foundation, and pilot funds from Lung SPORE P50-CA119997. The authors acknowledge Drs. Robert Holton and Mike Edler for critical review of this manuscript.

ABBREVIATIONS

5-FU	=	5-Fluorouracil
10-DAB	=	10-Deacetylbaccatin
BARD1	=	BRCA1 associated RING domain 1
BRCA1	=	Breast and ovarian cancer susceptibility gene 1
DFS	=	Disease-free survival
ER	=	Estrogen receptor
GTP	=	Guanine tri-phosphate
HER2	=	Human epidermal growth factor receptor 2
HNSCC	=	Head and neck squamous cell carcinoma
JNK	=	Jun N-terminal kinase
NSCLC	=	Non-small cell lung cancer
RT-PCR	=	Reverse transcriptase polymerase chain reaction

REFERENCES

[1] Wani, M.C.; Taylor, H.L.; Wall, M.E.; Coggon, P.; McPhail, A.T. Plant antitumor agents. VI. The isolation and structure of taxol, a novel antileukemic and antitumor agent from Taxus brevifolia. *J. Am. Chem. Soc.* **1971**, *93*(9), 2325-2327.

[2] Schiff, P.B.; Fant, J.; Horwitz, S.B. Promotion of microtubule assembly *in vitro* by taxol. *Nature* **1979**, *277*(5698), 665-667.

[3] Schiff, P.B.; Horwitz, S.B. Taxol stabilizes microtubules in mouse fibroblast cells. *Proc. Natl. Acad. Sci. USA* **1980**, *77*(3), 1561-1565.

[4] Luduena, R.F. Multiple forms of tubulin: different gene products and covalent modifications. *Int. Rev. Cytol.* **1998**, *178*, 207-275.

[5] Rao, S.; Krauss, N.E.; Heerding, J.M.; Swindell, C.S.; Ringel, I.; Orr, G.A.; Horwitz, S.B. 3'-(p-azidobenzamido)taxol photolabels the N-terminal 31 amino acids of beta-tubulin. *J. Biol. Chem.* **1994**, *269*(5), 3132-3134.

[6] Rao, S.; Orr, G.A.; Chaudhary, A.G.; Kingston, D.G.; Horwitz, S.B. Characterization of the taxol binding site on the microtubule. 2-(m-Azidobenzoyl)taxol photolabels a peptide (amino acids 217-231) of beta-tubulin. *J. Biol. Chem.* **1995**, *270*(35), 20235-20238.

[7] Rao, S.; He, L.; Chakravarty, S.; Ojima, I.; Orr, G.A.; Horwitz, S.B. Characterization of the Taxol binding site on the microtubule. Identification of Arg(282) in beta-tubulin as the site of photoincorporation of a 7-benzophenone analogue of Taxol. *J. Biol. Chem.* **1999**, *274*(53), 37990-37994.

[8] Nogales, E.; Wolf, S.G.; Downing, K.H. Structure of the alpha beta tubulin dimer by electron crystallography. *Nature* **1998**, *391*(6663), 199-203.

[9] Giannakakou, P.; Sackett, D.L.; Kang, Y.K.; Zhan, Z.; Buters, J.T.; Fojo, T.; Poruchynsky, M.S. Paclitaxel-resistant human ovarian cancer cells have mutant beta-tubulins that exhibit impaired paclitaxel-driven polymerization. *J. Biol. Chem.* **1997**, *272*(27), 17118-17125.

[10] Gonzalez-Garay, M.L.; Chang, L.; Blade, K.; Menick, D.R.; Cabral, F.A beta-tubulin leucine cluster involved in microtubule assembly and paclitaxel resistance. *J. Biol. Chem.* **1999**, *274*(34), 23875-23882.

[11] McGrogan, B.T.; Gilmartin, B.; Carney, D.N.; McCann, A. Taxanes, microtubules and chemoresistant breast cancer. *Biochim. Biophys. Acta* **2008**, *1785*(2), 96-132.

[12] Henderson, I.C.; Berry, D.A.; Demetri, G.D.; Cirrincione, C.T.; Goldstein, L.J.; Martino, S.; Ingle, J.N.; Cooper, M.R.; Hayes, D.F.; Tkaczuk, K.H.; Fleming, G.; Holland, J.F.; Duggan, D.B.; Carpenter, J.T.; Frei, E., III; Schilsky, R.L.; Wood, W.C.; Muss, H.B.; Norton, L. Improved outcomes from adding sequential Paclitaxel but not from escalating Doxorubicin dose in an adjuvant chemotherapy regimen for patients with node-positive primary breast cancer. *J. Clin. Oncol.* **2003**, *21*(6), 976-983.

[13] Citron, M.L.; Berry, D.A.; Cirrincione, C.; Hudis, C.; Winer, E.P.; Gradishar, W.J.; Davidson, N.E.; Martino, S.; Livingston, R.; Ingle, J.N.; Perez, E.A.; Carpenter, J.; Hurd, D.; Holland, J.F.; Smith, B.L.; Sartor, C.I.; Leung, E.H.; Abrams, J.; Schilsky, R.L.; Muss, H.B.; Norton, L. Randomized trial of dose-dense versus conventionally scheduled and sequential versus concurrent combination chemotherapy as postoperative adjuvant treatment of node-positive primary breast cancer: first report of Intergroup Trial C9741/Cancer and Leukemia Group B Trial 9741. *J. Clin. Oncol.* **2003**, *21*(8), 1431-1439.

[14] Mamounas, E.P.; Bryant, J.; Lembersky, B.; Fehrenbacher, L.; Sedlacek, S.M.; Fisher, B.; Wickerham, D.L.; Yothers, G.; Soran, A.; Wolmark, N. Paclitaxel after doxorubicin plus cyclophosphamide as adjuvant chemotherapy for node-positive breast cancer: results from NSABP B-28. *J. Clin. Oncol.* **2005**, *23*(16), 3686-3696.

[15] Martin, M.; Pienkowski, T.; Mackey, J.; Pawlicki, M.; Guastalla, J.P.; Weaver, C.; Tomiak, E.; Al-Tweigeri, T.; Chap, L.; Juhos, E.; Guevin, R.; Howell, A.; Fornander, T.; Hainsworth, J.; Coleman, R.; Vinholes, J.; Modiano, M.; Pinter, T.; Tang, S.C.; Colwell, B.; Prady, C.; Provencher, L.; Walde, D.; Rodriguez-Lescure, A.; Hugh, J.; Loret, C.; Rupin, M.; Blitz, S.; Jacobs, P.; Murawsky, M.; Riva, A.; Vogel, C. Adjuvant docetaxel for node-positive breast cancer. *N. Engl. J. Med.* **2005**, *352*(22), 2302-2313.

[16] Bear, H.D.; Anderson, S.; Brown, A.; Smith, R.; Mamounas, E.P.; Fisher, B.; Margolese, R.; Theoret, H.; Soran, A.; Wickerham, D.L.; Wolmark, N. The effect on tumor response of adding sequential preoperative docetaxel to preoperative doxorubicin and cyclophosphamide: preliminary results from National Surgical Adjuvant Breast and Bowel Project Protocol B-27. *J. Clin. Oncol.* **2003**, *21*(22), 4165-4174.

[17] Smith, I.C.; Heys, S.D.; Hutcheon, A.W.; Miller, I.D.; Payne, S.; Gilbert, F.J.; Ah-See, A.K.; Eremin, O.; Walker, L.G.; Sarkar, T.K.; Eggleton, S.P.; Ogston, K.N. Neoadjuvant chemotherapy in breast cancer: significantly enhanced response with docetaxel. *J. Clin. Oncol.* **2002**, *20*(6), 1456-1466.

[18] Hayes, D.F.; Thor, A.D.; Dressler, L.G.; Weaver, D.; Edgerton, S.; Cowan, D.; Broadwater, G.; Goldstein, L.J.; Martino, S.; Ingle, J.N.; Henderson, I.C.; Norton, L.; Winer, E.P.; Hudis, C.A.; Ellis, M.J.; Berry, D.A.; the Cancer and Leukemia Group. HER2 and response to paclitaxel in node-positive breast cancer. *N. Engl. J. Med.* **2007**, *357*(15), 1496-1506.

[19] Huang, C.H.; Millenson, M.M.; Sherman, E.J.; Borghaei, H.; Mintzer, D.M.; Cohen, R.B.; Staddon, A.P.; Seldomridge, J.; Treat, O.J.; Tuttle, H.; Ruth, K.J.; Langer, C.J. Promising survival in patients with recurrent non-small cell lung cancer treated with docetaxel and gemcitabine in combination as second-line therapy. *J. Thorac. Oncol.* **2008**, *3*(9), 1032-1038.

[20] Kubota, K.; Kawahara, M.; Ogawara, M.; Nishiwaki, Y.; Komuta, K.; Minato, K.; Fujita, Y.; Teramukai, S.; Fukushima, M.; Furuse, K. Vinorelbine plus gemcitabine followed by docetaxel versus carboplatin plus paclitaxel in patients with advanced non-small-cell lung cancer: a randomised, open-label, phase III study. *Lancet Oncol.* **2008**, *9*(12), 1135-1142.

[21] Barlesi, F. Lung cancer: moving forward with tailored strategies. *Lancet Oncol.* **2008**, *9*(12), 1116-1117.

[22] Markman, M. Pharmaceutical management of ovarian cancer : current status. *Drugs* **2008**, *68*(6), 771-789.

[23] Piccart, M.J.; Bertelsen, K.; James, K.; Cassidy, J.; Mangioni, C.; Simonsen, E.; Stuart, G.; Kaye, S.; Vergote, I.; Blom, R.; Grimshaw, R.; Atkinson, R.J.; Swenerton, K.D.; Trope, C.; Nardi, M.; Kaern, J.; Tumolo, S.; Timmers, P.; Roy, J.A.; Lhoas, F.; Lindvall, B.; Bacon, M.; Birt, A.; Andersen, J.E.; Zee, B.; Paul, J.; Baron, B.; Pecorelli, S. Randomized intergroup trial of cisplatin-paclitaxel versus cisplatin-cyclophosphamide in women with advanced epithelial ovarian cancer: three-year results. *J. Natl. Cancer Inst.* **2000**, *92*(9), 699-708.

[24] Vasey, P.A.; Jayson, G.C.; Gordon, A.; Gabra, H.; Coleman, R.; Atkinson, R.; Parkin, D.; Paul, J.; Hay, A.; Kaye, S.B. Phase III randomized trial of docetaxel-carboplatin versus paclitaxel-carboplatin as first-line chemotherapy for ovarian carcinoma. *J. Natl. Cancer Inst.* **2004**, *96*(22), 1682-1691.

[25] Stordal, B.; Pavlakis, N.; Davey, R.A systematic review of platinum and taxane resistance from bench to clinic: an inverse relationship. *Cancer Treat. Rev.* **2007**, *33*(8), 688-703.

[26] Schoffski, P.; Catimel, G.; Planting, A.S.; Droz, J.P.; Verweij, J.; Schrijvers, D.; Gras, L.; Schrijvers, A.; Wanders, J.; Hanauske, A.R. Docetaxel and cisplatin: an active regimen in patients with locally advanced, recurrent or metastatic squamous cell carcinoma of the head and neck. Results of a phase II study of the EORTC Early Clinical Studies Group. *Ann. Oncol.* **1999**, *10*(1), 119-122.

[27] Posner, M.R.; Hershock, D.M.; Blajman, C.R.; Mickiewicz, E.; Winquist, E.; Gorbounova, V.; Tjulandin, S.; Shin, D.M.; Cullen, K.; Ervin, T.J.; Murphy, B.A.; Raez, L.E.; Cohen, R.B.; Spaulding, M.; Tishler, R.B.; Roth, B.; Viroglio, R.C.; Venkatesan, V.; Romanov, I.; Agarwala, S.; Harter, K.W.; Dugan, M.; Cmelak, A.; Markoe, A.M.; Read, P.W.; Steinbrenner, L.; Colevas, A.D.; Norris, C.M., Jr.; Haddad, R.I. Cisplatin and fluorouracil alone or with docetaxel in head and neck cancer. *N. Engl. J. Med.* **2007**, *357*(17), 1705-1715.

[28] Ferlini, C.; Gallo, D.; Scambia, G. New taxanes in development. *Expert. Opin. Investig. Drugs* **2008**, *17*(3), 335-347.

[29] Mazumdar, A.; Henderson, Y.C.; El-Naggar, A.K.; Sen, S.; Clayman, G.L. Aurora kinase A inhibition and paclitaxel as targeted combination therapy for head and neck squamous cell carcinoma. *Head Neck* **2008**, *31*(5), 625-634.

[30] Hall, J.M.; Lee, M.K.; Newman, B.; Morrow, J.E.; Anderson, L.A.; Huey, B.; King, M.C. Linkage of early-onset familial breast cancer to chromosome 17q21. *Science* **1990**, *250*(4988), 1684-1689.

[31] Narod, S.A.; Feunteun, J.; Lynch, H.T.; Watson, P.; Conway, T.; Lynch, J.; Lenoir, G.M. Familial breast-ovarian cancer locus on chromosome 17q12-q23. *Lancet* **1991**, *338*(8759), 82-83.

[32] Vogelstein, B.; Kinzler, K.W. Has the breast cancer gene been found? *Cell* **1994**, *79*(1), 1-3.

[33] Miki, Y.; Swensen, J.; Shattuck-Eidens, D.; Futreal, P.A.; Harshman, K.; Tavtigian, S.; Liu, Q.; Cochran, C.; Bennett, L.M.; Ding, W.A strong candidate for the breast and ovarian cancer susceptibility gene BRCA1. *Science* **1994**, *266*(5182), 66-71.

[34] Futreal, P.A.; Liu, Q.; Shattuck-Eidens, D.; Cochran, C.; Harshman, K.; Tavtigian, S.; Bennett, L.M.; Haugen-Strano, A.; Swensen, J.; Miki, Y. BRCA1 mutations in primary breast and ovarian carcinomas. *Science* **1994**, *266*(5182), 120-122.

[35] Wilson, C.A.; Ramos, L.; Villasenor, M.R.; Anders, K.H.; Press, M.F.; Clarke, K.; Karlan, B.; Chen, J.J.; Scully, R.; Livingston, D.; Zuch, R.H.; Kanter, M.H.; Cohen, S.; Calzone, F.J.; Slamon, D.J. Localization of human BRCA1 and its loss in high-grade, non-inherited breast carcinomas. *Nat. Genet.* **1999**, *21*(2), 236-240.

[36] Narod, S.A.; Foulkes, W.D. BRCA1 and BRCA2: 1994 and beyond. *Nat. Rev. Cancer* **2004**, *4*(9), 665-676.

[37] Scully, R.; Livingston, D. In search of the tumour-suppressor functions of BRCA1 and BRCA2. *Nature* **2000**, *408*, 429-432.

[38] Venkitaraman, A.R. Cancer susceptibility and the functions of BRCA1 and BRCA2. *Cell* **2002**, *108*(2), 171-182.

[39] Scully, R.; Xie, A.; Nagaraju, G. Molecular functions of BRCA1 in the DNA damage response. *Cancer Biol. Ther.* **2004**, *3*(6), 521-527.

[40] Lane, T.F. BRCA1 and transcription. *Cancer Biol. Ther.* **2004**, *3*(6), 528-533.

[41] Kennedy, R.D.; Quinn, J.E.; Mullan, P.B.; Johnston, P.G.; Harkin, D.P. The role of BRCA1 in the cellular response to chemotherapy. *J. Natl. Cancer Inst.* **2004**, *96*(22), 1659-1668.

[42] Quinn, J.E.; Kennedy, R.D.; Mullan, P.B.; Gilmore, P.M.; Carty, M.; Johnston, P.G.; Harkin, D.P. BRCA1 functions as a differential modulator of chemotherapy-induced apoptosis. *Cancer Res.* **2003**, *63*(19), 6221-6228.

[43] Gilmore, P.M.; McCabe, N.; Quinn, J.E.; Kennedy, R.D.; Gorski, J.J.; Andrews, H.N.; McWilliams, S.; Carty, M.; Mullan, P.B.; Duprex, W.P.; Liu, E.T.; Johnston, P.G.; Harkin, D.P. BRCA1 interacts with and is required for paclitaxel-induced activation of mitogen-activated protein kinase kinase kinase 3. *Cancer Res.* **2004**, *64*(12), 4148-4154.

[44] Mullan, P.B.; Quinn, J.E.; Gilmore, P.M.; McWilliams, S.; Andrews, H.; Gervin, C.; McCabe, N.; McKenna, S.; White, P.; Song, Y.H.; Maheswaran, S.; Liu, E.; Haber, D.A.; Johnston, P.G.; Harkin, D.P. BRCA1 and GADD45 mediated G2/M cell cycle arrest in response to antimicrotubule agents. *Oncogene* **2001**, *20*(43), 6123-6131.

[45] Tassone, P.; Tagliaferri, P.; Perricelli, A.; Blotta, S.; Quaresima, B.; Martelli, M.L.; Goel, A.; Barbieri, V.; Costanzo, F.; Boland, C.R.; Venuta, S. BRCA1 expression modulates chemosensitivity of BRCA1-defective HCC1937 human breast cancer cells. *Br. J. Cancer* **2003**, *88*(8), 1285-1291.

[46] Chabalier, C.; Lamare, C.; Racca, C.; Privat, M.; Valette, A.; Larminat, F. BRCA1 downregulation leads to premature inactivation of spindle checkpoint and confers paclitaxel resistance. *Cell Cycle* **2006**, *5*(9), 1001-1007.

[47] Lafarge, S.; Sylvain, V.; Ferrara, M.; Bignon, Y.J. Inhibition of BRCA1 leads to increased chemoresistance to microtubule-interfering agents, an effect that involves the JNK pathway. *Oncogene* **2001**, *20*(45), 6597-6606.

[48] Zhou, C.; Smith, J.L.; Liu, J. Role of BRCA1 in cellular resistance to paclitaxel and ionizing radiation in an ovarian cancer cell line carrying a defective BRCA1. *Oncogene* **2003**, *22*(16), 2396-2404.

[49] Trenz, K.; Lugowski, S.; Jahrsdorfer, U.; Jainta, S.; Vogel, W.; Speit, G. Enhanced sensitivity of peripheral blood lymphocytes from women carrying a BRCA1 mutation towards the mutagenic effects of various cytostatics. *Mutat. Res.* **2003**, *544*(2-3), 279-288.

[50] Rottenberg, S.; Nygren, A.O. H.; Pajic, M.; van Leeuwen, F.W. B.; van der Heijden, I.; van de Wetering, K.; Liu, X.; de Visser, K.E.; Gilhuijs, K.G.; van Tellingen, O.; Schouten, J.P.; Jonkers, J.; Borst, P. Selective induction of chemotherapy resistance of mammary tumors in a conditional mouse model for hereditary breast cancer. *Proc. Natl. Acad. Sci. USA* **2007**, 0702955104.

[51] Orsulic, S.; Li, Y.; Soslow, R.A.; Vitale-Cross, L.A.; Gutkind, J.S.; Varmus, H.E. Induction of ovarian cancer by defined multiple genetic changes in a mouse model system. *Cancer Cell* **2002**, *1*(1), 53-62.

[52] Xing, D.; Orsulic, S.A Mouse model for the molecular characterization of brca1-associated ovarian carcinoma. *Cancer Res.* **2006**, *66*(18), 8949-8953.

[53] Thangaraju, M.; Kaufmann, S.H.; Couch, F.J. BRCA1 facilitates stress-induced apoptosis in breast and ovarian cancer cell lines. *J. Biol. Chem.* **2000**, *275*(43), 33487-33496.

[54] Wassmann, K.; Benezra, R. Mitotic checkpoints: from yeast to cancer. *Curr. Opin. Genet. Dev.* **2001**, *11*(1), 83-90.

[55] Wang, R.H.; Yu, H.; Deng, C.X. A requirement for breast-cancer-associated gene 1(BRCA1) in the spindle checkpoint. *Proc. Natl. Acad. Sci. USA* **2004**, *101*(49), 17108-17113.

[56] Joukov, V.; Groen, A.C.; Prokhorova, T.; Gerson, R.; White, E.; Rodriguez, A.; Walter, J.C.; Livingston, D.M. The BRCA1/BARD1 heterodimer modulates ran-dependent mitotic spindle assembly. *Cell* **2006**, *127*(3), 539-552.

[57] Sudo, T.; Nitta, M.; Saya, H.; Ueno, N.T. Dependence of paclitaxel sensitivity on a functional spindle assembly checkpoint. *Cancer Res.* **2004**, *64*(7), 2502-2508.

[58] Anand, S.; Penrhyn-Lowe, S.; Venkitaraman, A.R. AURORA-A amplification overrides the mitotic spindle assembly checkpoint, inducing resistance to Taxol. *Cancer Cell* **2003**, *3*(1), 51-62.

[59] Weaver, B.A.; Cleveland, D.W. Decoding the links between mitosis, cancer, and chemotherapy: The mitotic checkpoint, adaptation, and cell death. *Cancer Cell* **2005**, *8*(1), 7-12.

[60] Pujana, M.A.; Han, J.D.; Starita, L.M.; Stevens, K.N.; Tewari, M.; Ahn, J.S.; Rennert, G.; Moreno, V.; Kirchhoff, T.; Gold, B.; Assmann, V.; Elshamy, W.M.; Rual, J.F.; Levine, D.; Rozek, L.S.; Gelman, R.S.; Gunsalus, K.C.; Greenberg, R.A.; Sobhian, B.; Bertin, N.; Venkatesan, K.; yivi-Guedehoussou, N.; Sole, X.; Hernandez, P.; Lazaro, C.; Nathanson, K.L.; Weber, B.L.; Cusick, M.E.; Hill, D.E.; Offit, K.; Livingston, D.M.; Gruber, S.B.; Parvin, J.D.; Vidal, M. Network modeling links breast cancer susceptibility and centrosome dysfunction. *Nat. Genet.* **2007**, *39*(11), 1338-1349.

[61] Hsu, L.C.; White, R.L. BRCA1 is associated with the centrosome during mitosis. *Proc. Natl. Acad. Sci. USA* **1998**, *95*(22), 12983-12988.

[62] Hsu, L.C.; Doan, T.P.; White, R.L. Identification of a gamma-tubulin-binding domain in BRCA1. *Cancer Res.* **2001**, *61*(21), 7713-7718.

[63] Starita, L.M.; Machida, Y.; Sankaran, S.; Elias, J.E.; Griffin, K.; Schlegel, B.P.; Gygi, S.P.; Parvin, J.D. BRCA1-dependent ubiquitination of gamma-tubulin regulates centrosome number. *Mol. Cell Biol.* **2004**, *24*(19), 8457-8466.

[64] Sankaran, S.; Starita, L.M.; Groen, A.C.; Ko, M.J.; Parvin, J.D. Centrosomal microtubule nucleation activity is inhibited by BRCA1-dependent ubiquitination. *Mol. Cell. Biol.* **2005**, *25*(19), 8656-8668.

[65] Kurebayashi, J.; Yamamoto, Y.; Kurosumi, M.; Okubo, S.; Nomura, T.; Tanaka, K.; Sonoo, H. Loss of BRCA1 expression may predict shorter time-to-progression in metastatic breast cancer patients treated with taxanes. *Anticancer Res.* **2006**, *26*(1B), 695-701.

[66] Kim, S.J.; Miyoshi, Y.; Taguchi, T.; Tamaki, Y.; Nakamura, H.; Yodoi, J.; Kato, K.; Noguchi, S. High thioredoxin expression is associated with resistance to docetaxel in primary breast cancer. *Clin. Cancer Res.* **2005**, *11*(23), 8425-8430.

[67] Byrski, T.; Gronwald, J.; Huzarski, T.; Grzybowska, E.; Budryk, M.; Stawicka, M.; Mierzwa, T.; Szwiec, M.; Wisniowski, R.; Siolek, M.; Narod, S.A.; Lubinski, J. Response to neo-adjuvant chemotherapy in women with BRCA1-positive breast cancers. *Breast Cancer Res. Treat.* **2008**, *108*(2), 289-296.

[68] Wojciechowska-Lacka, A.; Markowska, J.; Skasko, E.; Kruczek, A.; Steffen, J. Frequent disease progression and early recurrence in patients with familial ovarian cancer primarily treated with paclitaxel and cis- or carboplatin (preliminary report). *Eur. J. Gynaecol. Oncol.* **2003**, *24*(1), 21-24.

[69] Quinn, J.E.; James, C.R.; Stewart, G.E.; Mulligan, J.M.; White, P.; Chang, G.K. F.; Mullan, P.B.; Johnston, P.G.; Wilson, R.H.; Harkin, D.P. BRCA1 mRNA expression levels predict for overall survival in ovarian cancer after chemotherapy. *Clin. Cancer Res.* **2007**, *13*(24), 7413-7420.

[70] Lee, M.N.; Tseng, R.C.; Hsu, H.S.; Chen, J.Y.; Tzao, C.; Ho, W.L.; Wang, Y.C. Epigenetic inactivation of the chromosomal stability control genes BRCA1, BRCA2, and XRCC5 in non-small cell lung cancer. *Clin. Cancer Res.* **2007**, *13*(3), 832-838.

[71] Taron, M.; Rosell, R.; Felip, E.; Mendez, P.; Souglakos, J.; Ronco, M.S.; Queralt, C.; Majo, J.; Sanchez, J.M.; Sanchez, J.J.; Maestre, J. BRCA1 mRNA expression levels as an indicator of chemoresistance in lung cancer. *Hum. Mol. Genet.* **2004**, *13*(20), 2443-2449.

[72] Wachters, F.M.; Wong, L.S. M.; Timens, W.; Kampinga, H.H.; Groen, H.J. M. ERCC1, hRad51, and BRCA1 protein expression in relation to tumour response and survival of stage III/IV NSCLC

patients treated with chemotherapy. *Lung Cancer* **2005**, *50*(2), 211-219.

[73] Wang, L.; Wei, J.; Qian, X.; Yin, H.; Zhao, Y.; Yu, L.; Wang, T.; Liu, B. ERCC1 and BRCA1 mRNA expression levels in metastatic malignant effusions is associated with chemosensitivity to cisplatin and/or docetaxel. *BMC Cancer* **2008**, *8*(1), 97.

[74] Rosell, R.; Skrzypski, M.; Jassem, E.; Taron, M.; Bartolucci, R.; Sanchez, J.J.; Mendez, P.; Chaib, I.; Perez-Roca, L.; Szymanowska, A.; Rzyman, W.; Puma, F.; Kobierska-Gulida, G.; Farabi, R.; Jassem, J. BRCA1: A novel prognostic factor in resected non-small-cell lung cancer. *PLoS ONE* **2007**, *2*(11), e1129.

[75] Reguart, N.; Cardona, A.F.; Carrasco, E.; Gomez, P.; Taron, M.; Rosell, R. BRCA1: a new genomic marker for non-small-cell lung cancer. *Clin. Lung Cancer* **2008**, *9*(6), 331-339.

Received: February 19, 2009 **Revised: March 11, 2009** **Accepted: March 20, 2009**

[Cancer Biology & Therapy 8:5, 422-434; 1 March 2009]; ©2009 Landes Bioscience

Research Paper

Ectopic expression of histone H2AX mutants reveals a role for its post-translational modifications

Jonathan Rios-Doria,[1] Aneliya Velkova,[1,2] Virna Dapic,[1] José M. Galán-Caridad,[3,†] Vesna Dapic,[3] Marcelo A. Carvalho,[1,‡] Johana Melendez[4] and Alvaro N.A. Monteiro[1,*]

[1]Risk Assessment, Detection and Intervention Program; H. Lee Moffitt Cancer Center & Research Institute; Tampa, FL USA; [2]University of South Florida Cancer Biology Ph.D. Program; Tampa, FL USA; [3]Strang Cancer Prevention Center; New York, NY USA; [4]Flow Cytometry Core; H. Lee Moffitt Cancer Center & Research Institute; Tampa, FL USA

†Present address: Integrated Program in Cell; Molecular and Biophysical Studies; Columbia University Medical Center; New York, NY USA; ‡Present address: Centro Federal de Educação Tecnológica de Química; Rio de Janeiro, Brazil

Abbreviations: ATM, ataxia-telangiectasia mutated; ATR, ATM and Rad3-related; BME, β-mercaptoethanol; BSA, bovine serum albumin; DBD, DNA binding domain; DNA-PK, DNA protein kinase; DSB, double strand breaks; EDTA, ethylene-diamine-tetra-acetic acid; γ-H2AX, histone H2AX phosphorylated at serine 139; GFP, green fluorescent protein; HEPES, 4-(2-hydroxyethyl)-1-piperazineethane-sulfonic acid; IR, ionizing radiation; MMS, methyl-methane sulfonate; PBS, phosphate buffered saline; PI, proteasome inhibitors; PI3K, phosphoinositide-3-kinase

Key words: histone, H2ax, ubiquitination, phosphorylation, half-life, DNA damage, apoptosis, cell cycle checkpoints

Recent evidence from a wide variety of biological systems has indicated important regulatory roles for post-translation histone modifications in cellular processes such as regulation of gene expression, DNA damage response and recombination. Phosphorylation of histone H2AX at serine 139 is a critical event in the response to DNA damage, but the functional implications of this modification are not yet clear. To investigate the role of H2AX phosphorylation we ectopically expressed epitope-tagged H2AX or mutants at the phosphorylation site. GFP-tagged wild type H2AX, H2AX Ser139Ala or H2AX Ser139Glu proteins were efficiently expressed, localizing exclusively to the interphase nucleus and to condensed chromosomes during mitosis. Biochemical fractionation indicated that epitope-tagged H2AX proteins are incorporated into nucleosomes. Expression of H2AX Ser139Ala, which disrupts the phosphorylation site partially suppressed early G_2/M arrest following ionizing radiation, and cells expressing this mutant were more sensitive to DNA damage. Conversely, expression of H2AX Ser139Glu, designed as phosphorylation mimic, induced a decrease in the number of cells in mitosis in the absence of DNA damage. Interestingly, this decrease induced by H2AX Ser139Glu was independent of the formation of 53BP1-containing foci and was partially suppressed in *CHK2*-deficient cells, suggesting a role for CHK2 in this process. Further analyses revealed that expression of either mutant lead to apoptosis and induced higher caspase-3/7 activity compared to expression of wild type H2AX. In addition, we also identified Lys119 as a site for ubiquitination that controls H2AX half-life. Phosphorylation of Ser139 and ubiquitination of K119 are not interdependent. Taken together these results demonstrate a role for H2AX Serine 139 phosphorylation in cell cycle regulation and apoptosis, and for Lysine 119 in the control of H2AX turnover.

*Correspondence to: Alvaro N.A. Monteiro; H. Lee Moffitt Cancer Center; 12902 Magnolia Drive; Tampa, FL 33612 USA; Tel.: 813.7456321; Fax: 813.9036847; Email: alvaro.monteiro@moffitt.org

Submitted: 10/27/08; Revised: 12/03/08; Accepted: 12/09/08

Previously published online as a *Cancer Biology & Therapy* E-publication: http://www.landesbioscience.com/journals/cbt/article/7592

Introduction

The response to DNA damage relies on a coordinated signaling network[1] and one of the earliest responses is phosphorylation of histone H2AX at Serine 139.[2] H2AX (*H2AFX;* OMIM 601772) is a minor variant of the highly conserved histone H2A that is part of the histone octamer in the core of the nucleosome in eukaryotic genomes.[3,4] H2AX differs from H2A and the other human H2A variants by having a longer C-terminal tail that contains an SQE motif, a consensus site for phosphorylation by PI3K-related kinases.[5] The kinases responsible for H2AX phosphorylation are the PI3K-like kinases ATM (Ataxia-Mutated), ATR (Ataxia and Rad3-related) and DNA-PK with each kinase thought to respond to different types of damage.[6-8]

After the induction of double strand breaks (DSB), phosphorylation of Ser 139 of H2AX radiates from the approximate site of damage to neighboring megabase regions of chromatin, although it seems not to be present in the immediate vicinity of the break.[9,10] Proteins implicated in the DNA damage response such as BRCA1, NBS1 and 53BP1 were found to form discrete foci that colocalized with H2AX phosphorylated at Serine 139, also called γ-H2AX.[11] The role of γ-H2AX in the recruitment of these factors is still under investigation, but experiments suggest that γ-H2AX is required for the retention, but not initial recruitment, of these factors to sites of DSB.[12] In addition, cells from mice with homozygous disruption of *H2aX* are hypersensitive to ionizing radiation (IR) and develop

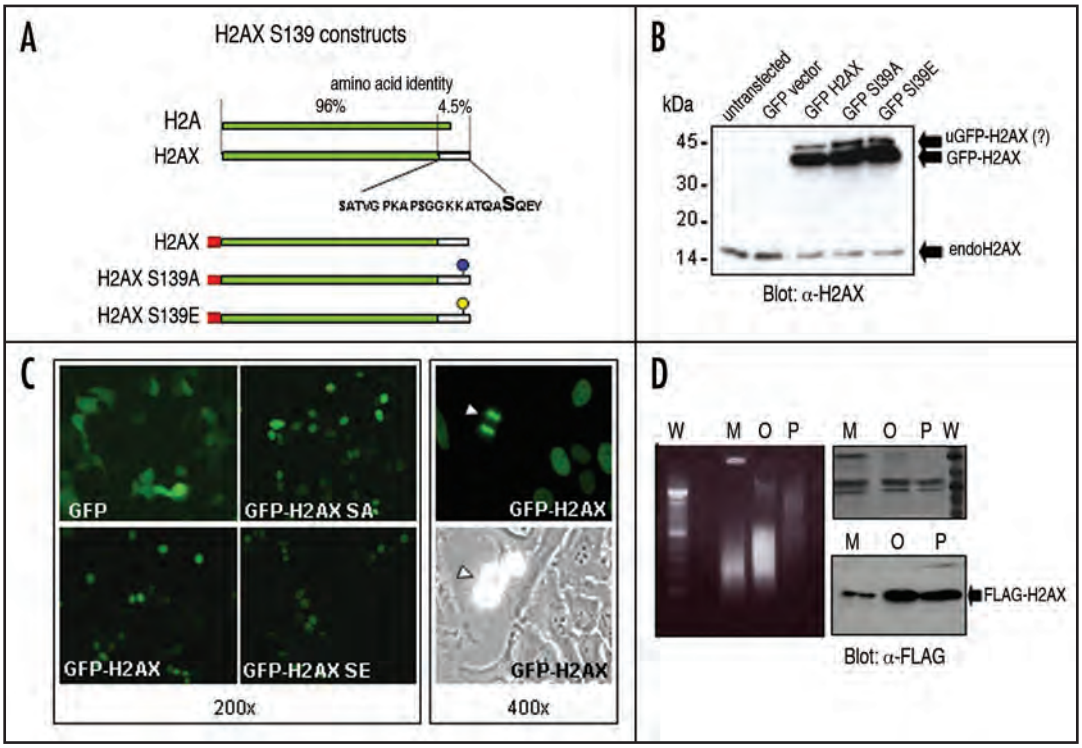

Figure 1. Expression of wild type H2AX and mutants. (A) Top diagram shows a comparison of H2A and H2AX indicating the percentage of amino acid similarity between the conserved part and the divergent tail. The amino acid sequence in the H2AX carboxy-terminal tail is depicted highlighting Serine 139. The bottom diagram shown wild-type H2AX, a mutant with a Serine139Alanine (S139A) mutation and a mutant with a Serine139Glutamic acid (S139E) mutation containing an N-terminal epitope (GFP or FLAG) tag. (B) Whole cell extracts of 293T cells transiently transfected with GFP Vector, GFP-H2AX, GFP-S139A and GFP-S139E were resolved by 12% SDS-PAGE and immunoblotted with α-H2AX antibody. Arrows indicate endogenous H2AX (endoH2AX), GFP-H2AX and slow migrating form of GFP-H2AX (uGFP-H2AX). (C) Left: Localization of ectopically expressed proteins in HeLa cells: GFP, note localization in nucleus and cytoplasm; GFP-H2AX, GFP-H2AX S139A and GFP-H2AX S139E localize exclusively to the nucleus; Right: HeLa cells in mitosis expressing GFP-H2AX (top) and phase contrast image of the same field (bottom), note localization in mitotic chromosomes. Magnification is 200x (left) and 400x (right). (D) Fractionation of nucleosomes in sucrose gradient. Ethidium bromide gel showing mono (M), oligo (O) and polynucleosome (P) fractions as indicated by a 100 bp marker (W), left; Coomassie-stained gel showing major histone components of all three fractions, top right; western blot with α-FLAG of all three fractions, bottom right.

genomic instability.[13,14] These data demonstrate that H2AX plays a key role in the DNA damage response.

After DNA damage, levels of γ-H2AX rise rapidly then decreased over several hours to return to pre-damage levels.[2] Removal of γ-H2AX is a necessary step to proceeding with the cell cycle.[15,16] This removal could happen by dephosphorylation of S139 residue and maintenance of nucleosome structure or, alternatively by degradation of γ-H2AX and subsequently nucleosome remodeling. However, it is still unclear what controls H2AX half-life.

Recently, it has been shown that *H2aX* may function as a haplo-insufficient tumor suppressor in the context of *Tp53* deletion.[17,18] Absence of H2aX seems to shift DNA repair towards an error-prone mode.[19] It is still not clear how disruption or decreased dosage of *H2aX* leads to cancer but induction of genomic instability in conjunction with defective DNA damage checkpoints seem to set the stage to cancer initiation. Fibroblasts from *H2aX* nullizygous mice display a functional G_2/M checkpoint at high doses of IR but defective at lower doses.[13,20] Conceivably, lower doses are a better model to study physiological responses to DNA damage as higher doses may trigger a series of redundant responses that may not be normally observed in living cells. Thus, these experiments suggest a role for H2AX in control of cell cycle.[20] However, information is still lacking on whether phosphorylation of serine 139 is required for the activation of the early G_2/M checkpoint in mammalian systems. Experiments in *S. cerevisiae* and *Schizosaccharomyces pombe* in which there was replacement of *yH2A* with mutants of Serine 129 (the corresponding residue to Serine 139 in H2AX) did not reveal any abnormal checkpoint response.[14,21,22] However, it is not surprising that there are intrinsic differences in the role of *H2AX* between the yeast and mammalian systems because *yH2A*, the ortholog of mammalian H2AX, makes up virtually all the H2A component in the yeast cell. Thus, in order to systematically address the role of H2AX post-translational modifications we characterized an experimental model of transient and stable expression of wild type H2AX as well as a series of Serine and Lysine mutants in its C-terminal tail.

Results

Epitope-tagged H2AX is correctly localized to nucleosomes. To investigate the role of H2AX Serine 139 phosphorylation, we engineered plasmids which contain GFP- or FLAG-tagged wild type (wt) H2AX, and mutants which harbor Serine to Alanine (S139A) or Serine to Glutamic Acid (S139E) substitutions (Fig. 1A). The S139E mutant was designed as a phospho-mimetic, whereas the S139A mutant cannot be phosphorylated at position 139. Western

blot analysis demonstrated roughly equivalent expression levels of wt and mutant GFP-H2AX forms and significant overexpression when compared to endogenous H2AX (Fig. 1B). Wt and mutant H2AX ectopically expressed in 293T cells localized exclusively to the nucleus and during mitosis GFP-H2AX was associated with chromosomes (Fig. 1C). Expression was also comparable among FLAG-H2AX forms with a slight difference in levels at 12 h and 24 h after transfection but reaching similar levels at 36 h (Suppl. Fig. 1A).

To rule out the possibility that the ectopically expressed H2AX forms were not incorporated in nucleosomes but loosely associated with chromatin we performed nucleosome fractionation studies (Fig. 1D). Using a sucrose gradient we obtained three fractions corresponding to mononucleosomes, oligonucleosomes and polynucleosomes as determined by ethidium bromide staining of the agarose gel (Fig. 1D; left). A parallel Coomassie staining of the SDS-PAGE confirmed the presence of major histone components in all three fractions (Fig, 1D; right, top). A western blot for the FLAG epitope confirmed the presence of the ectopically expressed H2AX even in the mononucleosome fraction (Fig. 1D, right, bottom). In summary, epitope-tagged H2AX forms are efficiently expressed by transient transfection, are localized in the nucleus and are incorporated into nucleosomes.

Because transient expression of GFP- or FLAG-H2AX forms resulted in levels of expression significantly higher than the endogenous H2AX protein, we tested whether this would lead to large scale changes in chromatin. Microccocal nuclease digestion of DNA from cells expressing FLAG-H2AX proteins did not reveal any difference when compared to untransfected cells (not shown). We also generated stable clones of 293T cells containing an integrated copy of a luciferase reporter gene driven by a GAL4 responsive promoter. Two independent clones were cotransfected with a FLAG-H2AX form and a GAL4 DNA binding domain (DBD) fusion to the transcription activating region of BRCA1.[23] Expression of H2AX forms did not significantly affect transcription of the reporter gene with the exception of wt H2AX in one of the clones (Suppl. Fig. 1B). In summary, epitope-tagged H2AX forms are efficiently expressed by transient transfection, are localized in the nucleus, and are incorporated into nucleosomes without causing major structural changes.

To confirm that the ectopically expressed H2AX could be phosphorylated after DNA damage, 293T cells expressing FLAG-H2AX and S139 mutants were irradiated with ten and 40 Gy and allowed 30 min for recovery. Ectopic wt H2AX was phosphorylated after DNA damage in a dose-dependent manner whereas the S139A and the S139E mutants fail to be phosphorylated (Suppl. Fig. 1C).

Stability of epitope-tagged H2AX depends on chromatin association. In order to determine whether the stability of different epitope-tagged forms varied in different compartments we transfected the wt, S139A and S139E mutants into 293T cells and incubated them for 36 hrs. This time point was chosen because all constructs showed their highest level and comparable expression (Suppl. Fig. 1A). Cells were then treated with cycloheximide to assess the stability of the ectopic proteins, irradiated or mock-treated, harvested at several time points following treatment and fractionated into cytosolic, nucleoplasm and chromatin fractions (Fig. 2A). While FLAG-H2AX forms were not detected in the cytoplasm (not shown), we detected two separate pools, one in the nucleoplasm and the other in the chromatin fraction (Fig. 2B). Levels of FLAG-H2AX forms rapidly decreased in the nucleoplasm fraction, in the presence and in the absence of IR. Multiple experiments failed to show any reproducible difference the in the half-life (~3.5 h) of FLAG-H2AX between irradiated and non-irradiated cells, and among the wt, S139A and S139E forms (Fig. 2B, compare top two rows).

Addition of proteasome inhibitors (PI) dramatically affected the steady state levels of the H2AX forms and indicated that their degradation is mediated by the proteasome (Fig. 2B; third row). Irradiated cells treated with PI were identical to non-irradiated ones (not shown). H2AX in the chromatin fraction was markedly more stable than the nucleoplasm fraction (Fig. 2B). We were unable to estimate the half-lives of the ectopic proteins in the nucleoplasm fraction in the presence of PI, or of proteins in the chromatin fraction because their increased stability called for longer incubation times with cycloheximide which lead to high toxicity.

While H2AX in the nucleoplasm was present as a single band of approximately ~16–18 kDa corresponding to the predicted molecular weight of FLAG-tagged H2AX (even in longer exposures), chromatin-associated H2AX presented at least two major bands, of ~16–18 kDa and ~25–27 kDa (Fig. 2B). Slight variations in molecular weight were due to different buffer conditions for fractionation. The ~9 kDa difference is suggestive of addition of one ubiquitin moiety. No consistent changes were seen upon irradiation (Fig. 2B, compare fourth and fifth rows). While a number of post-translationally modified forms of H2AX could be seen in the chromatin fraction, addition of proteasome inhibitor revealed additional post-translationally modified forms of H2AX. Their appearance following treatment with PI suggests that these are less stable forms that are stabilized by proteasome inhibition. While no other form was detectable in the nucleoplasm, we identified a large number of H2AX forms in the chromatin (Fig. 2B, sixth and seventh rows). To facilitate analysis we depicted in Figure 2C (right) all major and minor forms of H2AX encountered in different conditions after examining western blots results. The left panel in Figure 2C represents a long exposure of proteasome-treated chromatin fraction of wt H2AX. As the ladder pattern was indicative of ubiquitination we immunoprecipitated FLAG-tagged proteins from the cell lysate and probed the blot with anti-ubiquitin. A similar banding pattern emerged indicating that the major post-translationally modified H2AX forms were ubiquitinated (Fig. 2D).

Proteasome-dependent degradation is mediated by a modification of K119. Degradation by the proteasome has been shown to be mediated by ubiquitination of lysine residues in the target protein. To determine which lysine residue was the mediator of the degradation signal we constructed several mutants changing lysine residues present in the H2AX-specific tail (not present in H2A) for arginine as well as two lysines conserved in H2A (Fig. 3A). We treated cells with cycloheximide, harvested them at different time points, and analyzed the nucleoplasm fraction (Fig. 3A). Degradation was monitored by the disappearance of the signal and densitometric measurements were used to calculate the slope of the curves (Fig. 3B). The wild type K127R and K118R had similar slopes indicating that K118 and K127 play no significant role in the stability of H2AX (Fig. 3B). Mutants K134R and K133R displayed a slightly steeper slope suggesting that substitution of these residues slightly decreases the stability of H2AX, perhaps by shifting ubiquitination towards other sites. Mutant K119R is significantly more stable than other

forms indicating that K119 is the site targeted by a post-translational modification that controls H2AX stability (Fig. 3A and B).

In order to investigate whether the stabilization of H2AX by post-translational modification was dependent on the status of S139 we generated a series of double mutants, combining the mutants in S139 with the mutants with the K mutants. Mutation K119R conferred stability to all forms of H2AX independent of S139 (Fig. 3C). In addition, no other K mutant was able to significantly alter the stability of the other S139 forms of H2AX.

K119 is modified by ubiquitination and is not required for phosphorylation of S139. To determine whether K119 was post-translationally modified by ubiquitination we co-transfected cells with FLAG-H2AX or its S139 mutants and His-tagged ubiquitin. The chromatin fraction was used for pull-down assays with Nickel beads and blots were probed with α-H2AX antibody revealing that all forms of H2AX S139 mutants are ubiquitinated (Fig. 4A). However, there is a significant decrease in the precipitated band in cells transfected with K119R when compared with other forms (Fig. 4A). Note that input is comparable for all forms of H2AX. To verify whether this modification was also found in the endogenous H2AX we transfected cells with His-tagged ubiquitin only and increased the amount of protein loaded in the gel (Fig. 4B). A ubiquitinated endogenous H2AX form is present in cells in the presence and absence of irradiation (Fig. 4B). We noticed a slight increase in the ubiquitinated form after irradiation but this increase was not consistent over different experiments. Pull-down with Nickel beads and probing with α-FLAG antibody confirmed that H2AX K119R fails to be efficiently ubiquitinated (Fig. 4C). Also, mutant K119R can be phosphorylated at S139 (Fig. 4D arrow) when cells are subjected to DNA damage indicating that ubiquitination of K119 was not required for efficient phosphorylation of S139.

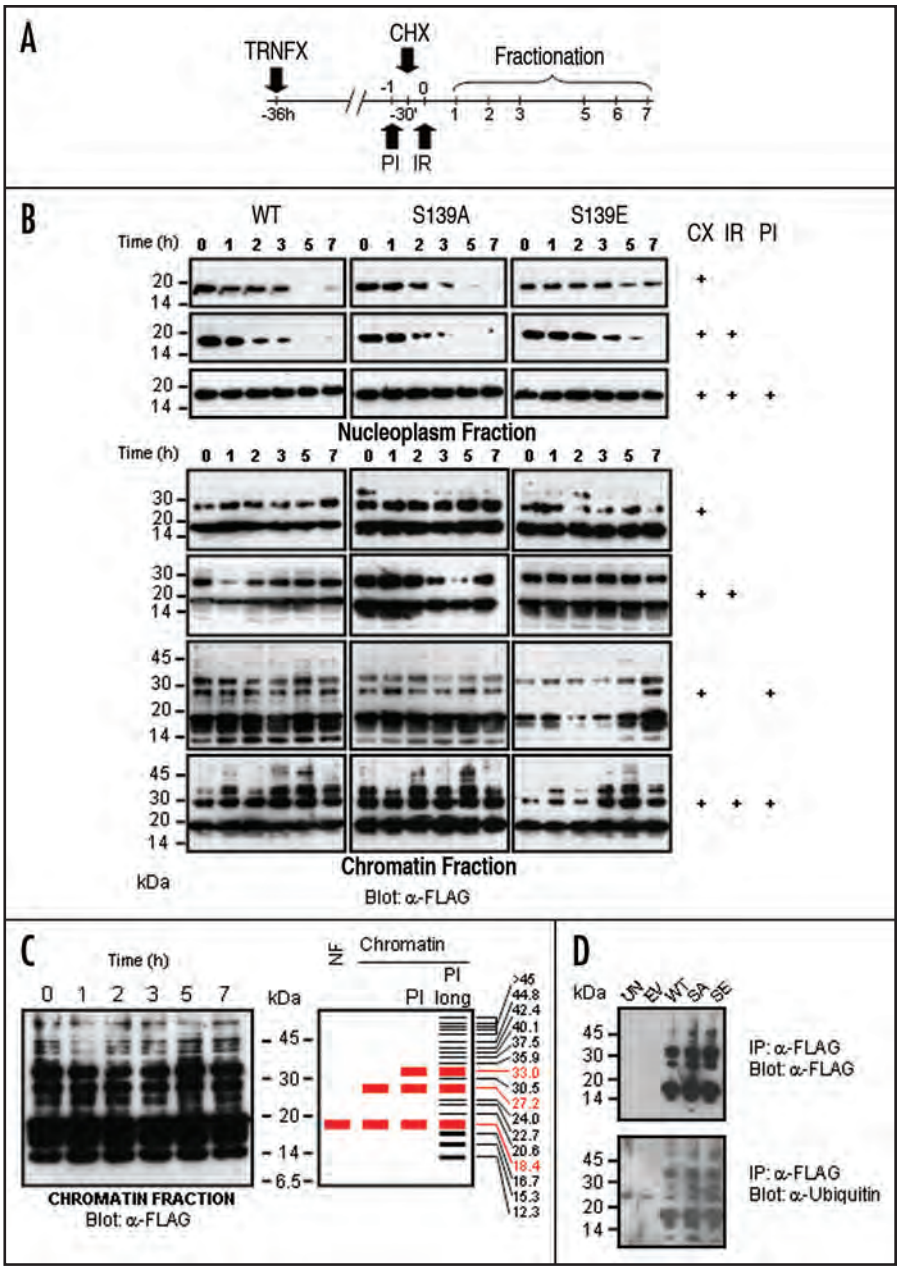

Figure 2. Post-translational modifications of ectopically expressed proteins. (A) Diagram illustrating the time course of treatment with proteasome inhibitors (P1), cycloheximide (CHX) and irradiation (IR). (B) Subcellular fractionation. Top three rows show nucleoplasm fraction levels of FLAG-H2AX forms after treatment with cycloheximide (first row), cycloheximide and irradiation (second row), and cycloheximide, irradiation and proteasome inhibitors (third row). Bottom four rows show chromatin fraction levels after treatment with cycloheximide (fourth row), cycloheximide and irradiation (fifth row), cycloheximide and proteasome inhibitors (sixth row) and cycloheximide, irradiation and proteasome inhibitors (seventh row). (C) A typical long exposure blot of chromatin fraction of FLAG-H2AX treated with cycloheximide, irradiation and proteasome inhibitors (left). A diagram detailing the major forms present after different treatments was derived (right). NF, nuclear fraction; PI, treated with proteasome inhibitors; PI Long, long exposure. (D) Lysates from cells transfected with empty vector (EV), FLAG-H2AX wild type (WT), FLAG-H2AX S139E (SE), FLAG-H2AX S139A (SA) and untransfected (UN) were immunoprecipitated with anti-FLAG antibody. Top panel is probed with anti-FLAG antibody to demonstrate expression. Bottom panel is probed with anti-ubiquitin.

Mutation of S139 to alanine leads to chromosomal aberrations. We generated a series of HCT116 cell line derivatives expressing the wt, S139A and S139E forms under the control of a Tet-Off system (Fig. 5). The S139E mutant was not efficiently repressed by the presence of doxycyclin and induction by removal of doxycyclin did not increase S139E beyond non-induced levels (Fig. 5A). We also observed some leakage of the wild type H2AX in the presence of doxycyclin but levels were significantly increased upon induction (Fig. 5A). The S139A mutant showed a tight regulation with very low levels of ectopic expression in non-induced conditions and a significant inducibility upon removal of doxycyclin (Fig. 5A). Cell lines were induced for seven days and their karyotype was analyzed. There was no significant difference in modal number of chromosomes in

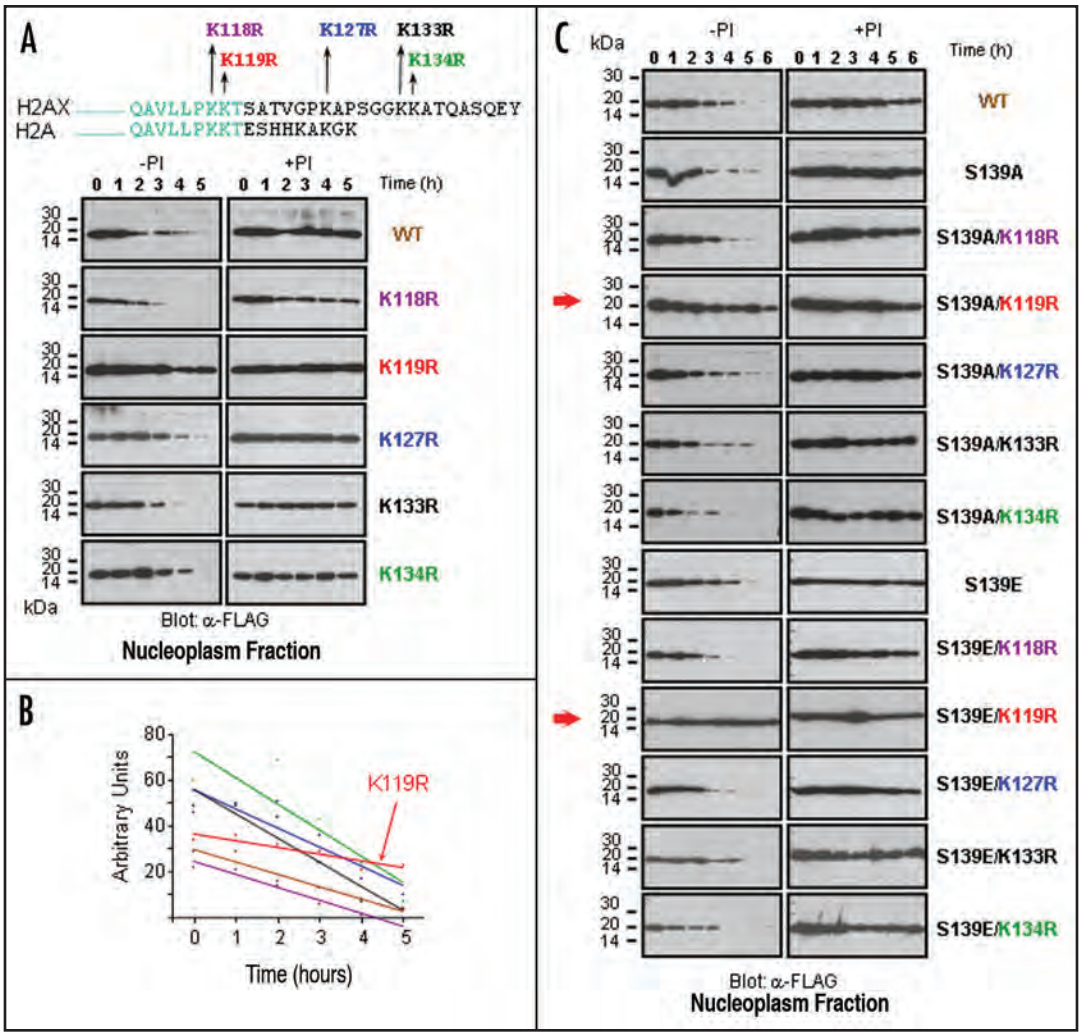

Figure 3. Mutation of Lysine 119 stabilizes H2AX protein levels. (A) Diagram showing amino acid sequence of H2AX and H2A C-terminal tail and sites of substitutions of Lysine residues to Arginine (top). Cells were transfected with different mutants and treated with cycloheximide in the presence (right) or absence (left) of proteasome inhibitors (PI). Cells were harvested and lysates were examined for the levels of FLAG-tag H2AX and its mutants at different time points. Note that K119R mutant is significantly more stable than all other constructs. (B) Densitometric measurements from the blots shown in (A) were used to plot the disappearance of H2AX mutants. Line colors correspond to different mutants as shown in (A). Note that the curve representing H2AX K119R has a clearly different slope from the wt or from the other mutants. (C) Double mutants of S139 and several K residues. Cells were transfected with different mutants and treated with cycloheximide in the presence (right) or absence (left) of proteasome inhibitors (PI). Cells were harvested and lysates were examined for the levels of FLAG-tag H2AX and its mutants at different time points. Note that K119R mutant is significantly more stable than all other constructs in the context of S139A or S139E (red arrows).

any of the cell lines (Suppl. Fig. 2). However, induced S139A cells displayed 11% of mitosis with chromosome abnormalities such as triradials and quadriradials (Fig. 5B). No gross abnormalities were found in non-induced S139A, or in induced or non-induced S139E or wild type.

H2AX mutants induce apoptosis and perturbation of G_2/M cell cycle checkpoint. During the course of our studies, we noticed that the S139A or S139E mutant appeared induce moderate cell death following transient transfection. Thus, we transiently transfected the GFP-H2AX forms into HeLa cells and quantified apoptosis by Annexin-V binding. This assay revealed a higher percentage of Annexin-V positive cells in both the S139E and the S139A transfected cells compared to wt H2AX (Fig. 6A). Increased apoptosis was confirmed by higher caspase-3/7 activity which was detected following expression of both mutants compared to wt H2AX (Fig. 6B). These results demonstrate that ectopic expression of H2AX S139A or S139E mutants induce apoptosis.

Recent studies have shown that one of the first detectable physiological events after IR is phosphorylation of histone H2AX at Serine 139.[2] Therefore we tested whether transfection of the H2AX S139E mutant would trigger the G_2/M checkpoints by assessing early G_2/M arrest (also called transient G_2/M checkpoint) as well as G_2 accumulation, which have been described as two different mechanisms for G_2/M arrest.[24] The early G_2/M checkpoint was assessed using histone H3 phosphorylated at Serine 10 (pH3), as marker for mitosis in a flow cytometric assay.[24,25] Analysis of the GFP-positive cell populations that stained for pH3 revealed that expression of the S139E mutant caused a significant reduction in the percentage of cells in mitosis, compared to the GFP negative cells (Fig. 6C). We also observed a modest reduction of cells in mitosis in GFP positive cells

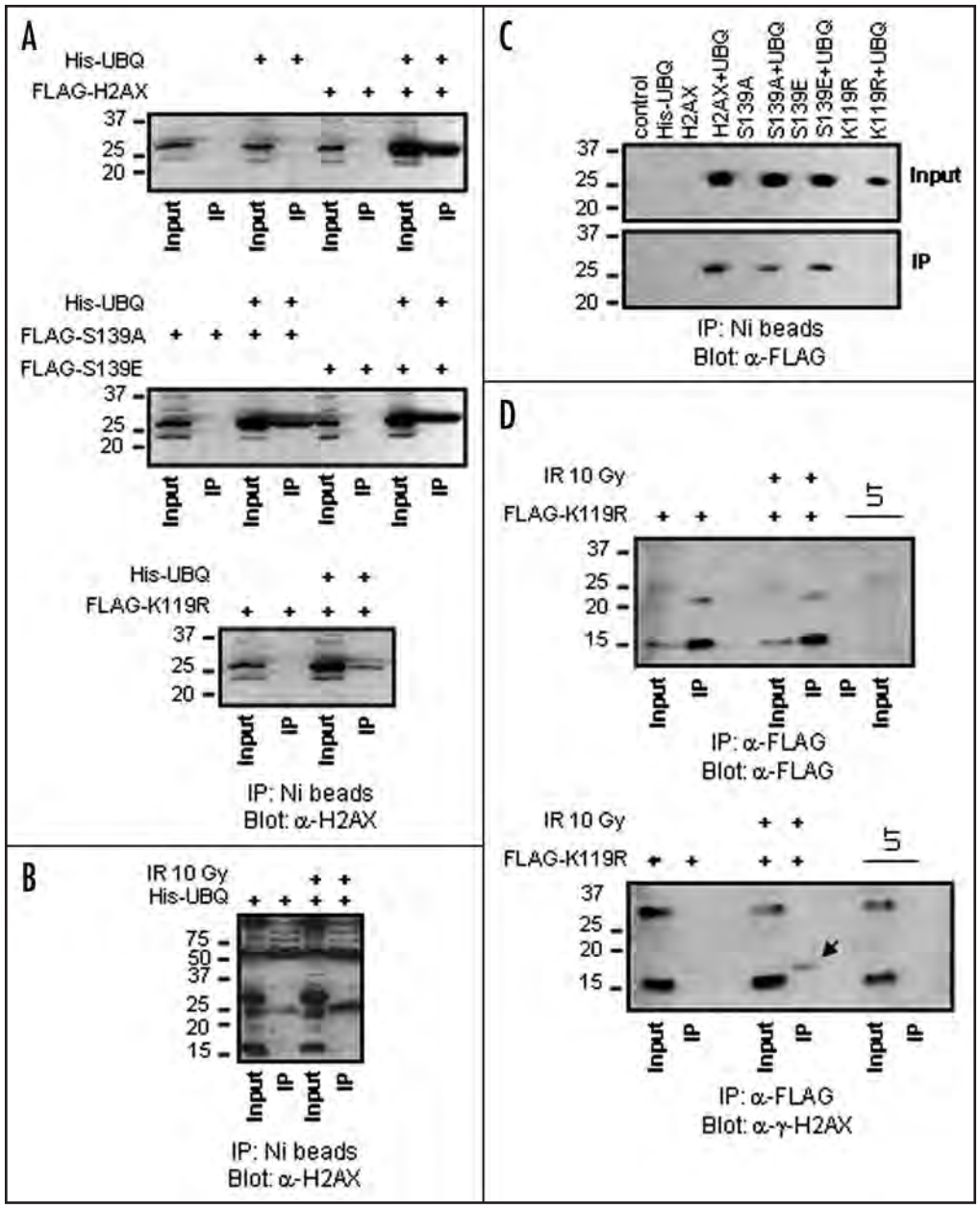

Figure 4. Ubiquitination of H2AX on K119. (A) Cells were co-transfected with constructs expressing His-tagged ubiquitin and FLAG-H2AX (top), FLAG-S139A, FLAG-S139E (middle), or FLAG-K119R (bottom). Lysates were precipitated (IP) with Ni-beads and blots were probed with α-H2AX. Note band corresponding to ubiquitinated H2AX in wt, S139A and S139E mutants but significantly reduced band in K119R mutant (bottom). (B) Cells were transfected with His-tagged ubiquitin and irradiated with 10 Gy after 24 hr post-tranfection. Lysates were precipitated (IP) with Ni-beads and blots were probed with α-H2AX. (C) Cells were co-transfected as in (A). Lysates were precipitated (IP) with Ni-beads and blots were probed with α-FLAG. Note band corresponding to ubiquitinated H2AX in wt, S139A and S139E mutants but absent in K119R mutant (bottom). (D) Mutation of K119 does not prevent phosphorylation of S139. Cells were transfected with FLAG-K119R and irradiated (IR) or mock-treated. Note band corresponding to phosphorylated S139 H2AX in α-FLAG immunoprecipitate only in presence of irradiation (black arrow). UT, untransfected.

transfected with the S139A mutant and wt H2AX. To assess G_2 accumulation, 293T cells were transfected with the GFP-S139E mutant for 48 h and stained with propidium iodide. Analysis of cell cycle histograms of the GFP negative and positive populations revealed no significant changes in cell cycle phase distribution following transfection of the S139E mutant (Suppl. Fig. 3A). This indicates that the S139E mutant has no effect on G_2/M accumulation.[24] While these data suggest that the S139E causes an early G_2/M arrest it is possible that this mutant exerts its effects in other cell cycle compartments that lead to a decrease in the percentage of cells in mitosis.

We next tested whether phosphorylation of S139 was necessary for IR-induced early G_2/M arrest. 293T cells were transfected with either the S139A mutant or wt H2AX and treated with 6 Gy of γ-radiation. Analysis of the GFP positive cells demonstrated that the S139A mutant partially suppressed early G_2/M arrest following IR (Fig. 6D).

Based on data in the transient experiments showing that the H2AX mutants partially suppressed early G_2/M arrest by IR (S139A), or triggered G_2/M arrest in the absence of IR (S139E) we set out to determine the effects of these perturbations on the sensitivity to DNA

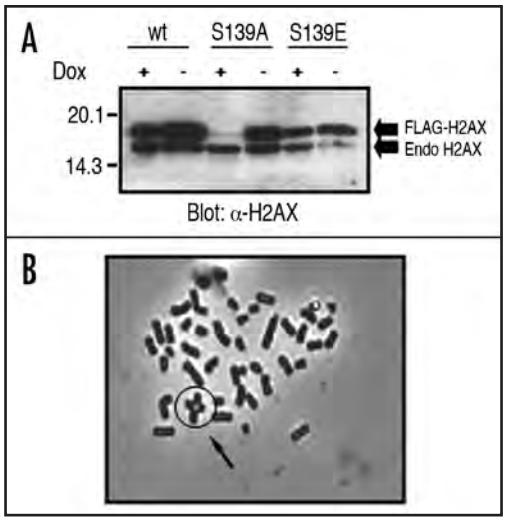

Figure 5. Induction of chromosome abnormalities in cells expressing H2AX S139A. (A) HCT116 Tet-off clones of cells expressing inducible FLAG-H2AX or mutants in the presence or absence of doxycyclin (Dox). (B) Chromosome spreads showing a chromosomal aberration (red circle, black arrow), a quadriradials, found in cells expressing H2AX S139A.

damage. To achieve that, we generated stable cells lines expressing GFP, GFP-H2AX, GFP-H2AX S139A or GFP-H2AX S139E (Suppl. Fig. 3B) and treated them with increasing doses of the radiomimetic drug MMS (Fig. 6E). While expression of wild type H2AX or the S139E mutant did not affect sensitivity to MMS, cells stably over-expressing GFP-S139A displayed a markedly increased sensitivity (Fig. 6E). These results suggest that the S139A mutant impairs, directly or indirectly, DNA damage repair in these cells.

γ-H2AX has been shown to colocalize with several DNA damage response factors, including 53BP1, after DNA damage.[26] Thus, we hypothesized that expression of the S139A or S139E mutants might induce IR-induced focus formation and colocalize with 53BP1. HeLa cells were mock transfected, or transfected with GFP-H2AX, GFP-S139A or GFP-S139E mutants, followed by immunostaining for 53BP1. 53BP1 staining of undamaged cells revealed a faint background punctate staining in every cell in the population with a few large 53BP1 foci (Fig. 7A, first row, first column, arrow). Once irradiated cells presented with several large IR-induced 53BP1 foci (Fig. 7A, first column, second row). The number of these large IR-induced foci was determined in the following manner. The average number of 53BP1 foci per GFP-positive cell was determined

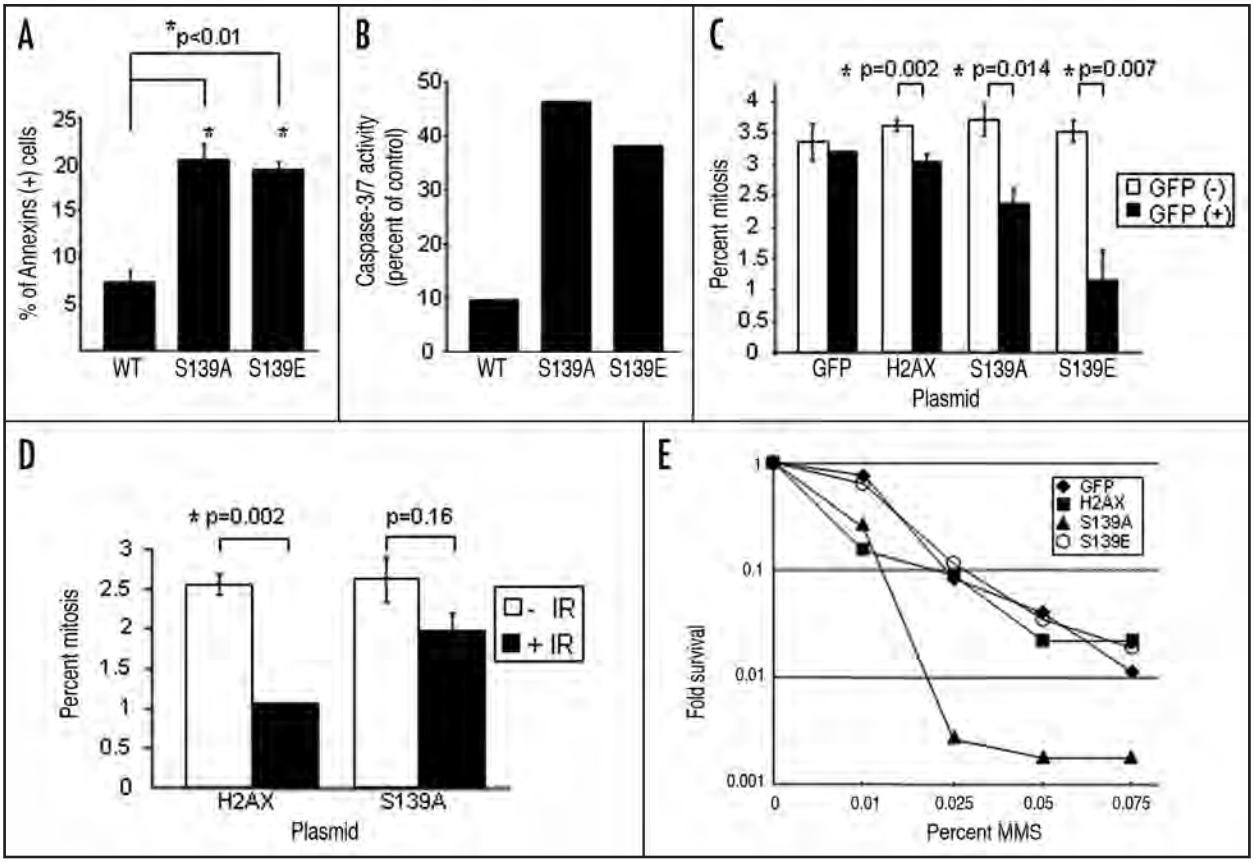

Figure 6. Effects of H2AX mutants on apoptosis and cell cycle checkpoints. (A) HeLa cells were transfected with GFP-H2AX, S139A or S139E and the percent increase of Annexin-V positive cells in the GFP positive cell population compared to the GFP negative cells in each sample was calculated. (B) HeLa cells were analyzed for caspase-3/7 activity 24 hours after transfection of H2AX, S139A, or the S139E constructs. Activity is relative to mock-transfected control cells. (C) Expression of S139E mutant triggers G_2/M arrest in the absence of DNA damage. 293T cells were transfected with GFP, the GFP Vector, GFP-H2AX, S139A or S139E for 48 hours, and the percentage of cells in mitosis was quantified by phosphorylated histone H3 (Serine 10) by flow cytometry. Comparisons of the percentage of mitotic cells between GFP Negative and GFP Positive cells were made. (D) Expression of S139A mutant abrogates the ionizing radiation-induced G_2/M arrest. 293T cells were transfected with the indicated constructs, irradiated with 6 Gy and analyzed one hour post-irradiation for phosphorylated histone H3. (E) Stable cell lines were treated with increasing doses of MMS for 50 minutes. Viability after 48 hours was measured by trypan blue exclusion.

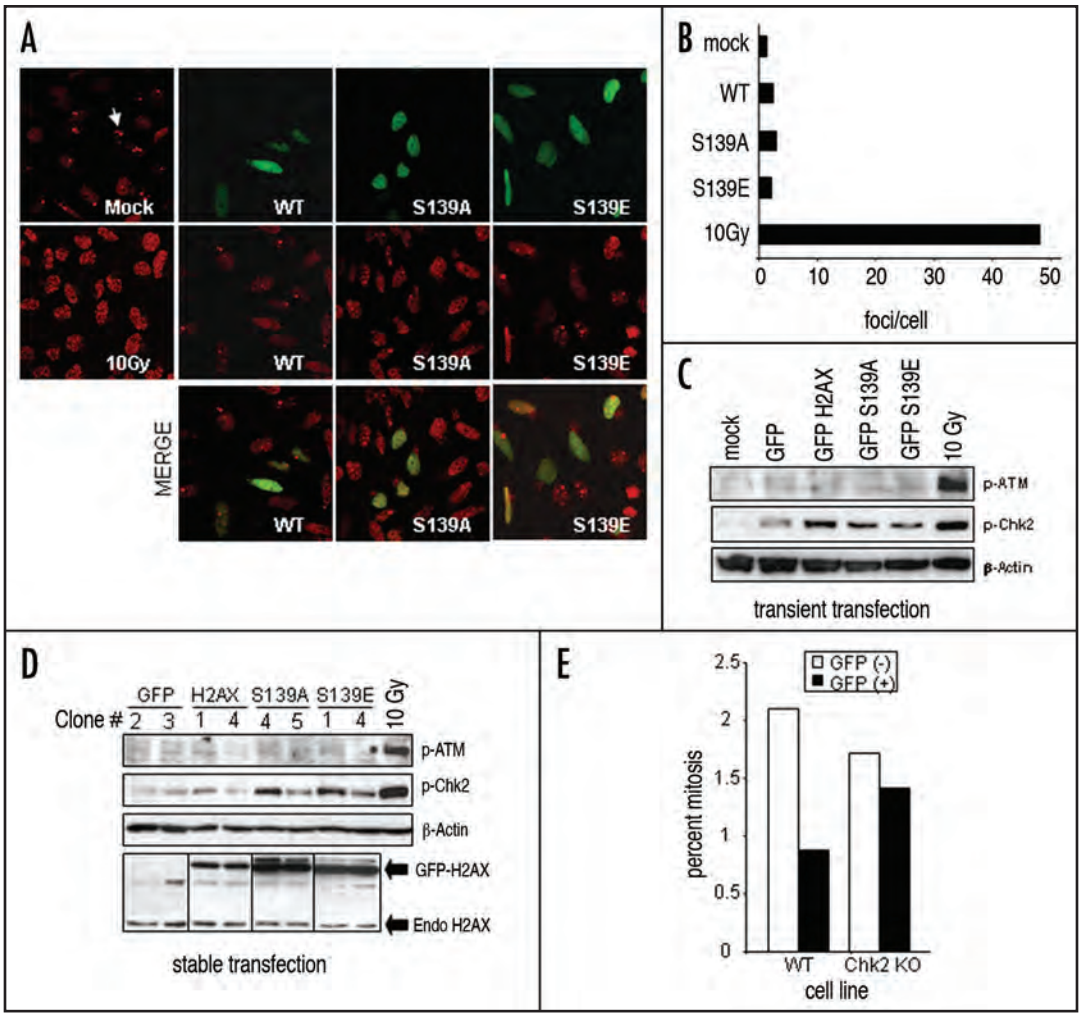

Figure 7. H2AX S139E does not induce 53BP1 foci. (A) HeLa cells were transfected with the indicated GFP-tagged constructs (green) and immunostained with 53BP1 antibody (red). Mock transfected and cells irradiated with 10 Gy are also shown (left columns). Images are at 630X magnification. The last row represents the merged images. (B) For mock-transfected cells, the number of foci per cell was quantitated automatically. For GFP-histone transfected cells, the number of foci per green cell was counted. (A) Expression of S139A or S139E activate Chk2. Whole cell lysates of 293T cells transiently transfected with the indicated constructs were immunoblotted with anti phospho-ATM Ser 1981 (top), Phospho Chk2 Thr 68 (middle) and β-Actin antibodies (bottom). An untransfected sample irradiated with 10 Gy is also shown. (D) Immunoblot analysis for phospho-ATM, phospho-Chk2, β-Actin and H2AX in HeLa clones stably expressing GFP, GFP-H2AX, GFP S139A and GFP S139E. (E) Chk2 is required for efficient early G_2/m arrest by GFP-S139E. HCT116 wild-type or Chk2$^{-/-}$ cells were transfected with GFP-S139E for 48 hours, and the percentage of GFP positive and negative cells in mitosis was calculated by phospho-H3 reactivity.

for the transfectants, whereas the number of foci per total number of cells was calculated for the mock transfected sample. This analysis demonstrated no significant induction of 53BP1 foci by any of the GFP-H2AX forms (Fig. 7A and B, compare with irradiated sample). Also, no difference was seen in number of foci between GFP-positive and GFP-negative cells in the same sample (Fig. 7A). In contrast, irradiating HeLa cells with 10 Gy induced ~48 foci per cell. These results demonstrate that the S139A or S139E mutants are not sufficient to induce foci that colocalize with 53BP1 and suggest that the observed effects on cell cycle checkpoint and apoptosis are independent of IR-induced foci formation.

To determine whether the H2AX forms activated other proteins involved in the DNA damage pathway, whole cell lysates of 293T cells transfected with the various H2AX forms were subjected to western blot analysis for phosphorylation of Ser1981 in ATM, Thr68 in CHK2 and Ser343 in NBS1. We barely detected any activation of ATM in transiently or stably transfected cells as judged by phosphorylation of Ser1981 (Fig. 7C and D, Top). Similarly, we did not detect any activation of NBS1 after transient or stable transfection of the various H2AX forms (not shown). However, we observed an increase in phosphorylation of Thr68 of CHK2 in both stable clones and transiently transfected cells (Fig. 7C and D). A small but significant activation was also seen in cells expressing GFP alone (Fig. 7C). We also observed similar activation of CHK2 upon transfection of FLAG-H2AX forms ruling out that the activation was due to the GFP moiety (data not shown). In stable clones, expression of the mutant forms induced a higher level of activation of CHK2 than the expression of the wt but that could be due to difference in expression levels in the stable clones (Fig. 7D). Importantly, H2AX expression levels in early passage clones were roughly equivalent for all GFP-H2AX forms but levels of wt GFP-H2AX decreased with passage (not shown). These data show that the effect on cell cycle

regulation and apoptosis described here seem to be independent of NBS1 activation and also independent of 53BP1 foci formation.

To determine whether CHK2 played a role in the effects of the H2AX mutants on the cell cycle, the ability of the GFP-S139E mutant to decrease the number of cells in mitosis in HCT116 wild-type and *CHK2* deficient cells was determined. Our data show that the S139E mutant induced a decrease in mitotic cells in the parental HCT116 cells, but failed to induce arrest in *CHK2*-deficient cells to the same extent (Fig. 7E). However, transfection of the S139A mutant into *CHK2*-deficient cells displayed the partial suppression of IR-induced G_2/M arrest seen in parental HCT116 (data not shown). These data suggest that CHK2 plays a role downstream of S139E, but does not appear to play a role in partial suppression of arrest by the S139A mutant after IR.

Discussion

Ectopic expression of H2AX as a model to study its function. We developed and characterized a series of reagents to study the biology of histone H2AX. The first series used an N-terminal FLAG tag fused in frame to the wild type H2AX, to H2AX with Ser139 mutated to Glutamic acid (S139E), or to H2AX with Ser139 mutated to Alanine (S139A). The S139E substitution was designed to behave as a phosphorylation mimic as this strategy has been successful in a number of different approaches.[27,28] Conversely, the S139A substitution was designed to represent an unphosphorylatable form of H2AX.

To monitor the association of the ectopic H2AX with chromatin we also generated a series of N-terminal GFP-tagged constructs. Other groups, studying histones have used GFP-histones successfully.[29-31] The GFP-histones were exclusively nuclear showing that the N-terminal fusion did not impair its nuclear localization. In addition, in mitotic cells GFP-H2AX was exclusively localized to the metaphase chromosomes. Similar results were obtained by another laboratory.[32] Tagged histones were present in fractions of purified mono and oligonucleosomes confirming that they are included into nucleosomes in vivo, and not just loosely associated with chromatin. In addition, ectopically expressed wt H2AX behaved similarly to endogenous H2AX as it was efficiently phosphorylated upon DNA damage.

Micrococcal nuclease digestion and transcriptional assays in cells expressing wt or mutant H2AX did not reveal large scale differences in chromatin structure when compared to untransfected cells. These results suggest that addition of epitope tags do not distort chromatin structure, in agreement with previous observations that incorporation of even a relatively large ubiquitin moiety in H2A has little effect on nucleosome structure.[33] It also suggests that absence (S139A mutant) or constitutive presence of a phosphorylation mimic (S139E mutant) does not lead to large scale changes in chromatin structure. Interestingly, expression of yH2A S129E (corresponds to H2AX S139E in humans) mutant in yeast led to a more relaxed chromatin suggesting that phosphorylation of yH2A could be acting to make the damaged sites more accessible to repair factors.[21] This discrepancy can be explained by taking into account the difference in relative composition of H2AX between yeast and mammalian cells. In the yeast experiment expression of yH2A S129E was obtained in a background lacking wt yH2A, thus it is expected that the mutant will make up close to 100% of the H2A pool in the cell. In mammalian cells H2AX make up from 5–20% of the total H2A component.[2] In our experiments mutants were expressed in addition to the endogenous H2A and its variants so that the levels of mutant H2AX incorporated in chromatin may not be enough to lead to large scale changes, although it is possible that more subtle changes occur.

Our system has several advantages but it also has inherent caveats. First, it is difficult to control or estimate the amount of H2AX as a fraction of the H2A component in the cell. Second, some results obtained after transient transfection could be due to an acute response to a change in the balance of H2A component. Likewise, cells expressing H2AX in a stable or inducible manner may undergo adaptation. The use of a combination of expression strategies should help in the interpretation of the results. Lastly, the S139E mutant which mimics DNA damage-induced phosphorylation of H2AX is expected to be homogenously distributed on the chromosome, different from the localized phosphorylation associated with DSB. In this sense, our model may better reflect diffuse H2AX phosphorylation caused by UV exposure.[34]

A role for K119 in H2AX turnover. Here we demonstrate that ectopically expressed H2AX was present in two cellular pools: chromatin and nucleoplasm. H2AX in the chromatin pool presented a much longer half-life than in the nucleoplasm. H2AX underwent post-translational modification by the addition of ubiquitin. The pattern of ubiquitination found in our experiments suggests that monoubiquitination is the major ubiquitinated form of H2AX. Upon stabilization by proteasome inhibitors a multiple ubiquitin conjugated form appeared. Mutation of K119 abolished ubiquitination and resulted in a stabilization of H2AX indicating that that ubiquitination of K119 is required for proteasome-dependent degradation. Interestingly, K119 is also the site of ubiquitination in H2A.[35] Proteasome inhibitors increased H2AX half-life suggesting that its turnover is mediated by the proteasome. This scenario is similar to that of H2A in HeLa cells in which ubiquitinated H2A turned over at a faster rate than non-modified H2A.[36]

A limitation of our studies is that half-life experiments were conducted in the nucleoplasmic pool and not on the chromatin pool. Histone proteins in chromatin are known to be extremely stable varying from ~100 h for H1 microinjected in HeLa nuclei to several days for other histones in mammalian cells in vitro and in vivo.[37-39] Longer incubation with cycloheximide induced severe toxicity which precluded experiments with the chromatin fraction.

In contrast to previously published data,[40] we found that ubiquitination of FLAG-H2AX was not dependent on DNA damage. Moreover, in our experiments phosphorylation of S139 was not required for ubiquitination of K119. One possible explanation for this discrepancy might be that the difference is quantitative rather than qualitative. Thus, experiments performed at the threshold of detection where ubiquitination is not detected under undamaged conditions but detected when cells are subjected to DNA damage, might be interpreted as ubiquitination been dependent on DNA damage. On the other hand experiments that are performed with more material might not reveal small changes. The modest enhancement of ubiquitination of H2A by RNF80 upon irradiation[41] suggests that changes may be small.

A role for S139 in cell cycle control and apoptosis. Our results demonstrate that ablation of the phosphorylation site by a

substitution to Alanine attenuated the IR-induced early G_2/M arrest. Similar results suggesting that phosphorylation of H2AX is required for early G_2/M arrest at low doses of IR were obtained in mouse cells nullizygous for *H2AX*.[20] Cells overexpressing the S139A mutant were also more sensitive to DNA damage, consistent with previously published results with yeast expressing a S129A mutant[22] and with H2AX-deficient cells.[13,14] Taken together these data indicate that overexpression of the S139A mutant results in a phenotype comparable to *H2AX*$^{-/-}$ cells and lends support to the notion that H2AX phosphorylation is required for checkpoint activation in mammalian cells.

Also, expression of H2AX S139E mutant leads to a significant decrease in the number of cells in mitosis. Irradiating cells expressing S139E with high doses of IR further reduced the fraction of cells in mitosis (data not shown) suggesting that this is a partial effect. There are several scenarios that can explain these observations. Because the effects of this mutant can be felt independent of external stimuli they could start after the expression levels reach a minimal threshold. Thus, a decrease in mitotic cells could be due to longer retention times of cells in other compartments due to G_1 arrest, S-phase delay, G_2 accumulation, or activation of early G_2/M checkpoint. It could also be due to shorter retention times in the mitotic compartment due to an accelerated mitotic exit. Flow cytometry analysis of propidium iodide-stained cells did not show increased accumulation of cells in G_1 or in G_2, which would indicate G_1 arrest or G_2 accumulation, respectively. However, it is still possible that S139E mutant causes S-phase delay, activation of G_2/M checkpoint or accelerated mitotic exit. Further research will be needed to clarify this issue.

Interestingly, expression of this mutant did not induce formation of 53BP1-containing foci in agreement with previous studies in mouse cells.[18] While transfection of either wt H2AX or the S139A mutant also resulted in a decrease in the percentage of cells in mitosis, these effects were very modest when compared to expression of the S139E mutant. It is possible that levels of H2A variants are tightly controlled and perturbations may result in small effects on cell cycle regulation.

H2AX is phosphorylated by ATM, ATR or DNA-PK in response to different stimuli with partially overlapping specificity.[7,8] Change in the overall tension and compaction of chromosomes have also been suggested as sufficient to trigger the DNA damage response.[42,43] We did not detect large scale changes but Heo et al. have shown that in experiments done in vitro, H2AX phosphorylation alters nucleosome structure.[44] Importantly, although we were unable to detect significant ATM activation upon transient or stable transfection of any of the H2AX forms, we did detect phosphorylated CHK2 in stable cell lines overexpressing H2AX, S139A and S139E. It is possible that CHK2 activation observed is a result of subtle changes in chromatin structure due to expression of the ectopic H2AX forms that trigger a low level ATM activity that cannot be detected by the methods (and antibody) used.

To determine the role of CHK2 in the S139E-induced decrease in mitotic cells we transfected wild type and *CHK2*-deficient HCT116 cells with the S139E and the S139A mutants. These experiments showed that although all H2AX forms activated CHK2 to some degree, absence of CHK2 partially abrogated the decrease in the percentage of cells in mitosis induced by the S139E mutant and did not have any effect on the modest arrest induced by the S139A mutant. We propose that there are additional factors involved that have not been identified that account for the molecular signals triggered by the H2AX mutants. Taken together, our data suggest that the effects of the S139E mutant on the cell cycle are at least partially dependent on CHK2 but are independent of 53BP1 focus formation.

Both the S139A and S139E mutant induce apoptosis to higher levels than wt H2AX. However, it is unclear if both mutants induce apoptosis through the same mechanism. It is conceivable that continuous presence of a damage signal over long periods of time, as represented by the S139E mutant, may lead to cell death. Induction of death by the S139A mutant might be due to accumulation of damage from replication errors in the context of a defective checkpoint. Alternatively, it has been shown that serine 139 is required for proper homologous recombination function[19] and this may lead either mutant to trigger apoptosis using the same mechanism.

The data presented here support the notion that histone H2AX has a pleiotropic role in the DNA damage response with the ability to modulate cell cycle control responses and apoptosis. Our data also suggests a role for CHK2 in cell cycle control mediated by H2AX. A role for CHK2 in cell cycle control by H2AX is consistent with recent experiments in yeast.[15,45] In yeast cells deficient for *PPH3*, the phosphatase that dephosphorylates γ-H2AX during damage repair,[15] the sustained activation of Rad9 and Rad53 (the yeast CHK2 homolog) correlated with the maintenance of G_2/M arrest.[15]

Experiments using mice with disrupted *H2AX* gene have revealed that H2AX plays an important role in the DNA damage response in mammalian cells.[13,14,17,18] However the mechanism by which H2AX exerts its effects has remained largely unknown. A tractable system to investigate the role of the Serine 139 phosphorylation has been established in the yeast *Saccharomyces cerevisiae* using replacement of yH2A gene (the ortholog of mammalian H2AX) with Serine 129 (the corresponding residue in yH2A) mutants.[21,22] However, it is unclear whether results from yeast can be generalized to mammalian systems given the intrinsic differences in the DNA damage pathways in yeast and mammalian cells, particularly at the level of CHK1 and CHK2 kinases.[46,47] For example, phosphorylation of serine 129 in yeast does not seem to affect cell cycle checkpoints.[21,22]

In the present paper we established a mammalian system of ectopic expression of H2AX and its mutants and discussed its advantages and potential pitfalls. We believe that such a system may represent a useful tool to study the biological role of histone H2AX.

Material and Methods

Constructs. GAL4 DBD BRCA1 (aa 1396–1863) was previously described.[48] Human histone *H2AX* (OMIM 601772) cDNA was obtained by PCR from a human mammary gland cDNA library (Clontech, Mountain View, CA), using the following primers: H2AX-(S)-EcoR1 (5'ATG AAT TCA TGT CGG GCC GCG GCA AGA C-3') and H2AX-(AS)-BamH1 (5'-TTG GAT CCT TAG TAC TCC TGG GAG GCC T-3'). The PCR product was cloned into pKS-Bluescript (Stratagene) and confirmed by sequencing. Mutants of Serine 139 to Alanine (S139A) and of Serine 139 to Glutamic acid (S139E) were generated by site-directed mutagenesis of the wild type construct using primers: for S139A (H2AX-(S)-EcoR1 and; H2AX S139A-(AS)-BamH1: 5'-TTG GAT CCT TAG TAC TCC TGG GCG GCC TGG GT-3'); for S139E (H2AX-(S)-EcoR1 and;

H2AX S139E-(AS)-BamH1: (5'-TTG GAT CCT TAG TAC TCC TGC TCG GCC TGG GT-3'). The wild type and mutant H2AX forms were then subcloned in frame to an N-terminal fusion of GFP in pEGP-C3 (Clontech) into pCMV FLAG2 (Sigma) in frame to an N-terminal fusion to FLAG epitope. To obtain pTRE-H2AX, pTRE-H2AX S139E and pTRE-H2AX S139A, we digested pKS-Bluescript containing the different H2AX forms with EcoR1 and BamH1 and ligated the inserts into similarly digested pTRE vectors (BD Biosciences).

Mutants of Lysine residues (K118R, K119R, K127R, K133R and K134R) were obtained through site-directed mutagenesis using the following primers: For K188R (K188R-S: 5'-CGT GCT GCT GCC CAG GAA GAC TAG TGC CAC CGT GGG GCC G-3'; K188R-AS: 5'-CGG CCC CAC GGT GGC ACT AGT CTT CCT GGG CAG CAG CAC G-3'); for K119R (K119R-S: 5'-CGT GCT GCT GCC CAA GAG GAC TAG TGC CAC CGT GGG GCC G-3'; K119R-AS: 5'-CGG CCC CAC GGT GGC ACT AGT CCT CTT GGG CAG CAG CAC G-3'); for K127R (K127R-S: 5'-GCC ACC GTG GGG CCG AGG GCA CCC TCG GGC GGC-3'; K127R-AS: 5'-GCC GCC CGA GGG TGC CCT CGG CCC CAC GGT GGC-3'); for K133R (K133R-S: 5'-CCC TCG GGC GGC AGG AAG GCA ACC CAG GCC TCC-3'; K133R-AS: 5'-GGA GGC CTG GGT TGC CTT CCT GCC CGG CGA GGG-3'); for K134R (K134R-S: 5'-CCC TCG GGC GGC AAG AGG GCA ACC CAG GCC TCC-3'; K134R-AS: 5'-GGA GGC CTG GGT TGC CCT CTT GCC GCC CGA GGG-3'). Site-directed mutagenesis for double mutants (containing a K mutation and an S139 mutation) were obtained using the same primers as above but with S139A or S139E mutant cDNAs as templates.

Cell lines and transfections. HeLa and human embryonic kidney (HEK) 293T cells were maintained in DMEM media supplemented with 7.5% FBS, 100 units/mL penicillin/streptomycin and 1.25 μg/mL amphotericin B (Sigma, St. Louis MO). HCT116 wild-type and *Chk2*$^{-/-}$ cells (kind gift from Bert Vogelstein) were maintained in McCoy's 5A media supplemented with 10%FBS, 100 units/mL penicillin/streptomycin and 1.25 μg/mL amphotericin B. Transient transfections using Fugene 6 (Roche) were performed according to manufacturer's protocol.

Stable HeLa cell lines were created by the addition of 600 μg/mL G418 (Sigma) three days after transfection with GFP-H2AX constructs. Cells were kept under selection for two wk, after which they were subjected to fluorescence activated cell sorting using FACSVantage SE with DIVA option. Sorted GFP positive cells were collected, replated and maintained with 200 μg/mL G418. Clones were generated from plating the stable pools at a 1:500 dilution in 150 mm tissue culture dishes and subsequently cloned with glass cylinders.

Stable HCT116 Tet-H2AX cell lines were created by initially transfecting HCT116 cells with pTet-Off (BD Biosciences) and adding 200 μg/mL G418. Clones were isolated using glass cylinders and tested for inducibility using a transient transfection of pTRE-luciferase in the presence and absence of doxycyclin. Transfections were performed in triplicate using Fugene 6 (Roche) and normalized with an internal control phGR-TK (Promega), which contains a Renilla luciferase gene under a constitutive TK basal promoter. Luciferase activity was measured using a dual luciferase assay system (Promega). A clone (HTO-23) was selected and subsequently cotransfected with pHygro and pTRE-H2AX, pTRE-H2AX S139E or pTRE-H2AX S139A. Clones were isolated using glass cylinder in the presence double selection (G418 and hygromycin).

Stable 293T-G5-luc cells were obtained by transfection of 293T cells with pG5-luc, which contains a firefly luciferase gene under the control of five GAL4 binding sites, and clones were isolated by glass cylinders in the presence of 200 μg/mL G418.

Early G_2/M checkpoint assay. Briefly, cells were transfected with GFP-tagged histones for 48 h, harvested, washed in PBS and fixed in 0.5% methanol-free formaldehyde (Polysciences, Warrington, PA). After washing, cells were incubated in 70% EtOH overnight at -20°C. The next day cells were washed in PBS and permeabilized in PBS/0.25% Triton X-100 for 15 min on ice. Cells were then washed, and 0.75 μg of α-phospho-histone H3 (Phosphoserine 10) antibody (Upstate, Charlottesville, VA) was added to cells resuspended in 100 μl of PBS/1% BSA for 2.5 h at room temperature. Cells were washed in PBS and resuspended again in PBS/1%BSA to which Alexa Fluor 680-R-phycoerythrin goat anti-rabbit IgG was added at a 1:200 dilution (Molecular Probes, Eugene, OR). Cells were washed twice, and samples were run on a BDFacsScan flow cytometer. The percentage of cells with phospho-H3 reactivity in the GFP positive and negative cell populations was calculated using FlowJo software (Treestar, Ashland, OR). For DNA content detection, cells were washed twice in PBS, and then resuspended in 40 ug/mL propidium iodide in PBS supplemented with 100 ug/mL RNAse A and analyzed in the BDFacsScan.

MMS sensitivity assay. The protocol was performed essentially as previously described.[49] Following treatment of HeLa stable cell lines with methyl methane sulfonate (MMS) for 50 min, they were washed with PBS, and fresh media was then added. Forty-eight hours later, attached and detached cells were harvested and viability was assessed using trypan blue exclusion (Invitrogen, Carlsbad, CA).

Apoptosis assays. For the Annexin-V assay, HeLa cells were transfected with the GFP-tagged H2AX, S139A or S139E constructs. Forty-eight hours after transfection, attached and detached cells were harvested and binding of Annexin-V was measured by flow cytometry according to the manufacturer's instructions (BD Biosciences, San Jose, CA). To measure caspase 3/7 activity, the Caspase-Glo kit was used (Promega, Madison, WI). Briefly, subconfluent HeLa cells were transfected with 50 ng/well of GFP-H2AX, S139A or S139E in 96-well plates. Caspase 3/7 activity was measured 24 h after transfection in a Victor 2 luminescent plate reader.

Subcellular fractionation, western blots and immunoprecipitations. Whole cell extracts were prepared by lyzing cells in RIPA buffer [120 mM NaCl, 50 mM Tris pH 7.4, 0.5% NP-40, 1 mM EDTA]. For extraction of histones, transfected cells were harvested, washed with PBS, and lyzed in Buffer A [20 mM Tris pH 7.4, 10 mM KCl, 1 μM EDTA, 0.2% NP40, 50% glycerol, 0.6 mM β-Mercaptoethanol (BME), 1 mM PMSF and 1X protease inhibitor cocktail (Roche)] for two min on ice. The pellet was resuspended in Buffer B [20 mM Tris pH 7.4, 10 mM KCl, 0.4 M NaCl, 1 μM EDTA, 50% glycerol, 0.6 mM BME, 1 mM PMSF, protease inhibitor cocktail] for 30 min on ice. After centrifugation, the pellet was resuspended in Acid Extraction Buffer (0.5 M HCl, 50% glycerol, 100 mM BME) for two min at room temperature. To the supernatant, Tris pH 7.4 (10 mM final concentration), NaOH (0.33 M final concentration) and protease inhibitors were added to 10 mM final concentration. Protein

concentrations were measured by the Bradford assay (Biorad). The following antibodies were used: α-H2AX, α-γH2AX and α-phospho-Histone H3 Serine 10 (Upstate), α-GFP (Chemicon), α-phospho CHK2 Threonine 68 (Cell Signaling), α-phospho ATM Serine 1981 (Upstate), α-Flag and β-Actin (Sigma). Beads were Protein A/G agarose (Santa Cruz) and Nickel-NTA-agarose (Qiagen).

Nucleosome fractionation. The procedure was carried out as previously described, with modifications.[50] 293T cells were transfected with wild-type Flag H2AX for 36 h, harvested, washed in PBS and resuspended in lysis buffer [20 mM HEPES pH 7.5, 0.25 M sucrose, 3 mM $MgCl_2$, 0.5% NP40, 3 mM BME, 0.4 M PMSF and protease inhibitors cocktail]. The cells were lyzed in a dounce homogenizer and centrifuged for 15 min at 3,000 *g*. Pelleting was repeated twice with lysis buffer and once with fractionation buffer [20 mM HEPES, pH 7.5, 3 mM $MgCl_2$, 0.2 mM EGTA, 3 mM BME, 0.4 M PMSF and protease inhibitor cocktail]. This was followed by resuspension of the pellet in two volumes of fractionation buffer. To the suspension, one total volume of fractionation buffer/0.6 M KCL/10% glycerol was added. After stirring at 4°C for ten min the nuclei were pelleted by centrifugation at 17,500 *g* for 30 min at 4°C .The nuclear pellet was resuspended in 20 volumes of medium salt buffer [20 mM HEPES pH 7.5, 0.4 M NaCl, 1 mM EDTA, 5% glycerol, 1 mM BME, 0.5 M PMSF and protease inhibitors], followed by centrifugation at 10,000 *g* for ten min at 4°C. The pellet was then resuspended in four volumes high salt buffer [20 mM HEPES pH 7.5, 0.65 M NaCl, 1 mM EDTA, 0.34 M sucrose, 1 mM BME, 0.5 M PMSF], and homogenized with 40–50 strokes in a dounce homogenizer to release the oligonucleosome fragments. The nuclei were then centrifuged at 10,000 *g* for 20 min at 4°C. The supernatant was dialyzed overnight against low salt buffer [20 mM HEPES pH 7.5, 0.1 M NaCl, 1 mM EDTA, 1 mM BME, 0.5 M PMSF], followed by the addition of $CaCl_2$ to a 3 mM final concentration and ten units/ml microccocal nuclease (Sigma). The reaction was incubated for ten min at 37°C, stopped with 0.1 volume 0.5 M EDTA, and subjected to a 10%–30% sucrose gradient, followed by ultracentrifugation for seven hrs. The 15 fractions were analyzed on a 1% agarose gel for the presence of nucleosome fragments. The positive fractions (which contained mono, oligo and poly-nucleosomes) were resolved by 12% SDS PAGE. Protein Bands were visualized by staining with Coomassie blue, and by immunoblotting with α-FLAG antibody.

Immunofluorescence. HeLa cells were plated onto chamber slides and transfected the next day with 0.5 μg of GFP vector, GFP-H2AX, GFP-S139A or GFP-S139E. Forty eight hours after transfection, mock transfected cells were irradiated with 10 Gy. One hour after irradiation, samples were fixed with 4% formaldehyde for five min followed by five min incubation with cold 100% EtOH. Cells were permeabilized with PBS/0.25% Triton X-100 for ten min on ice, washed with PBS, and then blocked for 30 min with PBS/5% BSA at room temperature. After blocking, 53BP1 antibody (Upstate) was added at a 1:1000 dilution to PBS/1% BSA for one hour at room temperature. Cells were washed and goat α-mouse AlexaFluor 555 (Molecular Probes) was added at 1:5,000 dilution in PBS/1% BSA for one hour at room temperature. Cells were washed four times and mounted with Prolong Gold medium (Molecular Probes). Quantitation of foci was performed using ImagePro software (MediaCybernetics, Silver Spring, MD).

Acknowledgements

The authors are indebted to members of the Monteiro Lab for helpful discussions. This work was supported by a DoD postdoctoral fellowship DAMD17-01-1-0403 (V.D.), a DoD predoctoral fellowship BC083181 (A.V.), by the Julia Murtha Fund (A.M.), NIH grant CA92309 (A.M.) and supplement CA92309-04S1 (J.R.D) and supported in part by the Molecular Imaging, Flow Cytometry, Analytic Microscopy and the Molecular Biology cores at the H.L. Moffitt Cancer Center & Research Institute.

Note

Supplementary materials can be found at:
www.landesbioscience.com/supplement/RiosDoriaCBT8-5-Sup.pdf

References

1. Zhou BB, Elledge SJ. The DNA damage response: Putting checkpoints in perspective. Nature 2000; 408:433-9.
2. Rogakou EP, Pilch DR, Orr AH, Ivanova VS, Bonner WM. DNA double-stranded breaks induce histone H2AX phosphorylation on serine 139. J Biol Chem 1998; 273:5858-68.
3. Redon C, Pilch D, Rogakou E, Sedelnikova O, Newrock K, Bonner W. Histone H2A variants H2AX and H2AZ. Curr Opin Genet Dev 2002; 12:162-9.
4. Hatch CL, Bonner WM, Moudrianakis EN. Minor histone 2A variants and ubiquinated forms in the native H2A:H2B dimer. Science 1983; 221:468-70.
5. Ivanova VS, Zimonjic D, Popescu N, Bonner WM. Chromosomal localization of the human histone H2A.X gene to 11q23.2-q23.3 by fluorescence in situ hybridization. Hum Genet 1994; 94:303-6.
6. Burma S, Chen BP, Murphy M, Kurimasa A, Chen DJ. ATM phosphorylates histone H2AX in response to DNA double-strand breaks. J Biol Chem 2001; 276:42462-7.
7. Ward IM, Chen J. Histone H2AX is phosphorylated in an ATR-dependent manner in response to replicational stress. J Biol Chem 2001; 276:47759-62.
8. Stiff T, O'Driscoll M, Rief N, Iwabuchi K, Lobrich M, Jeggo PA. ATM and DNA-PK function redundantly to phosphorylate H2AX after exposure to ionizing radiation. Cancer Res 2004; 64:2390-6.
9. Rogakou EP, Boon C, Redon C, Bonner WM. Megabase chromatin domains involved in DNA double-strand breaks in vivo. J Cell Biol 1999; 146:905-16.
10. Shroff R, Arbel-Eden A, Pilch D, Ira G, Bonner WM, Petrini JH, et al. Distribution and dynamics of chromatin modification induced by a defined DNA double-strand break. Curr Biol 2004; 14:1703-11.
11. Paull TT, Rogakou EP, Yamazaki V, Kirchgessner CU, Gellert M, Bonner WM. A critical role for histone H2AX in recruitment of repair factors to nuclear foci after DNA damage. Curr Biol 2000; 10:886-95.
12. Celeste A, Fernandez-Capetillo O, Kruhlak MJ, Pilch DR, Staudt DW, Lee A, et al. Histone H2AX phosphorylation is dispensable for the initial recognition of DNA breaks. Nat Cell Biol 2003; 5:675-9.
13. Celeste A, Petersen S, Romanienko PJ, Fernandez-Capetillo O, Chen HT, Sedelnikova OA, et al. Genomic instability in mice lacking histone H2AX. Science 2002; 296:922-7.
14. Bassing CH, Chua KF, Sekiguchi J, Suh H, Whitlow SR, Fleming JC, et al. Increased ionizing radiation sensitivity and genomic instability in the absence of histone H2AX. Proc Natl Acad Sci USA 2002; 99:8173-8.
15. Keogh MC, Kim JA, Downey M, Fillingham J, Chowdhury D, Harrison JC, et al. A phosphatase complex that dephosphorylates gammaH2AX regulates DNA damage checkpoint recovery. Nature 2005; 439:406-7.
16. Chowdhury D, Keogh MC, Ishii H, Peterson CL, Buratowski S, Lieberman J. Gamma-H2AX dephosphorylation by protein phosphatase 2A facilitates DNA double-strand break repair. Mol Cell 2005; 20:801-9.
17. Bassing CH, Suh H, Ferguson DO, Chua KF, Manis J, Eckersdorff M, et al. Histone H2AX: A dosage-dependent suppressor of oncogenic translocations and tumors. Cell 2003; 114:359-70.
18. Celeste A, Difilippantonio S, Difilippantonio MJ, Fernandez-Capetillo O, Pilch DR, Sedelnikova OA, et al. H2AX haploinsufficiency modifies genomic stability and tumor susceptibility. Cell 2003; 114:371-83.
19. Xie A, Puget N, Shim I, Odate S, Jarzyna I, Bassing CH, et al. Control of sister chromatid recombination by histone H2AX. MolCell 2004; 16:1017-25.
20. Fernandez-Capetillo O, Chen HT, Celeste A, Ward I, Romanienko PJ, Morales JC, et al. DNA damage-induced G_2-M checkpoint activation by histone H2AX and 53BP1. Nat Cell Biol 2002; 4:993-7.
21. Downs JA, Lowndes NF, Jackson SP. A role for Saccharomyces cerevisiae histone H2A in DNA repair. Nature 2000; 408:1001-4.
22. Redon C, Pilch DR, Rogakou EP, Orr AH, Lowndes NF, Bonner WM. Yeast histone 2A serine 129 is essential for the efficient repair of checkpoint-blind DNA damage. EMBO Rep 2003; 4:678-84.

23. Monteiro AN, August A, Hanafusa H. Evidence for a transcriptional activation function of BRCA1 C-terminal region. Proc Natl Acad Sci USA 1996; 93:13595-9.
24. Xu B, Kim ST, Lim DS, Kastan MB. Two molecularly distinct G_2/M checkpoints are induced by ionizing irradiation. Mol Cell Biol 2002; 22:1049-59.
25. Xu B, Kim S, Kastan MB. Involvement of Brca1 in S-phase and G(2)-phase checkpoints after ionizing irradiation. Mol Cell Biol 2001; 21:3445-50.
26. Fernandez-Capetillo O, Lee A, Nussenzweig M, Nussenzweig A. H2AX: The histone guardian of the genome. DNA Repair (Amst) 2004; 3:959-67.
27. Ishida N, Kitagawa M, Hatakeyama S, Nakayama Ki. Phosphorylation at serine 10, a major phosphorylation site of $p27^{Kip1}$, increases its protein stability. J Biol Chem 2000; 275:25146-54.
28. Potter LR, Hunter T. A constitutively "phosphorylated" guanylyl cyclase-linked atrial natriuretic peptide receptor mutant is resistant to desensitization. Mol Biol Cell 1999; 10: 1811-20.
29. Misteli T, Gunjan A, Hock R, Bustin M, Brown DT. Dynamic binding of histone H1 to chromatin in living cells. Nature 2000; 408:877-81.
30. Kanda T, Sullivan KF, Wahl GM. Histone-GFP fusion protein enables sensitive analysis of chromosome dynamics in living mammalian cells. Curr Biol 1998; 8:377-85.
31. Gautier T, Abbott DW, Molla A, Verdel A, Ausio J, Dimitrov S. Histone variant H2ABbd confers lower stability to the nucleosome. EMBO Rep 2004; 5:715-20.
32. Siino JS, Nazarov IB, Svetlova MP, Solovjeva LV, Adamson RH, Zalenskaya IA, et al. Photobleaching of GFP-labeled H2AX in chromatin: H2AX has low diffusional mobility in the nucleus. Biochem Biophys Res Commun 2002; 297:1318-23.
33. Kleinschmidt AM, Martinson HG. Structure of nucleosome core particles containing uH2A (A24). Nucleic Acids Res 1981; 9:2423-31.
34. Marti TM, Hefner E, Feeney L, Natale V, Cleaver JE. H2AX phosphorylation within the G_1 phase after UV irradiation depends on nucleotide excision repair and not DNA double-strand breaks. PNAS 2006; 103:9891-6.
35. Goldknopf IL, Busch H. Isopeptide linkage between nonhistone and histone 2A polypeptides of chromosomal conjugate-protein A24. Proc Natl Acad Sci USA 1977; 74:864-8.
36. Seale RL. Rapid turnover of the histone-ubiquitin conjugate, protein A24. Nucleic Acids Res 1981; 9:3151-8.
37. Wu LH, Kuehl L, Rechsteiner M. Dynamic behavior of histone H1 microinjected into HeLa cells. J Cell Biol 1986; 103:465-74.
38. Pina B, Suau P. Changes in histones H2A and H3 variant composition in differentiating and mature rat brain cortical neurons. Dev Biol 1987; 123:51-8.
39. Tsvetkov S, Ivanova E, Djondjurov L. Metabolic behaviors of the core histones in proliferating friend cells. Exp Cell Res 1989; 180:94-105.
40. Huen MS, Grant R, Manke I, Minn K, Yu X, Yaffe MB, et al. RNF8 transduces the DNA-damage signal via histone ubiquitylation and checkpoint protein assembly. Cell 2007; 131:901-14.
41. Mailand N, Bekker-Jensen S, Faustrup H, Melander F, Bartek J, Lukas C, et al. RNF8 ubiquitylates histones at DNA double-strand breaks and promotes assembly of repair proteins. Cell 2007; 131:887-900.
42. Kleckner N, Zickler D, Jones GH, Dekker J, Padmore R, Henle J, et al. A mechanical basis for chromosome function. Proc Natl Acad Sci USA 2004; 101:12592-7.
43. Bakkenist CJ, Kastan MB. DNA damage activates ATM through intermolecular autophosphorylation and dimer dissociation. Nature 2003; 421:499-506.
44. Heo K, Kim H, Choi SH, Choi J, Kim K, Gu J, et al. FACT-mediated exchange of histone variant H2AX regulated by phosphorylation of H2AX and ADP-ribosylation of Spt16. Mol Cell 2008; 30:86-97.
45. Rios-Doria J, Fay A, Velkova A, Monteiro AN. DNA damage response: Determining the fate of phosphorylated histone H2AX. Cancer Biol Ther 2006; 5:142-4.
46. McGowan CH, Russell P. The DNA damage response: Sensing and signaling. Curr Opin Cell Biol 2004; 16:629-33.
47. Bartek J, Falck J, Lukas J. CHK2 kinase—a busy messenger. Nat Rev Mol Cell Biol 2001; 2:877-86.
48. Phelan CM, Dapic V, Tice B, Favis R, Kwan E, Barany F, et al. Classification of BRCA1 missense variants of unknown clinical significance. J Med Genet 2005; 42:138-46.
49. Zhong Q, Chen CF, Li S, Chen Y, Wang CC, Xiao J, et al. Association of BRCA1 with the hRad50-hMre11-p95 complex and the DNA damage response. Science 1999; 285:747-50.
50. Zaret K. Chromatin assembly and analysis: Micrococcal nuclease analysis of chromatin structure. In: Ausubel FM, Brent R, Kingston R, Moore D, Seidman J, Smith JA, et al. Curr Protoc Mol Biol. New York: John Wiley & Sons, Inc 2005; 21:1-14.

2.26 **The Role of BRCA1 Domains and Motifs in Tumor Suppression**

Aneliya D. Velkova, Risk Assessment, Detection, and Intervention Program, H. Lee Moffitt Cancer Center & Research Institute, Tampa, FL and University of South Florida Cancer Biology PhD Program, Tampa, FL, USA; Marcelo A. Carvalho, Risk Assessment, Detection, and Intervention Program, H. Lee Moffitt Cancer Center & Research Institute, Tampa, FL, USA; Joseph O. Johnson, Analytic Microscopy Core, H. Lee Moffitt Cancer Center & Research Institute, Tampa, FL, USA; Sean V. Tavtigian, Genetic Susceptibility group, International Agency for Research on Cancer, Lyon, France; Alvaro N. A. Monteiro, Risk Assessment, Detection, and Intervention Program, H. Lee Moffitt Cancer Center & Research Institute, Tampa, FL, USA.

Germline mutations in the breast and ovarian cancer predisposition gene 1 (BRCA1) are responsible for the majority of hereditary breast cancer cases. There are over 1500 alleles of BRCA1 and one of the most challenging tasks for genetic counseling is to distinguish which are benign and which are cancer predisposing. We developed a system of functional assays to test the functions of domains anywhere in coding region of BRCA1. We did this by testing for biological processes and functions ascribed to BRCA1: DNA damage sensitivity and cell cycle checkpoint activation (early G2M, spindle assembly and intra-S-phase checkpoints). These assays can be used for further classification of BRCA1 unclassified variants for their cancer association as well as for analyzing BRCA1 function. We are also studying the function of under explored but conserved small motifs in BRCA1. Using as a bait in yeast two hybrid screening one of these motifs we identified cytoskeletal protein Filamin A as a specific BRCA1 binding partner. Their interaction is abrogated by a mutation found in breast cancer families. We systematically evaluated DNA damage signaling after treatment with ionizing radiation in cells that lack Filamin A. We found that these cells have an impaired BRCA1 and Rad51 foci formation and accumulate single stranded DNA. We also found that Filamin A is required for an efficient interaction between DNA-PKcs and Ku86. Our data showed that lack of Filamin A leads to an impairment in both homologous recombination and non-homologous end joining. [This work is supported by a predoctoral fellowship [BC083181] to Aneliya Velkova from the U.S. Department of Defense Breast Cancer Research Program].